Functional Polymers *via* Cu-mediated Radical Polymerization

Resat Aksakal

Submitted in partial fulfilment of the requirements of the Degree of Doctor of Philosophy

School of Engineering and Materials Science

Queen Mary, University of London

September 2017

Statement of Originality

I, Resat Aksakal, confirm that the research included within this thesis is my own work or that where it has been carried out in collaboration with, or supported by others, that this is duly acknowledged below and my contribution indicated. Previously published material is also acknowledged below.

I attest that I have exercised reasonable care to ensure that the work is original, and does not to the best of my knowledge break any UK law, infringe any third party's copyright or other Intellectual Property Right, or contain any confidential material.

I accept that the College has the right to use plagiarism detection software to check the electronic version of the thesis.

I confirm that this thesis has not been previously submitted for the award of a degree by this or any other university.

Signature:

Date: 21.09.2017

Details of collaboration and publications:

Parts of this thesis have been published in:

R. Aksakal, M Resmini and C.R. Becer, *Polym. Chem*., 2016, **7**, 171-175.

R. Aksakal, M. Resmini and C.R. Becer, *Polym. Chem.,* 2016, **7**, 6564 – 6569.

Abstract

This work reports the investigation of Cu-mediated polymerization systems and its limits, in order to obtain functional branched polymers, in particular star-shaped and graft-shaped polymers.

A novel initiator structure has allowed developing a new approach to synthesise sequence controlled multiblock star polymers via Cu-mediated reversible deactivation radical polymerization (RDRP) in water. This technique allows the preparation of pentablock star shaped polymers in just under 90 minutes of reaction time. The obtained polymers had a good agreement between theoretical and experimental molecular weights and excellent control over molecular weight distribution.

Alternatively, the Cu-mediated RDRP of star polymers using a British 1 penny coin was described, displaying similar results as in the literature, providing better experimental conditions. As the copper coin was recovered unharmed, the catalyst was found to be economically very effective.

Furthermore, poly(2-ethyl oxazoline) (PEtOx) was polymerized with good control and partially hydrolysed to poly(ethylene imine) (PEI) to yield PEtOx-*r*-PEI using a microwave reactor. The secondary amines of PEI was converted to macroinitiators, to allow the polymerization of acrylamides in aqueous medium, resulting in graft type polymers based on a poly(oxazoline) backbone with acrylamide side chains.

Finally, the synthesis of carbohydrate-monomers was described, which allows to obtain monomers with a different number of carbohydrates (one, two or three). These monomers were polymerised *via* aqueous SET-LRP, to explore their interaction with carbohydrate binding lectins and to understand the impact on binding of carbohydrate density on polymers and polymer chain length.

Table of Contents

List of Figures

List of Tables

Acknowledgments

First of all, my biggest thanks go to Prof. Marina Resmini and Dr. Remzi Becer, for giving me the opportunity to work on this project under their constant supervision and help during my entire time of PhD. I think this time, like other PhD students, has changed my life and although you might not be aware (or just too kind), YES, you are awesome, both as a supervisor and in person.

Now to the other awesome people of the Becer Group. I remember the first lab days of the group, the first BIG stores purchase of I don't know how many round bottom flasks and beakers *etc.*, the first experiments, the first instruments rolling in, our first lunch breaks (it was only me, Gokhan and Ed but still lots of fun) and I consider myself really lucky, but I have also seen in the early days of taking over the lab space, that we took lots of dirt, dust and impurities over as well "as evidenced by" failing reactions for weeks! The group slowly grew and grew and now hosts >10 full time students today. Only Ed and Gokhan would know how we suffered back then :) Then again, I must say that you guys were the first to show me the key skills in doing some of the experiments (Yeaah.. Just keep degassing for ehmm 10-15 minutes). While I also learned a lot about the instruments from Ed (who left the group too early), I unfortunately had to share my fumehood for years with you Gokhan. I was such an organized guy when I started, until we moved into a fumehood together (Warning!). Still regret it today. (if my examiners ask me what would I have done differently, there you have the answer).

Towards the end of my second year, Jacky joined the group. As you are one of the next people writing up, my advice to you would be to… stop saying "Oh, no, fail" for every unsuccessful GPC of polycaprolactone. That too will one day polymerize as you expect it to. Other newcomers were Manuel, Dominic, Tian, Martin, Elham and Laily. Laily! Laily! Laily! Is it finally working? I'm sure it does. Martin, Dominic and Elham you guys stay upstairs in the nice labs with AC, while we enjoyed the nice weather in the labs during summer. Gokhan az kac surdan. It was really fun to work with all of you, thank you for sparing chemicals every now and then, not you Dominic. You first need to bring the things you borrowed back! Yamin, make sure nobody kills the pump and definetly not the freeze drier! Oh yeah, with Menual came Vali, as if ein Bauer nicht genug war. I forgot where I was *quo vadis* with the Bauer example but anyway (Ach ja, an dieser Stelle bestelle ich Inge schöne Grüsse). Manuel, wiederhole bitte die 12 Gebote der green chemistry in richtiger Reihenfolge. Mausi (Vali),

Alarma! Ich werde dir weiterhin paper abstracts schicken, keine Sorge. Sonst weiss ich gar nicht was ich dir noch sagen soll, meine Augen sagen ja schon alles.

To the newer members Luka, part time member Eason (Eason, sorry but we need more NMR tubes) and the rest I had to chance to work with, have a coffee with or even just a chat, thank you for all your help and support. I might

Furthermore, I would like to thank Dr. Alban for his constant motivation from the north, the entire technical staff at QMUL, especially Chris Mole, Dr. Ben Gridley and ofcourse Armandino ("s…sprinkler") and everyone else who I didn't get to mention and say thanks.

Now to the most organized and cleanest member of the group, Suzan. If it wasn't for you, I don't know how I would have survived my last year. Thank you for all your support and constant

Chapter 1

Introduction

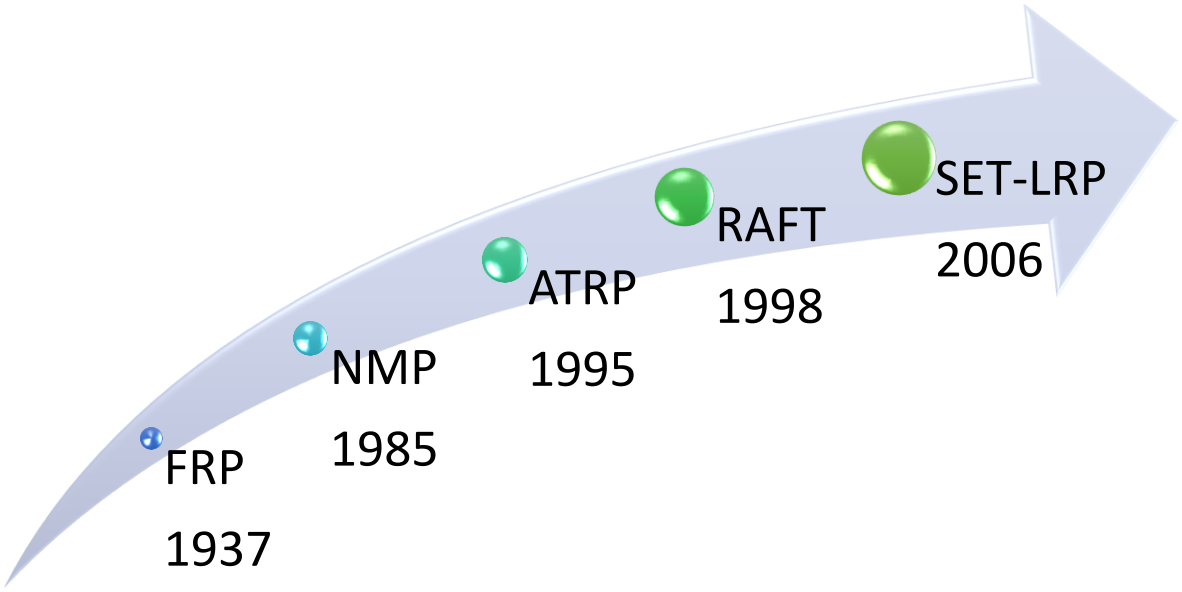

Controlled radical polymerisation (CRP) techniques are being constantly developed since the introduction of free radical polymerisation (FRP). This has opened numerous possibilities for researchers in understanding and designing macromolecules to tailored properties and structures. However, controlled polymerisation was already introduced as early as the introduction of anionic polymerisation. Therefore, an introduction to ionic polymerisation will be given in the following, prior to the development of efficient and sophisticated radical polymerisation techniques. Further, various CRP methods with some of their advantages and disadvantages will be discussed. Finally, an introduction to the synthesis of different polymer architectures will be given and some of the latest investigation of glycopolymers will be introduced in order to establish an understanding of their interactions with lectins.

1.1 Ionic Polymerization

1.1.1 Anionic Polymerization

The first example of an ionic polymerization was demonstrated by Szwarc in 1956, when the polymerization of styrene initiated by aromatic radical-anions such as sodium naphthalene.[1,2] The initiation step is much faster compared to propagation and initiators are expected to start only one chain. This allows access to well-defined polymers with control over their molecular weight. The propagating centers are not involved in bimolecular termination due to the electrostatic repulsion of similar charges. Additionally, the use of aprotic solvents as polymerization medium avoids the transfer of positive charged species, which could also induce termination events. Therefore, the polymerization proceeds until all monomers are consumed and can even be extended with the addition of more monomer. Due to this, anionic polymerization is termed as "living" polymerization, since the active chain ends only die once exposed to oxygen or intentionally terminated (*e.g.* by a polar reagent). Therefore however, appropriate care and extensive purification of reagents and solvents are required before being used for the polymerization. Additionally, this technique commonly requires temperatures as low as -78 °C, yet is still a very robust tool to yield well defined polymers. The mechanism of anionic polymerization is given below based on the polymerization of styrene with butyl lithium as initiator **(Scheme 1.1)**.

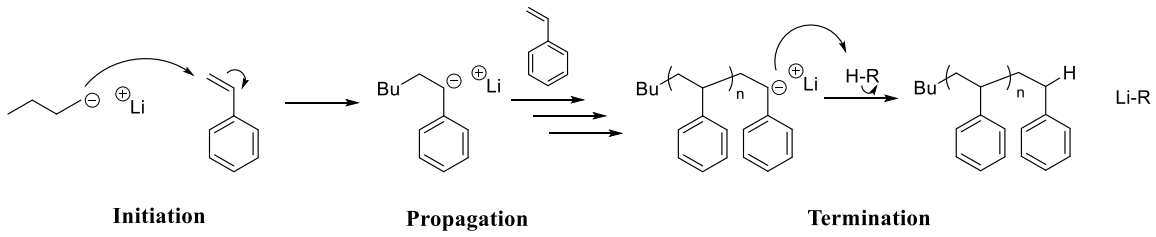

Scheme 1.1: Anionic polymerization of styrene with butyl lithium as initiator.

1.1.2 Cationic Polymerization

Similarly, cationic polymerization proceeds *via* propagating cationic chain ends, which are initiated in the presence of a *Lewis* acid. However this technique is less attractive due to unavoidable *β*-proton transfer, combination with the counterion or chain transfer to polymer. Through careful selection of reagents and solvent (ion salt as counterion, covalent esters or halides as dormant species), this technique can be expended to cationic "living" polymerization, which can be employed to polymerize 1,1-dialkyl olefins (*e.g.* isobutylene) or

dienes (*e.g.* butadiene, isoprene). The mechanism of cationic polymerization is given below based on the cationic polymerization of isobutylene initiated by boron trifluoride and water.

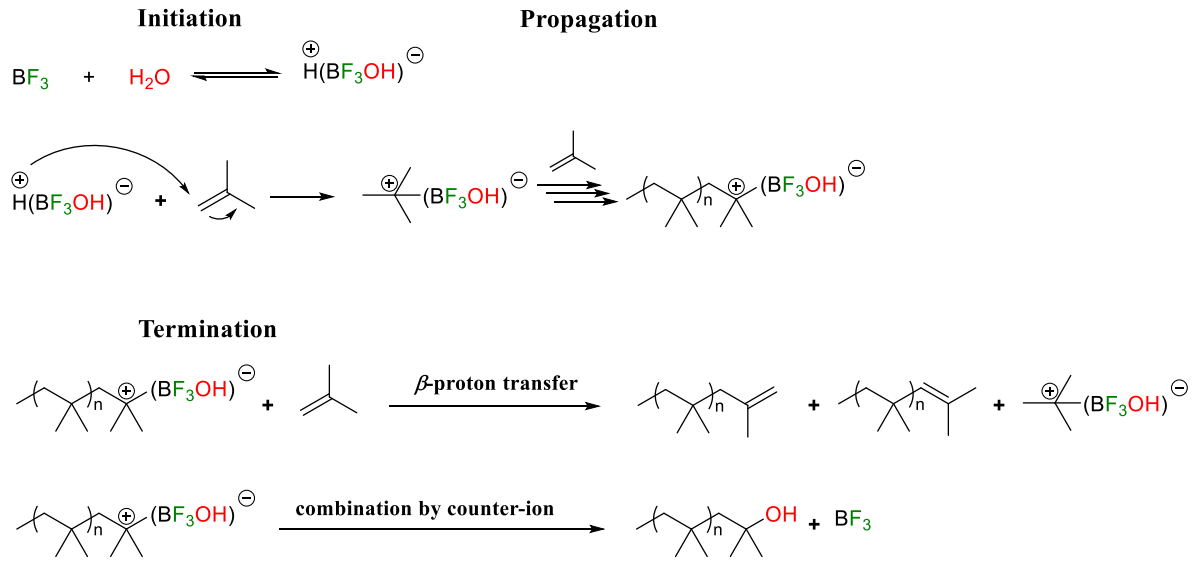

Scheme 1.2: Cationic polymerization of isobutylene initiated by boron trifluoride.

1.1.2.1 Cationic Ring Opening Polymerisation

A well-known class of cyclic monomers are the oxazolines, which the cationic ring opening polymerization (CROP) of was first described in 1966.[3-5] 2-Ethyl-2-oxazoline (EtOx) is a well-known monomer due to its biocompatibility and hydrophilicity.[6-8] The reaction mechanism of CROP is depicted below in Scheme 1.3, where 2-Ethyl-2-oxazoline is used as an example with acetyl halides[9].

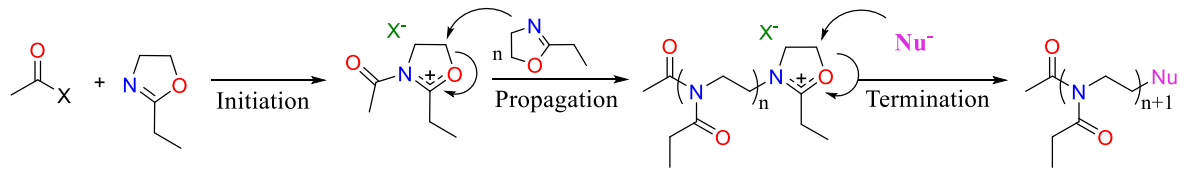

Scheme 1.3: Schematic representation of the acetyl halide initiatied CROP of 2-Ethyl-2-oxazoline.

In the 1980s and 1990s, this class of polymers was almost forgotten, due to their long reaction times. Their possibilities for application were not well investigated until the beginning of the 2000s. In 2004, Schubert *et al.* reported the accelerated synthesis of EtOx in a single-mode microwave reactor, which today gives easy access to a wide range of poly oxazolines.[10] In a range between 80 to 190 °C, the polymerization of EtOx (DP_n=60) was optimized to yield well defined polymers with low dispersities (PDI<1.2) under six hours and their livingness with

chain extensions of the same monomer was shown with higher molecular weights in the size exclusion chromatography (SEC) traces. The ideal temperature was identified as 140 °C. In a subsequent study, the range of monomers were expanded to 2-Methyl- (MeOx), 2-Nonyl- (NonOx) and fluorinated 2-Phenyl-2-oxazoline (PhOx) and polymerised in bulk.[11] It was also reported that fluorinated PhOx was the fastest reacting monomer, which was correlated to the substitution of the side chain with electron withdrawing groups. The above mentioned monomers were later chain extended with a library of 16 different monomers in order to obtain well-defined diblock copolymers[12], which was in a further study extended to triblock copolymers[13].

Schubert *et al.* also investigated the hydrolysis of PEtOx to poly(ethylene imine) (PEI) and explored different purification methods, to obtain "pharmagrade" PEI.[14] The hydrolysis of PEtOx was later optimised for microwave reactions by Hoogenboom *et al.*[15] Maximum acceleration was observed at 180 °C using dilute aqueous solutions of HCl. Both techniques can be used to fully hydrolyse PEtOx, in order to obtain PEI, whereas the microwave assisted hydrolysis of PEtOx was proven to be useful to target certain hydrolysis rates to obtain POx-*stat*-PEI. In a more recent study, Hoogenboom *et al.* reported the application of these polymers in gene delivery systems.[16] Random copolymers of *n*-propyl-2-oxazoline (nPrOx) and ethylenimine (PPrOx-*r*-PEI) were prepared by partial hydrolysis. Due to the increased hydrophobicity resulting from the PEI content, nanoparticles could be prepared at elevated temperatures. The prepared nanoparticles were then used to form polyplexes with DNA. The same group also reported the synthesis of glycopolymers from partially hydrolysed PEtOx.[17] Subsequently, linear forms of glucose and maltose were attached to the backbone *via* reductive amination, varying the ratio of PEtOx to carbohydrates systematically. Their solution properties were investigated, which revealed either fully water soluble or temperature dependent agglomerates of glycopolymers. Finally, their ability to bind to lectins were studied with Concanavalin A (ConA).

1.2 Radical Polymerisation

1.2.1 Free Radical Polymerisation

Today, the most commonly used method to obtain polymers is *via* free radical polymerisation, which was first introduced by *Flory* already in the 1930s.[18] This technique is widely dominating the synthesis of most of the daily commodity polymers (*e.g.* polystyrene) and still finds wide use in academia despite being one of the first polymerizations techniques. Its scalability and its

simple and straightforward reaction conditions are only a few of the many advantages, especially from the industrial point of view. Moreover, this technique offers a big pool of monomers that can be employed. Even when trace amounts of oxygen or stabilisers are present in the system, high molecular weight polymers can be obtained with ease, without requiring rigorous drying of solvents or extensive purification of other chemicals present. It is compatible with many solvents including water, however polymerizations can also be carried out in bulk, which makes it also attractive and cheap to employ.

1.2.1.1. Sequence of Events

Due to its long history, radical polymerisation is well studied and understood. The polymerization itself consists of a sequence of three steps, namely *initiation* of polymerization, *propagation* of chains and finally *termination* of the polymerization. The initiation of the polymerization involves two reactions, which usually starts with the homolytic decomposition of an initiator (I), that yields a pair of initiator radicals (2R·). The rate constant for the initiator dissociation is described as k_d (**Eq. 1.1**). Once the initiator radical is formed, the first monomer molecule (M) is added, which forms the chain-initiating radical (M·), where k_i is the rate constant for the initiation step (**Eq. 1.2**). The initiation step is followed by propagation. Here, the chain-initiating radical grows into a longer chain by reacting one by one with the rest of the monomers, as described in **Eq. 1.3,** where k_p is the rate constant for propagation.

$$\mathrm{I} \xrightarrow{k_d} 2\mathrm{R}\cdot \qquad \textbf{(1.1)}$$

$$\mathrm{R}\cdot + \mathrm{M} \xrightarrow{k_i} \mathrm{M}\cdot \qquad \textbf{(1.2)}$$

$$\mathrm{M}\cdot + \mathrm{nM} \xrightarrow{k_p} \mathrm{M_{n+1}}\cdot \qquad \textbf{(1.3)}$$

Although it can vary, typical k_p values for most monomers varies between 10^2–10^4 $\mathrm{L\cdot mol^{-1}\cdot s^{-1}}$ for radical polymerizations. Those encountered in step polymerizations on the other hand, are usually much lower (*e.g.* k_p for Nylon 6,6 = 10^{-3} $\mathrm{L\cdot mol^{-1}\cdot s^{-1}}$).[19] The termination step takes place once the propagating species has reacted with all the monomers and stopped growing (ignoring the occurrence of any early termination due to side reactions), where the radical on the propagating chains is annihilated. The termination of the polymerization can occur in two ways. More commonly, two radicals couple, in which two macromolecules combine and form a high molecular weight species. This mode of termination is called *combination* (**Eq. 1.4**). Termination can also occur *via disproportioniation*, in which a hydrogen atom is transferred

from one radical to the other, resulting in two polymer chains (**Eq. 1.5**). The polymer chains formed consist of one saturated end and an unsaturated end (double bond on chain end).

Combination: $$M_n\cdot + M_m\cdot \xrightarrow{k_{tc}} M_{n+m} \quad \textbf{(1.4)}$$

Disproportionation: $$M_n\cdot + M_m\cdot \xrightarrow{k_{td}} M_{n-1} = M_n + M_{m-1}M \quad \textbf{(1.5)}$$

For purposes of simplification, one can consider the chain lengths of the two resulting polymers the same, in order to avoid distinguishing between two termination reactions. The rate constants of terminations (k_{tc} and k_{td}) can be combined and simplified as follows:

$$k_t = a k_{tc} + (1 - a) k_{td} \quad \textbf{(1.6)}$$

In **Eq. 1.6** fractions of termination by coupling is represented by a, where (1-a) represents the fractions of termination by disproportionation.

Typical k_t values lie in the range of 10^6-10^8 $L\cdot mol^{-1}\cdot s^{-1}$. Although these values are orders of magnitude greater than k_p, propagation is not prevented due to low concentration of the radical species present in low concentrations and the dependency of the polymerization rate on k_t.

1.2.1.2. Rate Expression and Kinetics of Free Radical Polymerisation

Every polymerization can differ in kinetics depending on the components of the system. Important to note is that the fundamental difference comes from the propagation step, where large numbers of monomers are added to the active chain end. The rate of monomer addition (or termination) is directly related to the size of the radical, however this can be neglected as this effect greatly vanishes already at the length of a dimer or trimer.

The monomers present are consumed during both the initiation and the propagation step. Hence, the time dependent decrease of monomer concentration can be defined as the addition of the rate of initiation (R_i) and propagation (R_p) (**Eq. 1.7**). However, the majority of the monomers react during propagation, which allows the rate of initiaton to be neglected by a close approximation. The polymerization rate (monomer consumption) can thus be simplified to the rate of propagation (**Eq. 1.8**).

$$-\frac{d[M]}{dt} = R_i + R_p \quad \textbf{(1.7)}$$

$$-\frac{d[\mathrm{M}]}{dt} = R_p \tag{1.8}$$

With this simplification, we can redefine the rate of polymerization as the sum of many individual propagation steps. Since their rate constants are all equal, the rate of polymerization can be expressed as follows:

$$R_p = k_p[\mathrm{M}\cdot][\mathrm{M}] \tag{1.9}$$

where [M] is the monomer concentration and [M·] is the total concentration of all chain radicals. The radical concentration,however, has proven to be difficult to measure, since they are typically very low (10^{-8} M). **Eq. 1.9** is due to the existence of this term not directly usable and is therefore desirable to be eliminated from the expression. The radical concentration initially increases with the decomposition of the initiator. Once all the radicals are formed, the concentration of the formed radicals during propagation remains unchanged. With this *steady-state* assumption (*Bodenstein* approximation), it is likewise acceptable to state that the rate of initiation R_i and termination R_t remain equal (**Eq. 1.10**).

$$R_i = R_t = 2k_t[\mathrm{M}\cdot]^2 \tag{1.10}$$

The right side of the equation represents the rate of termination, without a specification as to whether termination occurs *via* disproportionation or combination, as both follow the same kinetic expression. The factor two in the rate of termination equation occurs as a result of the disappearance of two radicals at either incident of termination reaction. Rearranging **Eq. 1.10** and substitution into **Eq. 1.9** gives **Eq. 1.12** for the rate of polymerization.

$$[\mathrm{M}\cdot] = \left(\frac{R_i}{2k_t}\right)^{\frac{1}{2}} \tag{1.11}$$

$$R_p = k_p[M]\left(\frac{R_i}{2k_t}\right)^{\frac{1}{2}} \tag{1.12}$$

Thus, **Eq. 1.12** clearly show the dependence of the polymerisation rate on the square root of the initiation rate. The equation shows that doubling the initiation rate, does not double the rate of polymerization, but increases it by a factor of $\sqrt{2}$.

The rate of initiator decomposition into radicals by thermal hydrolysis is given by **Eq. 1.13**, where [I] is the initiator concentration and f is the initiator efficiency. The initiation efficiency

is defined as the fraction of the radicals produced during thermal hydrolysis and is usually less than one, as side reactions take place which leads to wastage of initiator radicals.

As mentioned above, the initiation step consists of two reactions (**Eq. 1.1** and **1.2**). In most polymerizations, the second reaction, in which the addition of the primary radical to monomer takes place, is much faster. Therefore, the homolysis of the initiator is the rate determining step which is given in **Eq. 1.14**. Substituting **Eq. 1.14** into **Eq. 1.12** gives **Eq. 1.15.**

$$R_d = 2fk_d[I] \quad \textbf{1.13}$$

$$R_i = 2fk_d[I] \quad \textbf{1.14}$$

$$R_p = k_p[\mathrm{M}]\left(\frac{fk_d[I]}{k_t}\right)^{\frac{1}{2}} \quad \textbf{1.15}$$

The above equation shows that the polymerization rate is proportional to the square root of the initiator, assuming that f is independent of monomer concentration, which is acceptable for high initiator efficiencies.

Although free radical polymerisation is very well understood and very widely employed in the industry, significant drawbacks such as total regulation over molecular weight, polymer structure and polymer topology needs to be realised. In the following years, more advanced systems/techniques have been developed, which give better control than free radical polymerisation and yet were termed "controlled" radical polymerisation. The most popular and widely used techniques will be introduced in the next section.

1.2.2. Controlled Radical Polymerisation

While commodity polymers are mostly synthesized *via* free radical or anionic polymerisation, several other applications benefit from using more precisely controlled polymers. Control over properties such as molecular weight, polydispersity (PDI), functionality and composition is accessible with "living" polymerization, pioneered by *Szwarc*. Early termination is minimized and molecular weight proceeds linearly with conversion until all monomer is consumed or intentionally terminated. In the 1990s, with the help of newly developed techniques, the characteristics of living polymerization were adapted to radical polymerization systems, referred to as controlled radical polymerization (CRP). CRP can be utilized with a broad range of (vinyl) monomers, solvents, temperatures *etc.* to obtain polymers for a variety of applications. Moreover, CRP allows a new level of materials design and is accessible to all levels of synthetic expertise due to the robustness of the polymerization conditions. The control

over polymerization is maintained with the ability of the system to reversibly terminate, which mediates the radical concentration and reactivity. Controlled radical polymerization has branched mainly into four techniques, namely nitroxide-mediated polymerization (NMP), reversible addition-fragmentation chain transfer (RAFT) polymerization, atom transfer radical polymerization (ATRP) and single electron transfer-living radical polymerization (SET-LRP).

1.2.2.1. Nitroxide Mediated Polymerization

One way to control the polymerization rate is by making use of stable radicals, which are present in the polymerization as *persistent radical* and act as a deactivator. Various stable radicals are used as mediators, such as nitroxides[20], (arylazo)oxy[21], triazolinyl[22], verdazyl[23], substituted triphenyl[24] *etc.* in these systems. The most efficient and well-studied of these stable radicals are nitroxides, which are generated from secondary amines or nitrones. Nitroxide radicals are stable due to steric hindrance and can be stored at room temperature. Hence, polymerization systems, where nitroxides are used, are termed nitroxide mediated polymerization (NMP), which was first discovered by *Solomon* and *Rizzardo* (CSIRO) in 1985 followed by a patent.[25] The two main components of this type of systems are: 1) the initiating radical to initiate the polymerization and 2) the stable nitroxide radical to control the polymerization rate by lowering the propagating radical concentration. This can be achieved by, either introducing a conventional radical initiator (*i.e.* AIBN, BPO) and the nitroxide radical or by directly using an alkoxyamine, which will create these by thermal decomposition. In the following scheme, the decomposition into a reactive radical and the cyclic nitroxide, 2,2,6,6-tetramethyl-1-piperidinoxyl (TEMPO) is shown (**Scheme 4**).

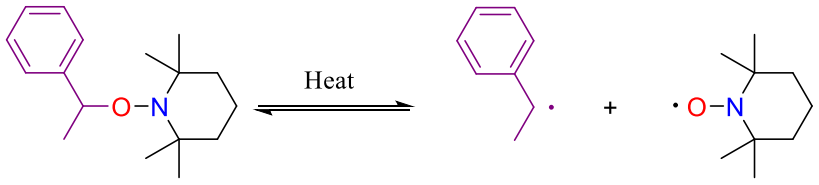

Alkoxyamine (Styryl TEMPO) | Reactive radical | Stable radical (TEMPO)

Scheme 4: The termal decomposition of alkoxyamine into a reactive radical and a stable radical (TEMPO).

Once the radicals are formed (*i.e.* the reaction vessel is heated), the polymerization is initiated, where the radicals are transferred to the monomer. An equilibrium is formed between propagation and reversible termination. The simplified mechanism of NMP is shown below on the polymerization of styrene.

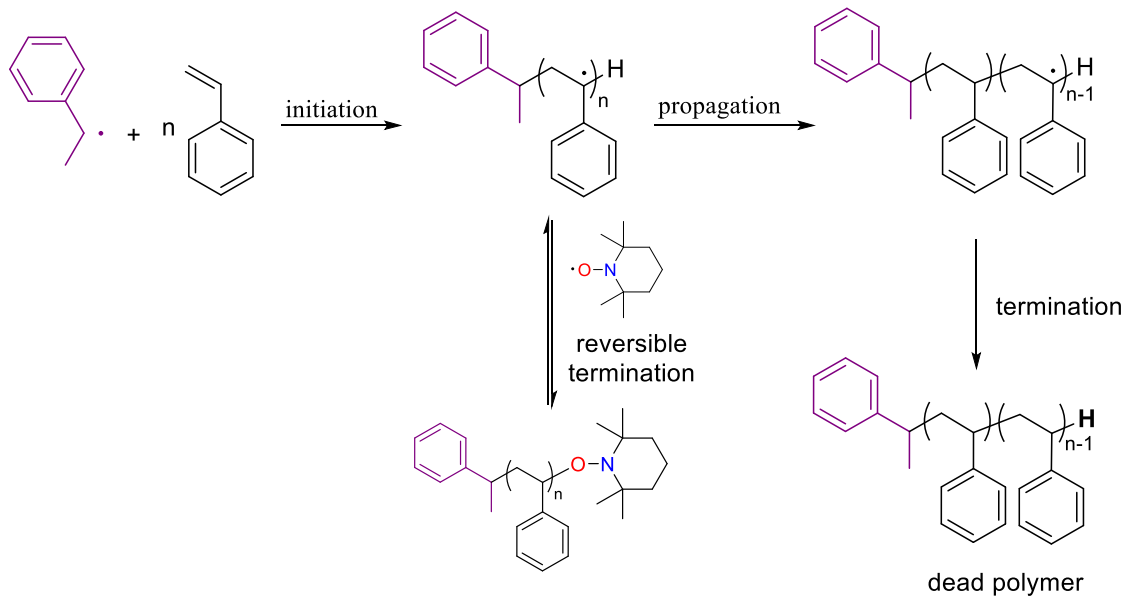

Scheme 5: Simplified mechanism of NMP of styrene.

In the early literature of NMP, Styrene and 4-vinylpyridine are the only examples that polymerize well, when TEMPO is used.[26] However, excessive heat (120-150 °C) and long reaction times (1-3 days) are required for this system. Hawker *et al.* investigated a range of alkoxyamines and developed this system further, in which acrylates, acrylamides and acrylonitrile-based monomers were successfully polymerised with polydispersities as low as 1.06.[27] Moreover, the development of a "universal" initiator allowed the ability to fine tune the composition, target molecular weights, define the end group, polymerise block copolymers and obtain polymers with low dispersities. The efficiency of 2,2,5-Trimethyl-4-phenyl-3-azahexane-3-nitroxide (*i.e.* TIPNO) was attributed to the presence of a hydrogen on the α-carbon and a higher equilibrium constant (K) value between the dormant and active chains compared to TEMPO, given in **Eq. 1.16**.[28]

$$K = \frac{[P\cdot][N\cdot]}{[P-N]} \qquad \textbf{(1.16)}$$

where $[P\cdot]$ is the concentration of actively growing macroradicals, $[N\cdot]$the concentration of the nitroxide radical and $[P-N]$ the concentration of the dormant, nitroxide capped chains K. The control over radical polymerisation is obtained by tuning the K value, which needs to be low, as it retards irreversible termination reactions and allows the chain end to be active for a longer time. The lower stability of the nitroxide capped chains, allow polymerizations at temperatures from 80°C to 100°C.

1.2.2.1.1. Monomer Compatibility

Over the years, a large library of monomers were successfully employed to synthesise polymers of various complex architectures. In general, a strong a relationship was found between the monomer and the nitroxide type employed, which was key to whether the polymerisation would succeed. In the following, a brief overview of the synthesis of polymers will be given grouped under different monomer classes.

As already mentioned, employing acyclic nitroxides provides high polymerization rates for styrene and styrene derivatives (substituted styrene) as in the case of *para*-substituted styrene, which behave similar. Using not so different reaction conditions, linear polymers can easily be obtained. For example, using BPO and TEMPO, Bertin *et al.* obtained diblock copolymers of 4-vinyl benzyl chloride (4-VBC) and styrene.[29] In this case, poly(4-VBC) was used as a macroinitiator, followed by the addition of styrene to the polymerization. Although full conversion was reached, a significant amount of leftover macroinitiator was obtained and the final dispersities were only slightly lower than 1.9. Similarly, Yoshida *et al.* reported the synthesis of diblock copolymers of styrene and benzyl chlorides with 2-, 3- and 4- vinyl groups.[30] The same group later on showed similar approaches to polymerize bromine substituent containing styrenics.[31] Following on these, styrenics with different functionalities such as; *N*-(*p*-vinylbenzyl)phtahalimide-[32], aminomethyl-[33], acetoxy-[34] or sulfonate-[34] bearing monomers were also reported.

In the case of acrylates, TEMPO hinders the synthesis of poly(acrylates) as a strong alkoxyamine C-ON bond is formed, which was demonstrated on *n*-butyl acrylate (*n*-BuA).[35,36] Sterically hindered TEMPO derivatives were shown to be slightly better in terms of control and livingness as this bond was found to be slightly weaker.[37,38] The use of acyclic initiators (SG1[39], TIPNO[27] and TIPNO analogues[40]), however, offered the best results. Cameron *et al.*[41] and Nicolas *et al.*[42] demonstrated this on the polymerization of *n*-BuA to obtain diblock and triblock polymers with styrene, respectively. The conditions were further extended on the copolymerization to other copolymers, including but not limited to 2-hydroxyethyl acrylate[43], 2-(dimethylamino)ethyl acrylate (DMAEA)[44], *t*-butyl acrylate (*t*BA)[45], oligo(ethylene glycol)acrylate (OEGA)[46] and *N*-acryloxysuccinimide (NAS)[47].

When it comes to methacrylates, NMP has proven to be challenging due to the β-hydrogen transfer from the propagating macroradicals to free nitroxide, which leads to formation of dead chains and to loss of control over polymerization.[48,49] This phenomenon was later directly

related to the structure of the nitroxide present. Nevertheless, diblock copolymers were synthesized by employing styrenic macroinitiators to polymerize methacrylics on the second block, such as poly(styrene-*b*-2-(dimethylamino)ethyl methacrylate)[50] or poly(styrene-*b*-*n*-butyl methacrylate)[48].

Similarly, only satisfactory control is achieved over the polymerisation of acrylamides to achieve diblock copolymers by chain extension. Diblock copolymers of *N*-isopropylacrylamide (NIPAM), one of the better known acrylamides, was likewise polymerized by employing a suitable macroinitiator consisting of either poly(*t*-butyl acrylamide) or poly(styrene).[51] Further examples include the polymerisation of *N*,*N*-dimethylacrylamide (DMA) or *N*,*N*-ethylacrylamide, using a poly(4-vinylpyridine) macroinitiator.[52]

In conclusion, it is evident that NMP is strongly monomer dependent. While styrenics work exceptionally well, acrylic monomers were also proven to be readily polymerisable. Their methacrylic counterparts however, suffer from side reactions, which lead to early termination of the polymerization. This problem has been overcome by employing a macroinitiator to polymerise both methacrylates and acrylamides. The polymerisation of branched structures will be discussed later in section 1.2.3.2 in detail.

1.2.2.2. Reversible Addition-Fragmentation Chain Transfer Polymerisation

Unlike in NMP and ATRP (see next section), where the polymerisation is regulated *via* reversible termination, reversible addition-fragmentation chain transfer (RAFT) polymerisation controls chain growth through reversible chain transfer. It was first reported by Chiefari *et al.*, who discovered that dithio-bearing compounds could be employed as efficient chain transfer agents (CTA).[53] The use of a CTA provides rapid exchange between the dormant and the living chains, throughout the polymerisation. The mechanism of the RAFT process is depicted below in **Scheme 6**.[54]

Initiaton

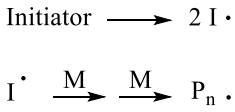

Reversible chain transfer/propagation

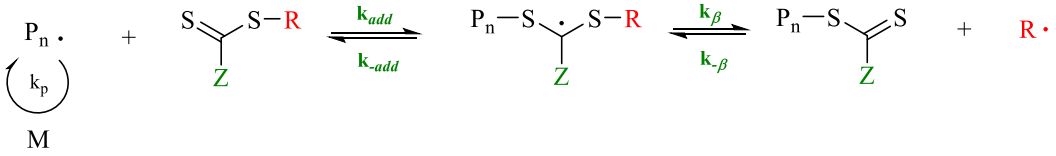

Reinitiaton

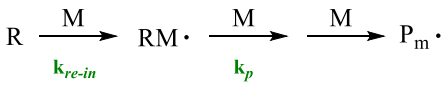

Chain equilibriation/propagation

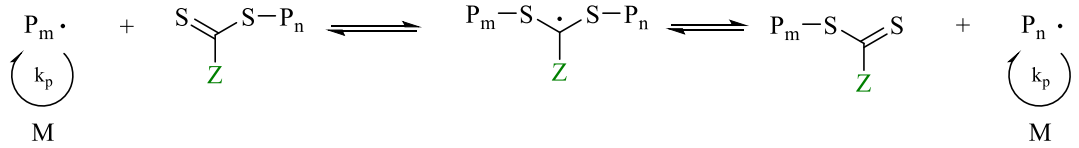

Termination

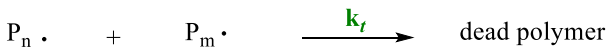

Scheme 6: Mechanism of the RAFT polymerization.

Contrary to NMP, RAFT polymerization allows the polymerisation of almost any monomer, when a suitable RAFT agent is used. Novel monomers with a range of functionalities can be employed to develop new synthetic materials, however the challenge herein lies in finding a suitable RAFT agent and in its usually multistep synthesis as many of them are commercially not available. The structure of the R and Z groups of the CTA are of critical importance. Especially the R group, is important in maintaining the equilibrium. It should be noted that the R group should be a better leaving group than the propagating radical and must efficiently reinitiate monomer.[55] The leaving (and reinitiating) ability of the R group depends on several factors. Steric hindrance, radical stability and polar effects can significantly influence this behaviour. For example, whereas increased radical stability enables the R group to be a good leaving group, a balance between the two needs to be found, as a too stable radical might lead to poorer reinitiation. Similarly, increased steric bulk is likely to increase the leaving ability,

but can impact the reinitiation.[56] One other possibility for the R group is to replace it with the analogue of the monomer, which will give the R group the ability to be structurally, but also electronically similar to the nature of the propagating radical, thus increasing reinitiation efficiency. A strong relation between the polymerization of methyl methacrylate and the nature of the R group was demonstrated by Chong *et al.*[57]

The Z group of the CTA is also highly influential in determining the polymerisation reactivity. Ideally, it should be activating the C=S bond toward radical addition and yield minimal stabilization of the radical formed.[58] If the stabilization is too high, fragmentation will not be preferred, which might lead to loss of control over the polymerization *via* inhibition or retardation of the growing chains.

Styrenics, acrylates, methacrylates, acrylamides, methacrylamides and vinylesters are typical classes of monomers, which are readily available and typically employed in RAFT polymerisation. In the case of styrenics, excellent control over the polymerization is maintained when dithioesters, trithiocarbonates or dithiocarbamates,[56] however the polymerization rates are in general comparably slower than for other monomers. On the other hand for both acrylates and acrylamides, the polymerization leads to very well controlled polymers with high purity and yield. The propagating radicals of these monomers are very reactive with low steric hindrance, which leads to very fast polymerization times. Yet only when trithiocarbonates or dithioesters are employed, the resulting polymers are well defined with PDIs < 1.2, whereas dithiocarbamates and xanthates lead to broader distributions between 1.2 – 2.5.[59,60] Due to sterics, tertiary radical forming monomers (methacrylates and methacrylamides) find it difficult to add to the C=S bond of the CTA. As described above, to increase the ability to add, the Z group needs to be of stabilizing nature. Due to this, dithiobenzoates tend to be the choice of CTA for these monomers, whereas xanthates offer poor control.[61]

The scope of potentials that RAFT offers is surely not limited by the choice of monomers, as the variations in the side chain in different monomer classes is possible. Using different monomers, more complex architectures can be obtained in a sequence defined fashion. Perrier *et al.* have demonstrated this by synthesizing an icosablock polymer with various acrylamides consisting of an average block length of three repeating units, with 94% chain end fidelity (PDI < 1.4).[62] The reaction conditions were later optimized and a decablock homopolymer was obtained, with a much better overall control (PDI = 1.15), whilst retaining the high livingness at 97%.[63] Yet a long polymerization time of 24h per block was required to

reach complete monomer conversion. By modifying the polymerisation conditions further on the homopolymerisation, the reaction times were significantly reduced, where only 2 hours were required per block to reach full conversion.[64] These findings were then extended on the synthesis of a dodecablock copolymer (12 blocks with four different acrylamides) and two high molecular weight pentablock copolymers (5 blocks with 3 different acrylamides) with an average degree of polymerization of 100 per block.

On the other hand, RAFT polymerisation does have drawbacks as well, especially, when employed by the industry. The CTA's bearing dithioester/trithiocarbonate groups usually add a range of colors (red, pink to yellow), which could falsely colorize the material. Furthermore these polymers with a RAFT end group can be unpleasant to handle, due to their odorous nature. On the other hand, most RAFT agents bear UV active groups that allows its detection, analytically.

1.2.2.3. Atom Transfer Radical Polymerization

Transition metal catalysts in atom transfer radical addition between alkyl halides and vinyl groups have been widely investigate.[65,66] Sawamato[67] and Matyjaszewski[68] independently developed this reaction further using Ruthenium and copper halides to obtain well-defined polymers. When copper rather than ruthenium is used, the process is typically termed atom transfer radical polymerisation (ATRP). Radical generation in ATRP involves an organic halide undergoing a reversible redox process catalysed by a transition metal compound such as copper halide. ATRP is dominated by an equilibrium between propagating radicals and dormant species, predominately in the form of initiating alkyl halides/macromolecular species (P_nX).[69] The dormant species periodically react with a rate constant of activation (k_{act}) with transition metal complexes in their lower oxidation state, Mt^m/L, acting as activators (Mt^m represents the transition metal species in oxidation state m and L is a ligand); to intermittently form growing radicals ($P_n\cdot$) and deactivators-transition metal complexes in their higher oxidation state, coordinated with halide ligands X-Mt^m+1 (**Scheme 1.7**) are used. The deactivator reacts with the propagating radical in a reverse reaction (k_{deact}) to regenerate the dormant species and the activator.

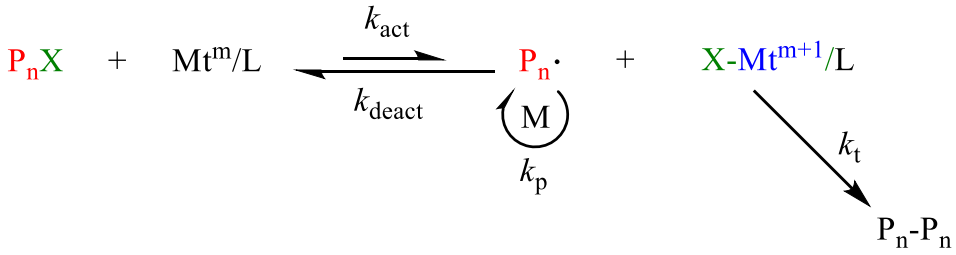

Scheme 7: Equlibrium of atom transfer radical polymerisation (ATRP).

To some extent, irreversible radical termination is always present in all reversible deactivation radical polymerisations (RDRP). In ATRP however, the small amount of bimolecular termination present at the initial stage of the reaction is beneficial for the polymerisation as it provides further control over the polymerisation. The typical deactivation route in ATRP is *via* CuX_2. When radicals terminate, it gives a slight excess of deactivation in the system, which slows down propagation by shifting the equilibrium towards the dormant species. This phenomenon is typically known as the persistent radical effect (PRE).[70,71]

The radical and the deactivating species in ATRP form through the homolytic atom transfer of the halogen radical from the dormant species (P_nX) to the active species (Mt^m/L), which is described to proceed *via* an inner sphere mechanism. Inner Sphere Electron Transfer (ISET) mechanism is more likely to happen in comparison with Outer Sphere Electron Transfer (OSET), as it is energetically favoured.[72]

Next to copper, many other transition metals can be employed in ATRP, in which the polymerisation proceeds with the same mechanism. Other common transition metals used are ruthenium[67,73,74], iron[75,76], nickel[77,78], palladium[79] and molybdenium[80]. The catalyst amount employed can be reduced drastically to ppm levels[81], which improved reaction conditions after the development of activator (re)generated by electron transfer ATRP (ARGET-ATRP)[82] and initiators for continuous activator regeneration ATRP (ICAR-ATRP)[83]. In ARGET-ATRP a small amount of catalyst is continuously regenerated by a reducing agent. Noteworthy reducing agents include FDA-approved tin(II) 2-ethylhexanoate ($Sn(EH)_2$), glucose[82,84], ascorbic acid[85], phenol[86] *etc*. Due to the low levels of catalyst and reducing agents, ARGET-ATRP can be defined as a "green" procedure. On the other hand, for ICAR-ATRP an external source of radical is typically employed (*e.g.* AIBN), to continuously regenerate the CuBr activator, which would otherwise be consumed by termination reactions. Although these systems offer attractive reaction conditions, long reaction times (24 – 48 h) and incomplete conversions (< 80 – 85%) represent some of the limitations.[69,87]

The ATRP rate relies heavily on the propagation rate and on the monomer concentration, as well as the concentration of the dormant species, activator and deactivator which can be described as in **Eq. 1.16**.

$$R_p = k_p[M][P_n^*] = k_p K_{ATRP}\left(\frac{[P_nX][(Cu^I)/L][M]}{[X\text{-}Cu^{II}/L]}\right) \quad \textbf{(1.16)}$$

In general, the ligand structure (L), monomer/dormant species (P_nX) structure as well as reaction conditions can heavily effect the activation or deactivation rate constants and hence K_{ATRP}. Although an increase of catalyst activity usually increases the ATRP rates, the persistent radical effect (see above) will lower the [Cu^I/L] (activator) to [X–Cu^{II}/L] (deactivator) ratio, leading to a decrease in K_{ATRP}.

For polymers prepared *via* ATRP, a relation between the polydispersity (M_w/M_n) and the system components can be drawn. The relationship thereof is described in **Eq. 1.17**.

$$\frac{M_w}{M_n} = 1 + \frac{1}{DP_n} + \left(\frac{k_p[P_nX]}{k_{deact}[X\text{-}(Cu^{II})/L]}\right)\left(\frac{2}{p} - 1\right) \quad \textbf{(1.17)}$$

whereas, p refers to conversion and k_p and k_{deact} describe the rate constants of propagation and deactivation respectively. Using a catalyst, which has an ability to rapidly deactivate the growing chains, the k_p to k_{deact} ratio can be lowered, which would yield lower polydispersities. In addition, reaching higher conversions or targeting higher molecular weights will similarly decrease polydispersity.

On the other hand, it is also important to consider termination reactions that occurs in more or less every controlled radical polymerization technique. It is of high importance to know how many of the growing chains terminate, which cannot be further chain extended or functionalised. This will not only impact the ratio of the components to each other, but the overall success of the polymerization. Therefore, the reaction conditions effecting chain end fidelity must be understood. A relation between rate of termination k_t and the dead chain fraction (DCF), can be described as in **Eq. 1.18**.

$$DCF = \frac{[T]}{[R-X]_0} = \frac{2DP_n k_t[\ln(1-p)^2]}{[M]_0 {k_p}^2 t} \quad \textbf{(1.18)}$$

whereas, concentration of terminated chains is T, initial concentration of initiator is $[R\text{-}X]_0$ and t is reaction time. **Eq. 1.18** indicates that DCF is low for slower rate polymerisations (high t). Likely, low conversion (p), low targeted DP, high monomer concentration and rapidly propagating monomers (lower $k_t/(k_p)^2$ value) will clearly decrease DCF.

From the above, it is evident that after optimisation of reaction conditions, better control over the ATRP of monomers and the structure and properties of the end polymer can be achieved.

1.2.2.4. Single Electron Transfer – Living Radical Polymerization

Single electron transfer – living radical polymerization (SET-LRP) was first introduced by Percec in organic media.[88,89] When carried out in polar media (such as DMSO, alcohols or water), it is possible to obtain "ultrafast" polymers of "ultrahigh" molecular weight at ambient temperature in the presence of an *N*-donor ligand and alkyl halide initiator as in ATRP. Therefore, SET-LRP also relies on an equilibrium between active and dormant species during a polymerization. In the case of SET-LRP however, it is proposed that Cu(0) acts as an electron donor, where the halogen is abstracted from the initiator *via* a heterolytic outher-sphere electron transfer (OSET) mechanism. An illustration of the mechanism is given below in **Scheme 1.8**.

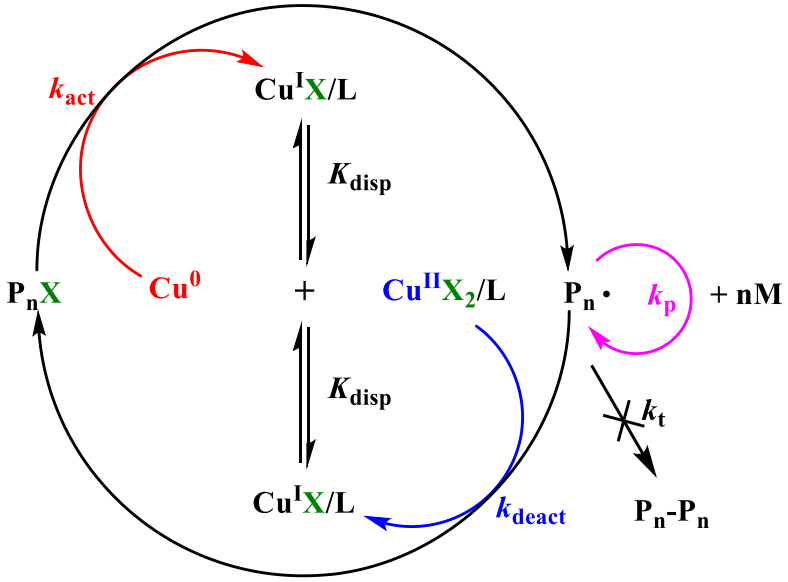

Scheme 1.8: Proposed mechanism of SET-LRP.

The crucial step in SET-LRP is the spontaneous disproportionation of the Cu(I)X species into extremely reactive Cu(0) and Cu(II)X_2 species. It is believed that the Cu(0) formed acts as the activator, whereas the Cu(II)X_2 species reversibly terminates the polymerization. In the presence of a ligand, Cu(I)X is unstable and the equilibrium favours disproportionation.[90]

Whilst the debate about what species really acts as the activator continues, the polymerization systems can be classified into two main categories by solvent, specifically organic- and aqueous SET-LRP.

1.2.2.4.1. Organic SET-LRP

The most common solvent to carry out SET-LRP in is DMSO, which is due to a number of reasons. The polarity of the solvent mainly plays a key role as this favours the proposed electron transfer.[91,92] Furthermore, DMSO has been found to coordinate the Cu(II)X_2 species, which shift the disproportionation equilibrium of Cu(I)X further to the right generating more deactivator.[91] In addition, DMSO has been found to be an appropriate solvent in dissolving a range of monomers, initiators and ligands, which otherwise can be challenging, when the aqueous system is employed. Activated or non-activated Cu(0) wire,[93] powder,[94,95] pellets,[96] plates,[97] colloidal copper[98] and a copper coin[99] have been previously reported as sources of catalyst. Polymerizations are typically initiated with the introduction of the copper source or the initiator.

A noteworthy example is the synthesis of ultrahigh molecular weight polymer of functional monomers, including acrylates, methacrylates and vinyl chloride, reported by Percec *et al.*, proposing that CuBr disproportionates into Cu(0) and Cu(II)Br_2 in the presence of Me_6TREN in DMSO[89], although this contrasts classical ATRP, in which Cu(II)Br_2 is generated in excess *via* bimolecular termination (*i.e.* loss of end group). Irrespective to the mechanism, when SET-LRP conditions are applied, a wide range of monomers can be polymerized using many initiators in organic media.

1.2.2.4.2. Aqueous SET-LRP

The above described "standard" conditions, however turn out to be less ideal, when water is employed as solvent. Although the polymerization of acrylates reaches full conversion with low dispersities, the polymerizations tend to be slow (typically 4-8 h). The control over the polymerization can be further increased by introducing Cu(II)Br_2 externally, which acts as the deactivating agent, yet slows down the polymerization even more. Contrary to acrylates, acrylamides are proven to be even more problematic, when employed for transition metal mediated (TMM) polymerizations.[100] Typically, only low conversions with little control over polymerization (*i.e.* high dispersity) could be reached or high amounts of Cu(II)-salts were required to retain control.[101] This further lead to loss of chain end fidelity, which proved the synthesis of copolymers highly difficult. Due to this, RAFT or NMP have been typically the choice of polymerisation for acrylamides.

In 2013, Haddleton *et al.* have reported a new aq. SET-LRP system, in which CuBr in presence of Me_6TREN is allowed to pre-disproportionate into Cu(0) and Cu(II)Br_2 under inert conditions, prior to the addition of the monomer and initiator.[102] Using this protocol, NIPAM was polymerised at different chain lenghts (DP_n = 8–320) between 30-60 minutes with excellent control over the polymerization (Đ<1.12). The protocol was applied to polymerise other water-soluble monomers, such as DMA, HEAm, OEGA including an acrylamide glycomonomer. However, loss of chain end functionality was observed in reactions at ambient temperature to some extent. This was overcome by carrying out the reaction in an ice bath. Further kinetic investigation of the polymerization of NIPAM by the same group, showed that full conversion was reached already within 11 minutes.[103]

Next to the protocols in DMSO and water, DMF[104], DMAC[105], alcohols[106,107], alcoholic beverages[108], water/alcohol mixtures[109], water/organic solvent mixtures[110], phosphate buffered saline (PBS)[102] and blood serum[111] are other examples, in which SET-LRP can be carried out. Especially solvents of complex media, display the surprising tolerance of this method towards impurities.

1.2.2.4.3. Monomer compatibility

Depending on the medium and technique used, SET-LRP allows a comprehensive range of monomers to be polymerized, such as acrylates[94,109,112-114], acrylamides[108,115,116], methacrylates[89,110,117], methacrylamides[118,119], zwitterionic monomers[120,121], semi-fluorinated monomers[122,123], glycomonomers[124,125], acrylonitrile[126,127], vinyl chloride[128], 2-vinyl pyridine[129] and styrene[130,131]. Furthermore, the polymerization of protected monomers was also reported, which allows in particular post polymerization functionalisation of segments/blocks of a polymeric chain. For example, (co)polymerizations of solketal acrylate (SA)[132], glycidyl acrylate (GA)[124] and trimethylsilyl propargyl acrylate (TMSPA)[124] and the efficient functionalisation thereof was reported by various groups.

1.2.2.4.4. Mechanistic controversy

Unlike other eminent radical polymerisation techniques, the underlying mechanism of SET-LRP is yet to be fully understood. The two proposed models are SET-LRP (Percec *et al.*) and SARA-ATRP (Matyjaszewski *et al.*) (**Scheme 1.9**).[87,90,133-139]

Both models are based on identical components to explain the rapid polymerization in polar media (*e.g.* DMSO) catalysed by copper in the presence of an *N*-donor ligand (*e.g.* Me_6TREN) that can complex Cu-species, yet strongly disagree on the mechanism. The models both agree

that Cu(II)Br_2 acts as the main deactivator and that the deactivation by CuBr is negligibly small, but differ mainly in the activation of the polymerization. In the following, the "war" between the two models will be explained briefly, with reference to each group's findings.

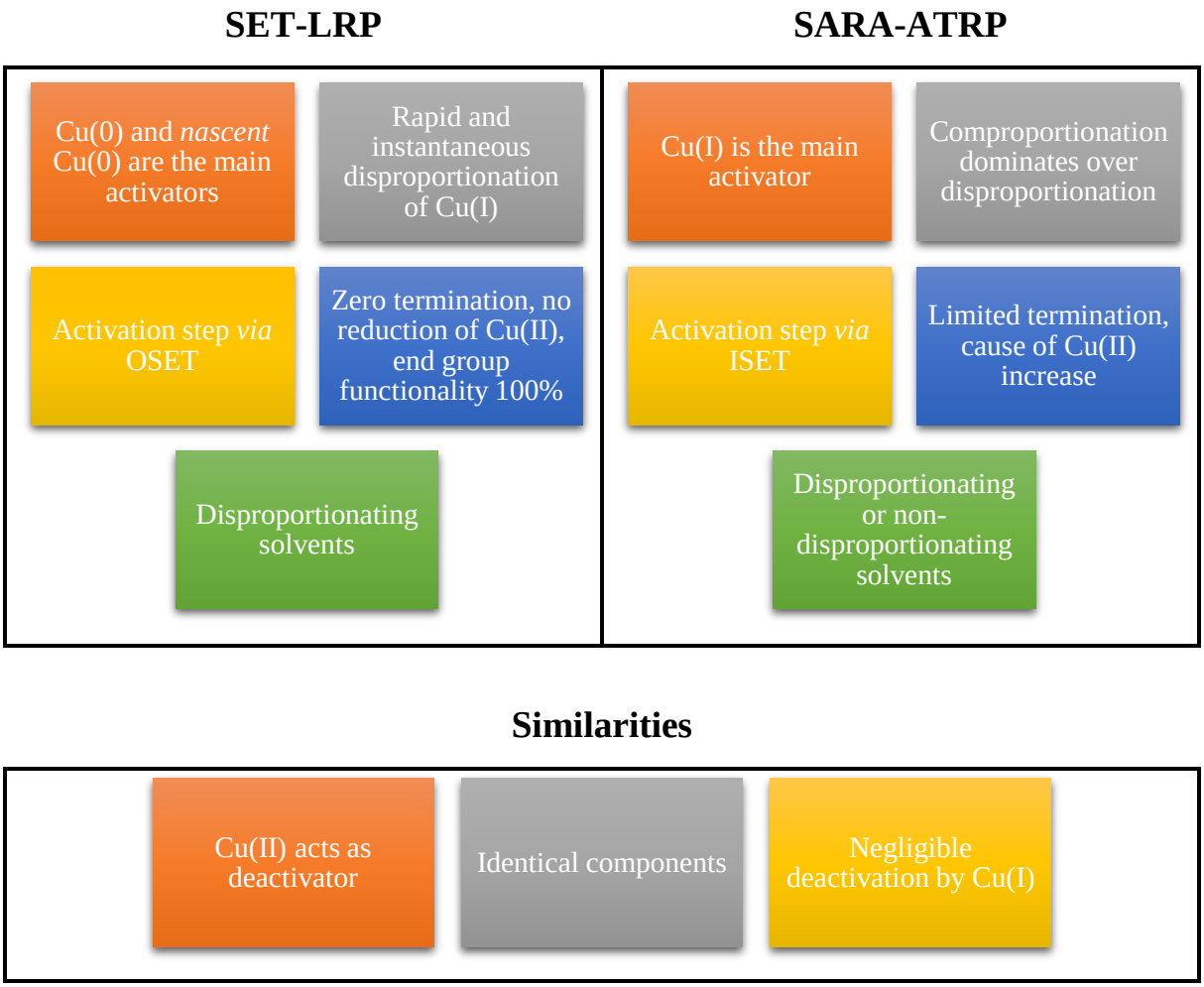

Scheme 1.9: Comparison of SET-LRP and SARA-ATRP.

As proposed by Percec, it is suggested that Cu(0)[89] or *nascent* Cu(0) particles[140,141] act as the main activator of the initiator, whereas no activation occurs by CuBr, as CuBr undergoes rapid disproportionation.[142] Furthermore, it is believed that the activation occurs *via* an Outer Sphere Electron Transfer (OSET) mechanism.[143] This has been reported with the experimental demonstration on the polymerization of methyl acrylate in DMSO, in which Cu(0)-wire was lifted from the polymerization mixture.[98] During the absence of the wire, the rate in conversion compared to the presence of the wire has been calculated to be 8 times slower. This suggested that a distinction between soluble CuBr and colloidal Cu(0) nanoparticles is necessary. Interestingly, when the wire was lifted at different conversions or the surface area of the wire was increased, the polymerizations proceeded at almost identical rates. The authors then

concluded that CuBr couldn't be the activator, as the change in the surface area of the copper was not reflected in the CuBr concentration. To investigate further, the polymerization mixture in an L-shaped Schlenk tube, was carefully decanted from one sided to the other, leaving the copper wire and colloidal Cu(0) particles in the original position, which lead the polymerization to a complete stop, even in the presence of soluble CuBr. In a following report, the accumulation of $CuBr_2$ was monitored *via* UV/vis spectroscopy, concluding that no reduction of $CuBr_2$ was present.[144] In addition, the conversion and chain end fidelity was carefully monitored *via* ^{1}H NMR spectroscopy, which showed 100% end group functionality. This suggested that, unlike bimolecular termination in ATRP, that PRE was indeed not the cause for the increase in the $CuBr_2$ concentration. Thus this increase must be due to disproportionation of CuBr. The disproportionation was further investigated in protic, dipolar aprotic and non-polar solvents.[142,145] It was found that the disproportionation in DMSO was maximum when 0.5 equivalents of Me_6TREN for 1 equivalnt of CuBr was employed. When solvents such as MeCN or toluene were used, two linear first-order kinetics were observed[146], while end group fidelity was poor with increasing conversion, implying that solvents that promote disproportionation are required for a good control over the polymerization.[147] This was later supported, when Haddleton and co-workers introduced the aqueous SET-LRP method described above, in which they observed the formation of Cu(0) nanoparticles.[102] These results, however, are only indicative to the role of Cu(0) and not direct proof.

Contrary to these, Matyjaszewski reports that CuBr is the main activator, whereas Cu(0) only acts as a supplemental activator and reducing agent (SARA) of the initiator.[148] The activity of CuBr and Cu(0) was compared and it was found that in order to achieve the same activity of 1 mM CuBr/Me_6TREN in DMSO, a Cu(0)-wire at a diameter of 0.25 mm would need to be at a length of 2000 m or greater.[149] Furthermore, Matyjaszewski's interpretation of Percec's lifting and decanting experiments, indicates that only 1% of the total surface area is actually in solution and thus only make a minimal contribution. In addition, the better control in DMSO over MeCN is simply attributed to the higher K_{ATRP} in DMSO.[72,150] Under typical ATRP conditions, comproportionation dominates over disproportionation and hence CuBr acts as the main activator. Matyjaszewski also reported that, as the activation by Cu(I) *via* ISET is about 10^{10} times faster than OSET, Percec's assumption of an OSET is wrong.[72] Finally, termination events will always occur, especially in faster systems at higher monomer conversions due to the loss of chain end functionality, increasing the concentration of $CuBr_2$. [151]

In conclusion, it is evident that the mechanism itself cannot be studied by separating different aspects into a series of multiple reactions and should be considered as one big picture. Although it is apparent, that there is more evidence for a SARA-ATRP taking place for the reactions in DMSO, more work needs to be carried out to understand the mechanism. On the other hand, the underlying mechanism in aqueous medium is yet to be fully investigated, as mechanistic studies to present are preliminary and limited. Nevertheless, the literature is full with elegant examples of novel polymers synthesised by reaction conditions, which are well exploited, proving SET-LRP to be a versatile tool to obtain well-controlled polymers with different architectures.

1.3 Control of Polymerization Towards Macromolecular Design

The most common ionic and radical polymerization techniques to obtain linear polymers are discussed above. In this section, synthesis techniques of higher order structures will be given, with a focus on their synthesis *via* SET-LRP.

Higher order structures consist of polymers with at least one branching point. Commonly, these type of polymers are classed under star polymers, comb/brush polymers, graft polymers and polymer networks, which are depicted in **Scheme 1.10.**

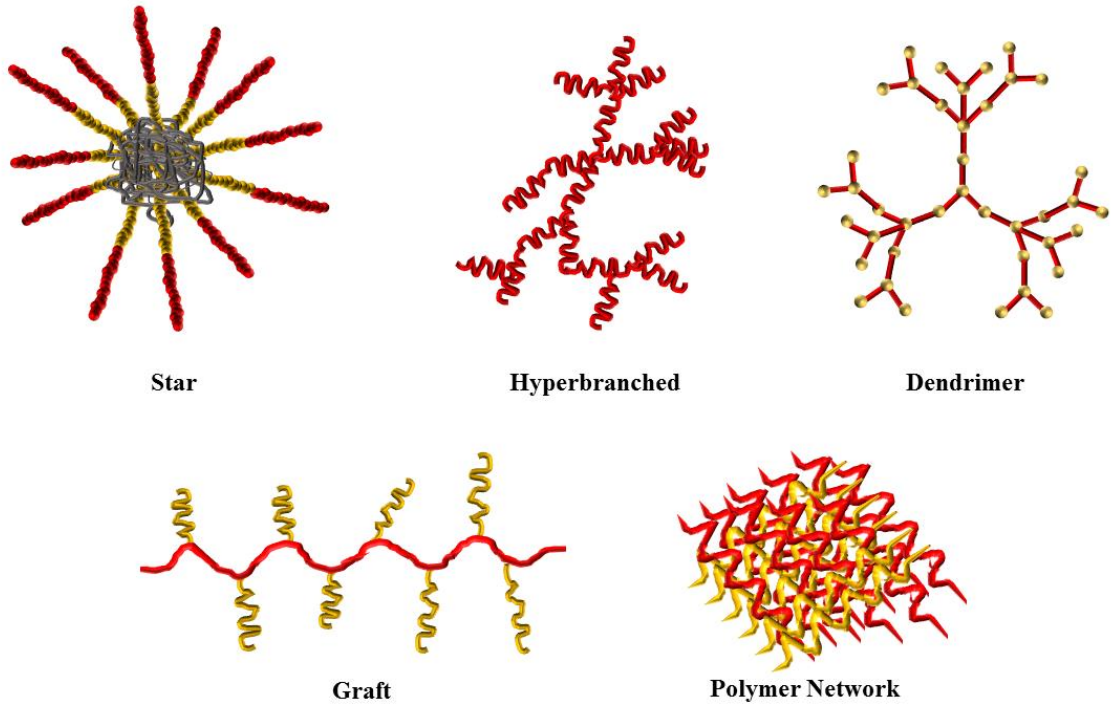

Scheme 1.10: Some examples of higher order polymeric structures that can be manufactured.

Hyperbranched polymers and dendrimers have been comprehensively reviewed in the past, while polymeric networks are mainly formed by excess crosslinking of other polymeric structures.[152-155] For the purpose of this report, only graft polymers and star polymers will be introduced in the next section.

1.3.1 Graft, Comb and Brush Polymers

Graft, comb and brush polymers belong to the same family of branched polymers. They mainly consist of a linear backbone, with polymeric side chains and differ in the chemical nature of the side chains. While comb polymers consist of the same side chain as the backbone, graft or brush polymers can have side chains of a different polymers. Graft and brush-like furthermore differ in the density of the side chains along the backbone. Comb and graft polymers are generally considered to have a low density of grafting, whereas the density of brush polymers is significantly higher. These polymers offer the possibility to tune both the length and the chemical nature of the backbone as well as the sidechains to increase the functionality of the polymer. In particular the possibility of using these polymers as amphiphiles has attracted considerable interest of researchers.[156,157]

1.3.1.1 Synthetic Routes

Graft polymers are usually obtained in at least two steps *via* "grafting through", "grafting onto" or "grafting from" approach.

Schulz and Milkovich reported the first example of the "grafting through" approach in 1982.[158] This approach, typically involves the polymerization of a macromonomer. The principal advantage of this method is that various type of functional macromonomers such as drug conjugated macromonomers or even macromonomers carrying targeting moieties can be attached to the backbone *via* homo- or copolymerisation. Although this approach allows the synthesis of fully grafted polymers, it usually requires an additional purification step as the polymerization of the macromonomers generally don't reach full conversion.

The "grafting onto" method obtains polymers, in which a predefined polymeric side chain is attached to backbone *via* coupling reactions. As the targeted density of grafting is high, an efficient coupling reaction is necessary. Typically, a large excess of sidechains to backbone is introduced, which requires additional steps of purification. With the introduction of "click" chemistry however, this drawback of sterics has been largely overcome.

Finally, the "grafting from" approach, involves the formation of side chains directly on the backbone. This can be achieved by introducing initiating sites to the pre-obtained backbone that could serve as a macroinitiator for further polymerisations. With effective reactions and polymerisation techniques, this approach tends to be the most efficient in obtaining the desired structure with the minimum number of steps (*i.e.* reaching full monomer conversion).

Although SET-LRP remains to be a rapidly expanding field, the above mentioned methods have already been employed to obtain polymers of different structures and functionalities, however mostly in combination with other polymerization techniques. For example, Huang *et al.* reported the synthesis of an amphiphilic graft copolymer *via* the grafting from approach.[159] For this, a hydroxyl functional monomer was first polymerized *via* living coordination polymerization, which was subsequently functionalised into a SET-LRP initiator, to polymerize 2-(Dimethylamino)ethyl acrylate (DMAEA). The obtained polymers were assessed for their ability to form micelles in aqueous solutions, which was characterised by the determination of the critical micelle concentration (*cmc*) *via* fluorescence spectroscopy. The same group later reported the polymerization of a hydrophilic graft copolymer, consisting of a PHEA backbone with PDMAEA side chains using a combination of RAFT and SET-LRP *via* the grafting from strategy.[160] First, a trifunctional acrylic monomer was polymerised *via* RAFT to give a well-defined PHEA based homopolymer bearing a Cl-containing SET-LRP initiating backbone. The obtained macroinitiator was next employed to polymerise DMAEA *via* SET-LRP.

Davis *et al.* applied SET-LRP for the first time in a grafting from approach with iron oxide nano particles (IONPs), which are used as MRI contrast agents.[161] In their report, IONPs were first functionalised into a SET-LRP initiator, which was used to polymerize OEGA as an antifouling layer. It was found that these particles had higher stability in serum. Similarly, a grafting to approach was attempted, yet the grafting density was found to be not as high as in their previous methodology.

Recently, Haddleton *et al.* reported the synthesis of comb polymers *via* the grafting through method using aqueous SET-LRP, consisting of polymeric EtOx based sidechains with dispersities below 1.23.[162] Interestingly, quantitative conversions were reached for all polymers despite the length of the sidechain. These polymers were subsequently conjugated to peptides, showing the versatility of this approach, when SET-LRP is employed.

In conclusion, it is evident that organic SET-LRP can be employed to obtain grafted polymers, yet the potential of aqueous SET-LRP in the other methodologies are yet to be investigated. All three techniques have advantages over the other, however the selection of the right method and polymerization technique is largely dependent on the structure of the graft polymer that is expected.

1.3.2 Star Polymers

Star polymers can be achieved *via* three methodologies, namely "arm first", "core first" and "coupling onto", which are similar to the above described for the synthesis of graft polymers.

The arm first method requires the pre polymerization of linear polymers, that can be linked to a central core in the next step. Typically, a difunctional crosslinker is employed (*e.g. bis*acrylate), that makes use of the livingness of polymer over the chain end fidelity. When this method is employed, high number of arms per star polymer can be achieved if required. The crosslinking however can be inefficient and might require purification steps which can be time consuming.

Similarly, the coupling onto method also requires the prior synthesis of the arms. These arms are then conjugated to a central core directly using a multifunctional molecule, without using a crosslinker. This methodology yields polymers, where the number of arms per star could be tuned by using the appropriate conjugation. Yet in both methods, extra purification is required as 100% chain end fidelity can't be retained at full conversion or as an excess amount of arms per multifunctional core require to be used.

The most promising method to obtain star polymers is the core first method if high number of arms are not targeted. For this, a multifunctional core is used to grow the polymers on the "arms".

Monteiro *et al.* reported the block copolymerization of a 4-arm star polymer consisting of MA and SA *via* the core first method in organic SET-LRP. Subsequent deprotection of SA produced amphiphilic star polymers that self-assembled in water.[132] Moreover, Whittaker *et al.* reported the synthesis of a multiblock star copolymer, initiated by a 5-arm glucose initiator, resulting in low dispersities and full conversions throughout the polymerization (24 h per block).[163] Similarly, Haddleton *et al.* employed an octa-functional star initiator based on lactose, to polymerize lipophilic monomers with excellent control over PDI, without any significant star-

star coupling when the polymerizations were carried out in a solvent that promoted phase separation throughout the polymerization.[164]

In a different approach, Qiao *et al.* investigated the preparation of core-crosslinked star polymer formation of linear arms in a one-pot methodology, where MA was polymerised into a linear arm and subsequently crosslinked with a diacrylate *via* organic SET-LRP.[165] In a subsequent report, the method was translated to the aqueous SET-LRP system, in which NIPAM or HEA was polymerised and in the next step crosslinked with *N,N'*-Methylene bisacrylamide.[166]

The synthesis of a core-first star polymer in aqueous SET-LRP is demonstrated for the first time in this report and will be described in the following chapter.

1.4 Glycopolymers

Macromolecules which bear sugar moieties are considered as alternative structures to oligosaccharides.[167] Considerable interest has been directed to the synthesis of glycopolymers in the recent years as synthetic ligands that function in a multivalent binding process with human proteins. The weak interactions between proteins and ligands can be dramatically enhanced by the multivalent effect of densely packed carbohydrate molecules ("cluster glycoside effect").[168] This high affinity of carbohydrate ligands with lectins are observed to be mainly due to hydrogen bonding and *van der Waal's* interactions.[169,170] However, over the years of research in glycopolymer synthesis, it is becoming more and more evident that the glycopolymer molecular weight, glycopolymer topology, positioning of the sugar, distance of the sugar from the backbone and the distance to the neighbouring sugars all have influence in binding to lectins. For example, Kiesling *et al.* reported that the affinity of mannose bearing glycopolymers to ConA increased with increasing molecular weight.[171] Similarly, Miura *et al.* showed a similar trend for the binding of lactose glycopolymers to RCA120, which was attributed to the number of carbohydrate units present.[172]

One other way to modify the binding to lectin can also be regulated by introducing structural control over the glycopolymer.[125] For example, Becer *et al.* synthesised a series of mannose bearing glycopolymers with structural differences and investigated the interaction between the glycopolymers and DC-SIGN using surface plasmon resonance (SPR). It was shown that the more abundant mannose compared to its commoners is, the higher will be the binding. Furthermore, incorporation of fucose enhanced the binding affinity, while a similar effect was not evident for glucose.

Recently Hartmann *et al.* reported the synthesis of monodisperse glycopolymer segments for the first time.[173] Herein, a backbone was synthesised on solid phase, with clickable alkyne moieties. Then, mannose sugars were introduced to the solid phase *via* "click" chemistry. The obtained mono-, di- and trivalent structures were then subjected to binding studies with ConA, which were investigated using SPR. It was found that the binding increased with number of mannose units present on the sequence defined backbone, but decreased with increasing spacing between the mannose units. It is suggested that the spacing between the sugar units should be close to the distance between two binding sites of ConA.

In addition, the role of the distance of the sugar from the backbone was also investigated. By employing the exact same backbone, the distance of the sugar was varied by introducing allylamine as an orthogonal handle and 2-hydroxypropylamine to yield a water soluble backbone. Tandem postpolymerization was then utilised to obtain glycopolymers with precise chain length, carbohydrate density and a well-defined backbone. As expected, the polymer, which had the sugar further away from the polymer, was found to increase inhibition due to increased ability of the carbohydrate monomer to move, indicating that the longer the side-chain spacer is, the more effective the inhibition will be.[174]

Next to linear polymers, Becer *et al.* also reported the synthesis of star shaped *β*-CD based glycopolymers *via* SET-LRP. These polymers exhibited strong binding to DC-SIGN according to SPR measurements. The polymers were further tested for delivery of an anti-HIV drug and found that polymers with a hydrophobic core, exhibit high loading capacity, indicating promising applications in HIV-therapeutic and drug delivery.[175]

1.5. Aims and Objectives

The primary aim of this work is the synthesis of functional polymers with branched structures *via* Cu-mediated radical polymerisation and the synthesis of novel glycosylated polymers.

Control of polymer structure are becoming increasingly important. These materials can be used in a variety of applications as mentioned above, which require tailored properties and architecture. SET-LRP allows the rapid synthesis of well-defined multiblock linear polymers with excellent control over the polymerisation It has been shown that the synthesis can be carried out within minutes under mild reaction conditions. There is, however, a lack of investigation and understanding for how these systems work, when multiarm initiators are employed (*i.e.* initiators with multiple initiating sites).

In the following work, the synthesis of star shaped polymers *via* the core first approach was investigated for aqueous SET-LRP conditions. Initially, a three arm initiator was employed to polymerise *N*-Isopropylacrylamide (NIPAM), while optimising the reaction conditions with increasing chain length. The obtained polymers displayed thermoresponsive behaviour once heated, which were further characterised for their cloud points *via* turbidimetry. The optimisation of reaction conditions allowed for further chain extension with other acrylamide based monomers, to finally obtain a three-arm multiblock star shaped polymer.

Furthermore, a new catalyst system for the synthesis of star shaped polymers investigated, in which a British 1 penny coin was used as the copper source. Four-arm star shaped polymers from acrylate based monomers were obtained to investigate influence of the copper source on polymerisations. In order to gain a better understanding of the polymerisation behaviour with increasing conversion, samples were taken periodically and analysed *via* gas chromatography (GC) and size exclusion chromatography (SEC).

In an attempt to investigate the limitations of initiators, a poly(2-ethyl oxazoline) (PEtOx) based multiarm initiator was synthesised. For this purpose, PEtOx consisting of *ca.* 100 repeating units, was partially hydrolysed to poly(ethylene imine) (PEI) to yield PEtOx-*r*-PEI, which was transformed to a SET-LRP initiator. Previously described reaction conditions were applied to obtain homopolymers and copolymers of NIPAM and *N*-Hydroxyethyl acrylamide.

Finally to increase functionality, the synthesis and polymerisation of monomers with various sugar densities were investigated. The number of sugars attached on a monomer can allow the tuning of the sugar density along the polymer chain, without altering the total chain length. For this purpose, *N*-[Tris(hydroxymethyl)methyl]acrylamide was used as the precursor and the synthesis and polymerisation of the glycomonomers were characterised *via* nuclear magnetic resonance (NMR), GC and SEC.

1.6. References

1. M. Szwarc, M. Levy and R. Milkovich, *J. Am. Chem. Soc.*, 1956, **78**, 2656-2657.
2. M. Szwarc, *J. Polym. Sci. Part A: Polym. Chem.*, 1998, **36**, IX-XV.
3. D. A. Tomalia and D. P. Sheetz, *J. Polym. Sci. Part A: Polym. Chem.*, 1966, **4**, 2253-2265.
4. T. G. Bassiri, A. Levy and M. Litt, *J. Polym. Sci. Part B: Polym. Lett.*, 1967, **5**, 871-879.
5. W. Seeliger, E. Aufderhaar, W. Diepers, R. Feinauer, R. Nehring, W. Thier and H. Hellmann, *Angew. Chem. Int. Ed*, 1966, **5**, 875-888.
6. R. Hoogenboom and H. Schlaad, *Polym. Chem.*, 2017, **8**, 24-40.
7. R. Hoogenboom, *Angew. Chem. Int. Ed.*, 2009, **48**, 7978-7994.
8. B. Verbraeken, B. D. Monnery, K. Lava and R. Hoogenboom, *European Polymer Journal*, 2017, **88**, 451-469.
9. B. Verbraeken and R. Hoogenboom, *Angew. Chem. Int. Ed.*, 2017, **56**, 7034-7036.
10. F. Wiesbrock, R. Hoogenboom, C. H. Abeln and U. S. Schubert, *Macromol. Rapid Commun.*, 2004, **25**, 1895-1899.
11. F. Wiesbrock, R. Hoogenboom, M. A. M. Leenen, M. A. R. Meier and U. S. Schubert, *Macromolecules*, 2005, **38**, 5025-5034.
12. F. Wiesbrock, R. Hoogenboom, M. Leenen, S. F. G. M. van Nispen, M. van der Loop, C. H. Abeln, A. M. J. van den Berg and U. S. Schubert, *Macromolecules*, 2005, **38**, 7957-7966.
13. R. Hoogenboom, F. Wiesbrock, H. Huang, M. A. M. Leenen, H. M. L. Thijs, S. F. G. M. van Nispen, M. van der Loop, C.-A. Fustin, A. M. Jonas, J.-F. Gohy and U. S. Schubert, *Macromolecules*, 2006, **39**, 4719-4725.
14. L. Tauhardt, K. Kempe, K. Knop, E. Altuntaş, M. Jäger, S. Schubert, D. Fischer and U. S. Schubert, *Macromol. Chem. Phys.*, 2011, **212**, 1918-1924.
15. V. R. de la Rosa, E. Bauwens, B. D. Monnery, B. G. De Geest and R. Hoogenboom, *Polym. Chem.*, 2014, **5**, 4957-4964.
16. M. Mees, E. Haladjova, D. Momekova, G. Momekov, P. S. Shestakova, C. B. Tsvetanov, R. Hoogenboom and S. Rangelov, *Biomacromolecules*, 2016, **17**, 3580-3590.
17. M. A. Mees, C. Effenberg, D. Appelhans and R. Hoogenboom, *Biomacromolecules*, 2016, **17**, 4027-4036.
18. P. J. Flory, *J. Am. Chem. Soc.*, 1937, **59**, 241-253.
19. G. Odian, in *Principles of Polymerization, Fourth Edition*, John Wiley & Sons, 2004.
20. R. D. Puts and D. Y. Sogah, *Macromolecules*, 1996, **29**, 3323-3325.
21. J. D. Druliner, *Macromolecules*, 1991, **24**, 6079-6082.
22. M. Steenbock, M. Klapper and K. Müllen, *Macromol. Chem. Phys.*, 1998, **199**, 763-769.
23. S. J. Teertstra, E. Chen, D. Chan-Seng, P. O. Otieno, R. G. Hicks and M. K. Georges, *Macromolecular Symposia*, 2007, **248**, 117-125.
24. E. De León-Sáenz, G. Morales, R. Guerrero-Santos and Y. Gnanou, *Macromol. Chem. Phys.*, 2000, **201**, 74-83.
25. D. H. Solomon, E. Rizzardo and P. Cacioli, *Journal*, 1986.
26. M. K. Georges, R. P. N. Veregin, P. M. Kazmaier and G. K. Hamer, *Macromolecules*, 1993, **26**, 2987-2988.
27. D. Benoit, V. Chaplinski, R. Braslau and C. J. Hawker, *J. Am. Chem. Soc.*, 1999, **121**, 3904-3920.

28. T. Fukuda, T. Terauchi, A. Goto, K. Ohno, Y. Tsujii, T. Miyamoto, S. Kobatake and B. Yamada, *Macromolecules*, 1996, **29**, 6393-6398.
29. D. Bertin and B. Boutevin, *Polym. Bull.*, 1996, **37**, 337-344.
30. E. Yoshida and T. Fujii, *J. Polym. Sci. Part A: Polym. Chem.*, 1997, **35**, 2371-2378.
31. E. Yoshida, *J. Polym. Sci. Part A: Polym. Chem.*, 1996, **34**, 2937-2943.
32. M. Mariani, M. Lelli, K. Sparnacci and M. Laus, *J. Polym. Sci. Part A: Polym. Chem.*, 1999, **37**, 1237-1244.
33. K. Ohno, Y. Izu, Y. Tsujii, T. Fukuda and H. Kitano, *European Polymer Journal*, 2004, **40**, 81-88.
34. K.-i. Fukukawa, L. Zhu, P. Gopalan, M. Ueda and S. Yang, *Macromolecules*, 2005, **38**, 263-270.
35. A. Debuigne, T. Radhakrishnan and M. K. Georges, *Macromolecules*, 2006, **39**, 5359-5363.
36. M. K. Georges, J. L. Lukkarila and A. R. Szkurhan, *Macromolecules*, 2004, **37**, 1297-1303.
37. C. A. Knoop and A. Studer, *J. Am. Chem. Soc.*, 2003, **125**, 16327-16333.
38. K. O. Siegenthaler and A. Studer, *Macromolecules*, 2006, **39**, 1347-1352.
39. C. Farcet, J. Nicolas and B. Charleux, *J. Polym. Sci. Part A: Polym. Chem.*, 2002, **40**, 4410-4420.
40. L. Marx and P. Hemery, *Polymer*, 2009, **50**, 2752-2761.
41. N. R. Cameron and A. J. Reid, *Macromolecules*, 2002, **35**, 9890-9895.
42. J. Nicolas, B. Charleux, O. Guerret and S. Magnet, *Angew. Chem. Int. Ed.*, 2004, **43**, 6186-6189.
43. K. Bian and M. F. Cunningham, *Macromolecules*, 2005, **38**, 695-701.
44. K. Bian and M. F. Cunningham, *J. Polym. Sci. Part A: Polym. Chem.*, 2006, **44**, 414-426.
45. K.-H. Kuo, W.-Y. Chiu and K.-C. Cheng, *Polym. Int.*, 2008, **57**, 730-737.
46. B. Lessard and M. Marić, *Macromolecules*, 2008, **41**, 7870-7880.
47. N. Handké, T. Trimaille, E. Luciani, M. Rollet, T. Delair, B. Verrier, D. Bertin and D. Gigmes, *J. Polym. Sci. Part A: Polym. Chem.*, 2011, **49**, 1341-1350.
48. C. Burguière, M.-A. Dourges, B. Charleux and J.-P. Vairon, *Macromolecules*, 1999, **32**, 3883-3890.
49. M. Souaille and H. Fischer, *Macromolecules*, 2001, **34**, 2830-2838.
50. J. Lokaj, P. Vlček and J. Kříž, *Macromolecules*, 1997, **30**, 7644-7646.
51. O. Gibbons, W. M. Carroll, F. Aldabbagh and B. Yamada, *J. Polym. Sci. Part A: Polym. Chem.*, 2006, **44**, 6410-6418.
52. A. Fischer, A. Brembilla and P. Lochon, *European Polymer Journal*, 2001, **37**, 33-37.
53. J. Chiefari, Y. K. Chong, F. Ercole, J. Krstina, J. Jeffery, T. P. T. Le, R. T. A. Mayadunne, G. F. Meijs, C. L. Moad, G. Moad, E. Rizzardo and S. H. Thang, *Macromolecules*, 1998, **31**, 5559-5562.
54. G. Moad, E. Rizzardo and S. H. Thang, *Aust. J. Chem.*, 2012, **65**, 985-1076.
55. C. Boyer, V. Bulmus, T. P. Davis, V. Ladmiral, J. Liu and S. Perrier, *Chem. Rev.*, 2009, **109**, 5402-5436.
56. G. Moad, J. Chiefari, Y. K. Chong, J. Krstina, R. T. A. Mayadunne, A. Postma, E. Rizzardo and S. H. Thang, *Polym. Int.*, 2000, **49**, 993-1001.
57. Y. K. Chong, J. Krstina, T. P. T. Le, G. Moad, A. Postma, E. Rizzardo and S. H. Thang, *Macromolecules*, 2003, **36**, 2256-2272.
58. J. Chiefari, R. T. A. Mayadunne, C. L. Moad, G. Moad, E. Rizzardo, A. Postma and S. H. Thang, *Macromolecules*, 2003, **36**, 2273-2283.

59. C. Barner-Kowollik, M. Buback, B. Charleux, M. L. Coote, M. Drache, T. Fukuda, A. Goto, B. Klumperman, A. B. Lowe, J. B. McLeary, G. Moad, M. J. Monteiro, R. D. Sanderson, M. P. Tonge and P. Vana, *J. Polym. Sci. Part A: Polym. Chem.*, 2006, **44**, 5809-5831.
60. S. Perrier, C. Barner-Kowollik, J. F. Quinn, P. Vana and T. P. Davis, *Macromolecules*, 2002, **35**, 8300-8306.
61. E. Rizzardo, J. Chiefari, R. T. A. Mayadunne, G. Moad and S. H. Thang, in *Controlled/Living Radical Polymerization*, 2000, vol. 768, pp. 278-296.
62. G. Gody, T. Maschmeyer, P. B. Zetterlund and S. Perrier, 2013, **4**, 2505.
63. G. Gody, T. Maschmeyer, P. B. Zetterlund and S. Perrier, *Macromolecules*, 2014, **47**, 639-649.
64. G. Gody, T. Maschmeyer, P. B. Zetterlund and S. Perrier, *Macromolecules*, 2014, **47**, 3451-3460.
65. F. Minisci, *Acc. Chem. Res.*, 1975, **8**, 165-171.
66. J. Iqbal, B. Bhatia and N. K. Nayyar, *Chem. Rev.*, 1994, **94**, 519-564.
67. M. Kato, M. Kamigaito, M. Sawamoto and T. Higashimura, *Macromolecules*, 1995, **28**, 1721-1723.
68. J.-S. Wang and K. Matyjaszewski, *J. Am. Chem. Soc.*, 1995, **117**, 5614-5615.
69. K. Matyjaszewski, *Macromolecules*, 2012, **45**, 4015-4039.
70. H. Fischer, *Macromolecules*, 1997, **30**, 5666-5672.
71. H. Fischer, *Chem. Rev.*, 2001, **101**, 3581-3610.
72. C. Y. Lin, M. L. Coote, A. Gennaro and K. Matyjaszewski, *J. Am. Chem. Soc.*, 2008, **130**, 12762-12774.
73. V. Percec, B. Barboiu, A. Neumann, J. C. Ronda and M. Zhao, *Macromolecules*, 1996, **29**, 3665-3668.
74. H. Takahashi, T. Ando, M. Kamigaito and M. Sawamoto, *Macromolecules*, 1999, **32**, 6461-6465.
75. T. Ando, M. Kamigaito and M. Sawamoto, *Macromolecules*, 1997, **30**, 4507-4510.
76. K. Matyjaszewski, M. Wei, J. Xia and N. E. McDermott, *Macromolecules*, 1997, **30**, 8161-8164.
77. H. Uegaki, Y. Kotani, M. Kamigaito and M. Sawamoto, *Macromolecules*, 1997, **30**, 2249-2253.
78. H. Uegaki, Y. Kotani, M. Kamigaito and M. Sawamoto, *Macromolecules*, 1998, **31**, 6756-6761.
79. P. Lecomte, I. Drapier, P. Dubois, P. Teyssié and R. Jérôme, *Macromolecules*, 1997, **30**, 7631-7633.
80. E. Le Grognec, J. Claverie and R. Poli, *J. Am. Chem. Soc.*, 2001, **123**, 9513-9524.
81. Y. Wang, N. Soerensen, M. Zhong, H. Schroeder, M. Buback and K. Matyjaszewski, *Macromolecules*, 2013, **46**, 683-691.
82. K. Matyjaszewski, W. Jakubowski, K. Min, W. Tang, J. Huang, W. A. Braunecker and N. V. Tsarevsky, *Proceedings of the National Academy of Sciences*, 2006, **103**, 15309-15314.
83. H. Dong, W. Tang and K. Matyjaszewski, *Macromolecules*, 2007, **40**, 2974-2977.
84. A. de Vries, B. Klumperman, D. de Wet-Roos and R. D. Sanderson, *Macromol. Chem. Phys.*, 2001, **202**, 1645-1648.
85. K. Min, H. Gao and K. Matyjaszewski, *Macromolecules*, 2007, **40**, 1789-1791.
86. Y. Gnanou and G. Hizal, *J. Polym. Sci. Part A: Polym. Chem.*, 2004, **42**, 351-359.
87. A. Anastasaki, V. Nikolaou, G. Nurumbetov, P. Wilson, K. Kempe, J. F. Quinn, T. P. Davis, M. R. Whittaker and D. M. Haddleton, *Chem. Rev.*, 2016, **116**, 835-877.

88. V. Percec, A. V. Popov, E. Ramirez-Castillo, M. Monteiro, B. Barboiu, O. Weichold, A. D. Asandei and C. M. Mitchell, *J. Am. Chem. Soc.*, 2002, **124**, 4940-4941.
89. V. Percec, T. Guliashvili, J. S. Ladislaw, A. Wistrand, A. Stjerndahl, M. J. Sienkowska, M. J. Monteiro and S. Sahoo, *J. Am. Chem. Soc.*, 2006, **128**, 14156-14165.
90. B. M. Rosen and V. Percec, *Chem. Rev.*, 2009, **109**, 5069-5119.
91. S. Monge, V. Darcos and D. M. Haddleton, *J. Polym. Sci. Part A: Polym. Chem.*, 2004, **42**, 6299-6308.
92. C. A. Bell, M. R. Whittaker, L. R. Gahan and M. J. Monteiro, *J. Polym. Sci. Part A: Polym. Chem.*, 2008, **46**, 146-154.
93. M. Enayati, R. L. Jezorek and V. Percec, *Polym. Chem.*, 2016, **7**, 4549-4558.
94. N. H. Nguyen, B. M. Rosen, G. Lligadas and V. Percec, *Macromolecules*, 2009, **42**, 2379-2386.
95. W. Ding, C. Lv, Y. Sun, H. Luan, T. Yu and G. Qu, *Polym. Bull.*, 2011, **67**, 1499-1505.
96. M. E. Levere, I. Willoughby, S. O'Donohue, A. de Cuendias, A. J. Grice, C. Fidge, C. R. Becer and D. M. Haddleton, *Polym. Chem.*, 2010, **1**, 1086-1094.
97. T. Zhang, Y. Du, F. Mueller, I. Amin and R. Jordan, *Polym. Chem.*, 2015, **6**, 2726-2733.
98. M. E. Levere, N. H. Nguyen, H.-J. Sun and V. Percec, *Polym. Chem.*, 2013, **4**, 686-694.
99. R. Aksakal, M. Resmini and C. R. Becer, *Polym. Chem.*, 2016, **7**, 6564-6569.
100. J. T. Rademacher, M. Baum, M. E. Pallack, W. J. Brittain and W. J. Simonsick, *Macromolecules*, 2000, **33**, 284-288.
101. P.-E. Millard, N. C. Mougin, A. Böker and A. H. E. Müller, in *Controlled/Living Radical Polymerization: Progress in ATRP*, American Chemical Society, 2009, vol. 1023, ch. 9, pp. 127-137.
102. Q. Zhang, P. Wilson, Z. Li, R. McHale, J. Godfrey, A. Anastasaki, C. Waldron and D. M. Haddleton, *J. Am. Chem. Soc.*, 2013, **135**, 7355-7363.
103. F. Alsubaie, A. Anastasaki, P. Wilson and D. M. Haddleton, *Polym. Chem.*, 2015, **6**, 406-417.
104. L. Voorhaar, S. Wallyn, F. E. Du Prez and R. Hoogenboom, *Polym. Chem.*, 2014, **5**, 4268-4276.
105. X. Jiang, S. Fleischmann, N. H. Nguyen, B. M. Rosen and V. Percec, *J. Polym. Sci. Part A: Polym. Chem.*, 2009, **47**, 5591-5605.
106. N. H. Nguyen and V. Percec, *J. Polym. Sci. Part A: Polym. Chem.*, 2011, **49**, 4756-4765.
107. G. Lligadas and V. Percec, *J. Polym. Sci. Part A: Polym. Chem.*, 2008, **46**, 2745-2754.
108. C. Waldron, Q. Zhang, Z. Li, V. Nikolaou, G. Nurumbetov, J. Godfrey, R. McHale, G. Yilmaz, R. K. Randev, M. Girault, K. McEwan, D. M. Haddleton, M. Droesbeke, A. J. Haddleton, P. Wilson, A. Simula, J. Collins, D. J. Lloyd, J. A. Burns, C. Summers, C. Houben, A. Anastasaki, M. Li, C. R. Becer, J. K. Kiviaho and N. Risangud, *Polym. Chem.*, 2014, **5**, 57-61.
109. X. Leng, N. H. Nguyen, B. van Beusekom, D. A. Wilson and V. Percec, *Polym. Chem.*, 2013, **4**, 2995-3004.
110. N. H. Nguyen, X. Leng, H.-J. Sun and V. Percec, *J. Polym. Sci. Part A: Polym. Chem.*, 2013, **51**, 3110-3122.
111. Q. Zhang, Z. Li, P. Wilson and D. M. Haddleton, *Chem. Commun.*, 2013, **49**, 6608-6610.
112. S. R. Samanta, M. E. Levere and V. Percec, *Polym. Chem.*, 2013, **4**, 3212-3224.
113. S. R. Samanta, V. Nikolaou, S. Keller, M. J. Monteiro, D. A. Wilson, D. M. Haddleton and V. Percec, *Polym. Chem.*, 2015, **6**, 2084-2097.

114. A. Simula, V. Nikolaou, A. Anastasaki, F. Alsubaie, G. Nurumbetov, P. Wilson, K. Kempe and D. M. Haddleton, *Polym. Chem.*, 2015, **6**, 2226-2233.
115. N. H. Nguyen, B. M. Rosen and V. Percec, *J. Polym. Sci. Part A: Polym. Chem.*, 2010, **48**, 1752-1763.
116. Q. Zhang, P. Wilson, A. Anastasaki, R. McHale and D. M. Haddleton, *ACS Macro Lett.*, 2014, **3**, 491-495.
117. S. Fleischmann and V. Percec, *J. Polym. Sci. Part A: Polym. Chem.*, 2010, **48**, 2236-2242.
118. M. Vorobii, A. de los Santos Pereira, O. Pop-Georgievski, N. Y. Kostina, C. Rodriguez-Emmenegger and V. Percec, *Polym. Chem.*, 2015, **6**, 4210-4220.
119. J. A. Syrett, M. W. Jones and D. M. Haddleton, *Chem. Commun.*, 2010, **46**, 7181-7183.
120. U. Edlund, C. Rodriguez-Emmenegger, E. Brynda and A.-C. Albersson, *Polym. Chem.*, 2012, **3**, 2920-2927.
121. T. Tischer, C. Rodriguez-Emmenegger, V. Trouillet, A. Welle, V. Schueler, J. O. Mueller, A. S. Goldmann, E. Brynda and C. Barner-Kowollik, *Adv. Mater.*, 2014, **26**, 4087-4092.
122. S. R. Samanta, R. Cai and V. Percec, *Polym. Chem.*, 2014, **5**, 5479-5491.
123. S. R. Samanta, R. Cai and V. Percec, *Polym. Chem.*, 2015, **6**, 3259-3270.
124. Q. Zhang, A. Anastasaki, G.-Z. Li, A. J. Haddleton, P. Wilson and D. M. Haddleton, *Polym. Chem.*, 2014, **5**, 3876-3883.
125. Q. Zhang, J. Collins, A. Anastasaki, R. Wallis, D. A. Mitchell, C. R. Becer and D. M. Haddleton, *Angew. Chem. Int. Ed.*, 2013, **52**, 4435-4439.
126. X.-H. Liu, G.-B. Zhang, B.-X. Li, Y.-G. Bai and Y.-S. Li, *J. Polym. Sci. Part A: Polym. Chem.*, 2010, **48**, 5439-5445.
127. J. Ma, H. Chen, M. Zhang and L. Chen, *J. Polym. Sci. Part A: Polym. Chem.*, 2011, **49**, 2588-2593.
128. M. J. Sienkowska, B. M. Rosen and V. Percec, *J. Polym. Sci. Part A: Polym. Chem.*, 2009, **47**, 4130-4140.
129. H. Wu, Y. Wan, W. Wang, Y. Wang, N. Zhou, W. Zhang, X. Li, Z. Zhang and X. Zhu, *Polym. Chem.*, 2015, **6**, 2620-2625.
130. J. Tom, B. Hornby, A. West, S. Harrisson and S. Perrier, *Polym. Chem.*, 2010, **1**, 420-422.
131. J. Gao, Z. Zhang, N. Zhou, Z. Cheng, J. Zhu and X. Zhu, *Macromolecules*, 2011, **44**, 3227-3232.
132. M. R. Whittaker, C. N. Urbani and M. J. Monteiro, *J. Polym. Sci. Part A: Polym. Chem.*, 2008, **46**, 6346-6357.
133. D. Konkolewicz, Y. Wang, P. Krys, M. Zhong, A. A. Isse, A. Gennaro and K. Matyjaszewski, *Polym. Chem.*, 2014, **5**, 4396-4417.
134. Y. Gao, T. Zhao, D. Zhou, U. Greiser and W. Wang, *Chem. Commun.*, 2015, **51**, 14435-14438.
135. S. Harrisson, P. Couvreur and J. Nicolas, *Macromolecules*, 2012, **45**, 7388-7396.
136. D. Konkolewicz, Y. Wang, M. Zhong, P. Krys, A. A. Isse, A. Gennaro and K. Matyjaszewski, *Macromolecules*, 2013, **46**, 8749-8772.
137. S. Harrisson and J. Nicolas, *ACS Macro Lett.*, 2014, **3**, 643-647.
138. F. Alsubaie, A. Anastaski, V. Nikolaou, A. Simula, G. Nurumbetov, P. Wilson, K. Kempe and D. M. Haddleton, *Macromolecules*, 2015, **48**, 5517-5525.
139. F. Alsubaie, A. Anastasaki, V. Nikolaou, A. Simula, G. Nurumbetov, P. Wilson, K. Kempe and D. M. Haddleton, *Macromolecules*, 2015, **48**, 6421-6432.
140. G. Lligadas, B. M. Rosen, C. A. Bell, M. J. Monteiro and V. Percec, *Macromolecules*, 2008, **41**, 8365-8371.

141. N. H. Nguyen, H.-J. Sun, M. E. Levere, S. Fleischmann and V. Percec, *Polym. Chem.*, 2013, **4**, 1328-1332.
142. M. E. Levere, N. H. Nguyen, X. Leng and V. Percec, *Polym. Chem.*, 2013, **4**, 1635-1647.
143. T. Guliashvili and V. Percec, *J. Polym. Sci. Part A: Polym. Chem.*, 2007, **45**, 1607-1618.
144. M. E. Levere, N. H. Nguyen and V. Percec, *Macromolecules*, 2012, **45**, 8267-8274.
145. B. M. Rosen, X. Jiang, C. J. Wilson, N. H. Nguyen, M. J. Monteiro and V. Percec, *J. Polym. Sci. Part A: Polym. Chem.*, 2009, **47**, 5606-5628.
146. G. Lligadas, B. M. Rosen, M. J. Monteiro and V. Percec, *Macromolecules*, 2008, **41**, 8360-8364.
147. N. H. Nguyen, M. E. Levere, J. Kulis, M. J. Monteiro and V. Percec, *Macromolecules*, 2012, **45**, 4606-4622.
148. K. Matyjaszewski, N. V. Tsarevsky, W. A. Braunecker, H. Dong, J. Huang, W. Jakubowski, Y. Kwak, R. Nicolay, W. Tang and J. A. Yoon, *Macromolecules*, 2007, **40**, 7795-7806.
149. C.-H. Peng, M. Zhong, Y. Wang, Y. Kwak, Y. Zhang, W. Zhu, M. Tonge, J. Buback, S. Park, P. Krys, D. Konkolewicz, A. Gennaro and K. Matyjaszewski, *Macromolecules*, 2013, **46**, 3803-3815.
150. M. Zhong, Y. Wang, P. Krys, D. Konkolewicz and K. Matyjaszewski, *Macromolecules*, 2013, **46**, 3816-3827.
151. Y. Wang, M. Zhong, Y. Zhang, A. J. D. Magenau and K. Matyjaszewski, *Macromolecules*, 2012, **45**, 8929-8932.
152. A. Duro-Castano, J. Movellan and M. J. Vicent, *Biomaterials Science*, 2015, **3**, 1321-1334.
153. M. A. Mintzer and M. W. Grinstaff, *Chem. Soc. Rev.*, 2011, **40**, 173-190.
154. S. Svenson and D. A. Tomalia, *Advanced Drug Delivery Reviews*, 2005, **57**, 2106-2129.
155. J. B. Wolinsky and M. W. Grinstaff, *Advanced Drug Delivery Reviews*, 2008, **60**, 1037-1055.
156. X. Jiang, X. Jiang, G. Lu, C. Feng and X. Huang, *Polym. Chem.*, 2014, **5**, 4915-4925.
157. Y. Li, H. J. Heo, G. H. Gao, S. W. Kang, C. T. Huynh, M. S. Kim, J. W. Lee, J. H. Lee and D. S. Lee, *Polymer*, 2011, **52**, 3304-3310.
158. G. O. Schulz and R. Milkovich, *J. Appl. Polym. Sci.*, 1982, **27**, 4773-4786.
159. G. Lu, Y. Li, H. Guo, W. Du and X. Huang, *Polym. Chem.*, 2013, **4**, 3132-3139.
160. F. Sun, C. Feng, H. Liu and X. Huang, *Polym. Chem.*, 2016, **7**, 6973-6979.
161. J. S. Basuki, L. Esser, P. B. Zetterlund, M. R. Whittaker, C. Boyer and T. P. Davis, *Macromolecules*, 2013, **46**, 6038-6047.
162. J. Collins, S. J. Wallis, A. Simula, M. R. Whittaker, M. P. McIntosh, P. Wilson, T. P. Davis, D. M. Haddleton and K. Kempe, *Macromol. Rapid Commun.*, 2017, **38**, DOI: 10.1002/marc.201600534
163. C. Boyer, A. Derveaux, P. B. Zetterlund and M. R. Whittaker, *Polym. Chem.*, 2012, **3**, 117-123.
164. C. Waldron, A. Anastasaki, R. McHale, P. Wilson, Z. Li, T. Smith and D. M. Haddleton, *Polym. Chem.*, 2014, **5**, 892-898.
165. E. H. H. Wong, A. Blencowe and G. G. Qiao, *Polym. Chem.*, 2013, **4**, 4562-4565.
166. T. G. McKenzie, E. H. H. Wong, Q. Fu, S. J. Lam, D. E. Dunstan and G. G. Qiao, *Macromolecules*, 2014, **47**, 7869-7877.
167. L. L. Kiessling, J. E. Gestwicki and L. E. Strong, *Angew. Chem. Int. Ed.*, 2006, **45**, 2348-2368.
168. J. J. Lundquist and E. J. Toone, *Chem. Rev.*, 2002, **102**, 555-578.

169. R. T. Lee and Y. C. Lee, *Glycoconjugate J.*, 2000, **17**, 543-551.
170. J. Holgersson, A. Gustafsson and M. E. Breimer, *Immunol Cell Biol*, 2005, **83**, 694-708.
171. J. E. Gestwicki, C. W. Cairo, L. E. Strong, K. A. Oetjen and L. L. Kiessling, *J. Am. Chem. Soc.*, 2002, **124**, 14922-14933.
172. Y. Miura, D. Koketsu and K. Kobayashi, *Polym. Adv. Technol.*, 2007, **18**, 647-651.
173. D. Ponader, F. Wojcik, F. Beceren-Braun, J. Dernedde and L. Hartmann, *Biomacromolecules*, 2012, **13**, 1845-1852.
174. S.-J. Richards, M. W. Jones, M. Hunaban, D. M. Haddleton and M. I. Gibson, *Angew. Chem. Int. Ed.*, 2012, **51**, 7812-7816.
175. Q. Zhang, L. Su, J. Collins, G. Chen, R. Wallis, D. A. Mitchell, D. M. Haddleton and C. R. Becer, *J. Am. Chem. Soc.*, 2014, **136**, 4325-4332.

Chapter 2

Pentablock star shaped polymers in less than 90 minutes *via* aqueous SET-LRP

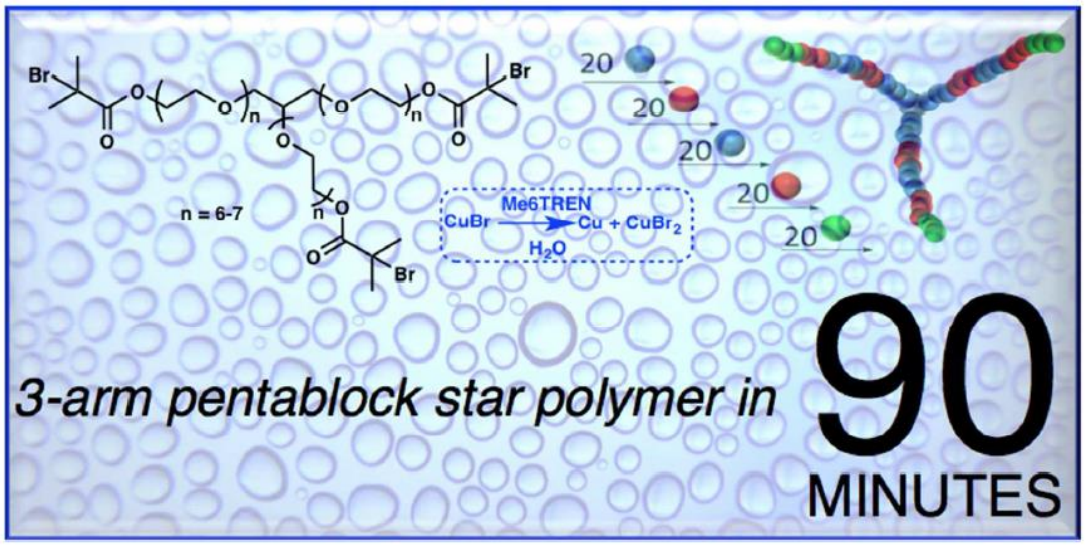

The synthesis of multi-block star-shaped copolymers via SET-LRP in aqueous solution has been reported. This aqueous polymerization technique allows rapid and direct access to acrylamide based star-shaped polymers. It is possible to synthesize an A-B-A-B-C penta-block copolymer in less than 90 minutes reaction time in total. To achieve this, a water-soluble 3-arm initiator based on a glycerol structure has been investigated for the first time. Using N-isopropylacrylamide 3-arm star-shaped polymers were prepared with DP = 60 to 240 with full conversions in <30 minutes with polydispersities <1.11. The scope of the reaction was demonstrated by synthesizing diblock copolymers using a combination of NIPAM, DMA and HEAm in different ratios. In addition a sequence controlled 3-arm pentablock copolymer has been obtained with excellent control over molecular weight distribution (Đ < 1.14) as evidenced by SEC, ^{1}H NMR, and MALDI-ToF MS.

Parts of this chapter have been published;

R. Aksakal, M Resmini and C.R. Becer, Polym. Chem., 2016, 7, 171-175.

2.1. Introduction

Synthesis of structurally complex precision polymers has been an essential requirement in order to successfully mimic biomacromolecules and biological systems.[1,2] More recently the main focus has moved to the regulation of the building block sequence and folding in linear or branched polymers, to obtain control over their secondary structure, all of which allow researchers to design and tailor unique features to enable biologically inspired functionalities as in DNA, RNA, peptides or proteins.[3,4] Star shaped polymers exhibit distinct physical and biological properties that can be used in a broad range of applications including drug delivery,[5,6] lectin recognition,[7,8] treatment of cancer,[9] as well as photonics.[10]

Star-shaped polymers can be prepared by arm-first, coupling-onto and core-first approaches. In the arm-first approach, linear polymer chains are synthesized before crosslinking with a difunctional monomer. However, this technique allows the formation of multi-arm star-shaped polymers with large number of arms (>100) and the conversion to core cross-linked stars (CCS) is often incomplete, which results in a broad distribution of number of arms per molecule.[11] Additional purification steps are usually required to separate unreacted chains from the desired end product.[12] Similarly, the coupling-onto approach also requires pre-synthesis of arms and then conjugation to a multifunctional core *via* efficient coupling reactions (*e.g.* "click" reaction).[13,14] Although it is possible to obtain stars with pre-defined number of arms, this approach requires complete modification of the active chain end groups prior to conjugation to the core. On the other hand, in the core-first approach a core molecule is functionalized into a multifunctional initiator, where the arms are grown directly from. This approach is not only highly efficient, reaching nearly always quantitative monomer conversion, but also the number of arms is predefined, which allows control over the repeating units per arm and total size. In addition, core-first stars retaining high chain-end fidelity can be further used to polymerize other monomers to obtain star block copolymers, therefore introducing more complexity to the polymer.

Although all three methodologies are well established, numerous studies were carried out to optimize the synthesis of star-shaped polymers using controlled radical polymerization techniques. Due to the highly reactive nature of radicals, the main challenge has been to avoid undesired side reactions such as star-star coupling or termination of growing arms.[15,16] The key approach has been to reduce the number of

active radicals present in the solution at any time to suppress the termination reactions. However, this resulted in extended reaction times and/or highly diluted reactions solutions. Yet the problem to use highly polar organic solvents, such as DMSO, together with multistep purifications in order to obtain multi block star copolymers, remains unsolved.

Current methods published in the literature mainly consist of either homo-/diblock copolymers with short reaction times or multi-block star copolymers with reaction times up to days, even with blocks consisting of as few as 5 repeating units (DP_n).[17,18] For this reason there has been a drive towards developing more efficient protocols with fewer steps to obtain high DP_n multi-block star shaped copolymers.

In recent years, aqueous Cu(0)-mediated single electron transfer living radical polymerization (SET-LRP) has gained great popularity, as nearly 100% chain end fidelity is retained at full conversion.[19] Utilizing water as the reaction solvent has a great advantage not only because of water being an environmentally friendly and cheap solvent, but also to provide faster polymerization kinetics for acrylamides.[20]

Recently, SET-LRP in acetone has been performed by Zhu *et al.* to synthesize pH-responsive A_2B_2 and fluorescent A_3B type mikto-arm stars using a combination of SET-LRP and RAFT.[21] Similarly, the combination of SET-LRP and NMP to polymerize star shaped acrylates was reported by Save *et al.*[22] Moreover, Whittaker *et al.* reported the synthesis of low molecular weight 4-arm poly(methyl acrylate) and also demonstrated high chain-end fidelities, however with broad polydispersities (*Đ*), which was attributed to star-star coupling, yet the degree of coupling was not fully investigated. The technique was optimized later, when a 5-arm glucose core was used to polymerize different acrylates, with each individual block polymerising for 24h.[17,23] Haddleton *et al.* reported successful synthesis of 8-arm acrylate stars with high molecular weight and narrow molecular weight distribution.[24] Furthermore, they observed phase separation of the polymer from the reaction media, which was deemed to be beneficial in reducing star-star coupling in certain cases.

In a more recent study, Qiao *et al.* demonstrated the synthesis of core crosslinked star polymers in a one-pot two-step reaction, where MA was polymerized and crosslinked in a second step with ethylene glycol diacrylate in DMSO.[25] In a later work, they have shown the synthesis of stimuli-responsive heteroarm star polymers by the arm-first

approach, where a poly(ethylene glycol) methyl ether (PEG) macro initiator was used to polymerize *N*-isopropyl acrylamide (NIPAM) and 2-hydroxyethyl acrylate (HEA).[12]

In this chapter, aqueous SET-LRP has been investigated to overcome the above mentioned drawbacks associated with the core first approach and even take this approach to the next level by preparing sequence controlled polymers. Here the synthesis of a hydrophilic star-core with 3 initiating sites is reported, which is utilized to obtain well-defined core-first multi-block stars (**Scheme 2.1)** in less than 90 minutes with well-defined monomer sequences. Although aqueous SET-LRP is a versatile polymerization technique to obtain linear polymers, there is a lack in investigation when it comes to star shaped polymers. It is believed that this will allow the synthesis of precision star shaped polymers, which can be obtained under mild conditions

2.2. Results and Discussion

In order to investigate the optimum reaction conditions, SET-LRP of NIPAM was initiated using a water-soluble 3-arm initiator (**Gly-Br$_3$**). For this purpose, commercially available glycerol ethoxylate (M_n ~ 1000 g/mol) was functionalized into a 3-arm initiator (**Scheme 2.1**).

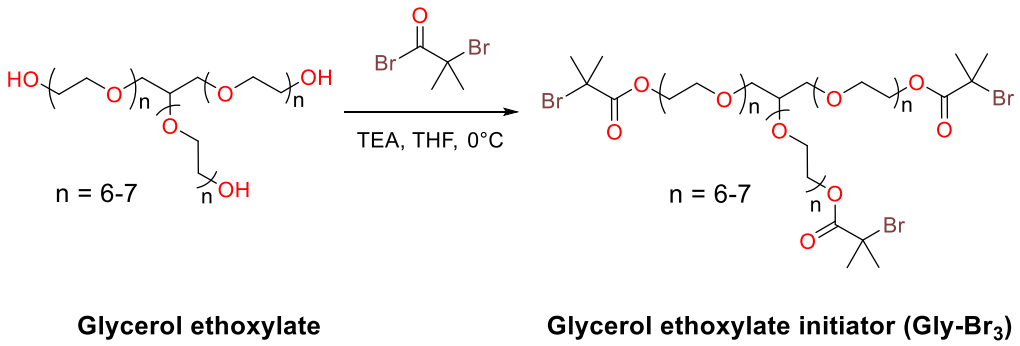

Scheme 2.1: Synthesis of water soluble and 3-arm star initiator Glycerol ethoxylate (Gly-Br$_3$).

The synthesis of Gly-Br$_3$ was confirmed by MALDI-ToF-MS analysis, displaying the corresponding shift in peak distribution to higher *m/z* ratio and a change in the isotopic pattern due to the bromines. (**Figure 1**). Initially, glycerol ethoxylate gives a distribution between 700-1400 *m/z*, with a spacing between signals, corresponding to one ethylene oxide repeating unit. Whilst this spacing is maintained, signals for Gly-Br$_3$ are observed at a higher *m/z* ratio (between 1200-1800), without any indication for the presence of unreacted glycerol ethoxylate.

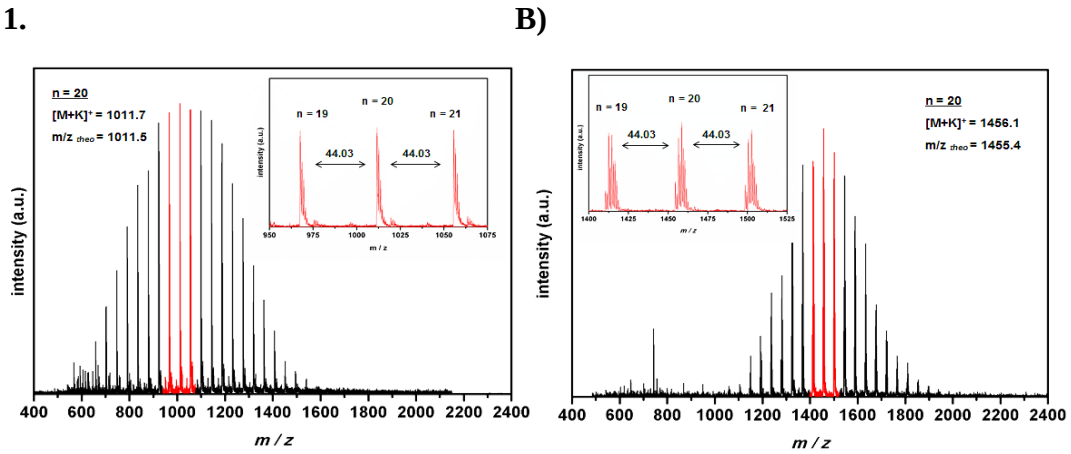

Figure 1: MALDI-ToF-MS spectra of **A)** Glycerol ethoxylate and **B)** Glycerol ethoxylate initiator (Gly-Br$_3$) confirming the functionalisation into the 3-arm star initiator.

In addition, both ^{1}H NMR and ^{13}C NMR spectra were recorded, supporting the successful synthesis of the initiator (**Figure 2.2**). The methyl groups on the initiatior are visible at 1.92 ppm, whereas the CH_2 groups next to the ester appear at 4.27 ppm. The two integrals of the signals are in a ratio of 3:1 which was expected. Furthermore, the integral of the ethylene glycol repeating unit (labelled d) reveals an average of 6 to 7 repeating units per arm, which was calculated from the ratio between the repeating units and the initiator signal (labelled a). The appearance of the signal for the methyl groups at 32 ppm additionally confirms the presence of the initiating group.

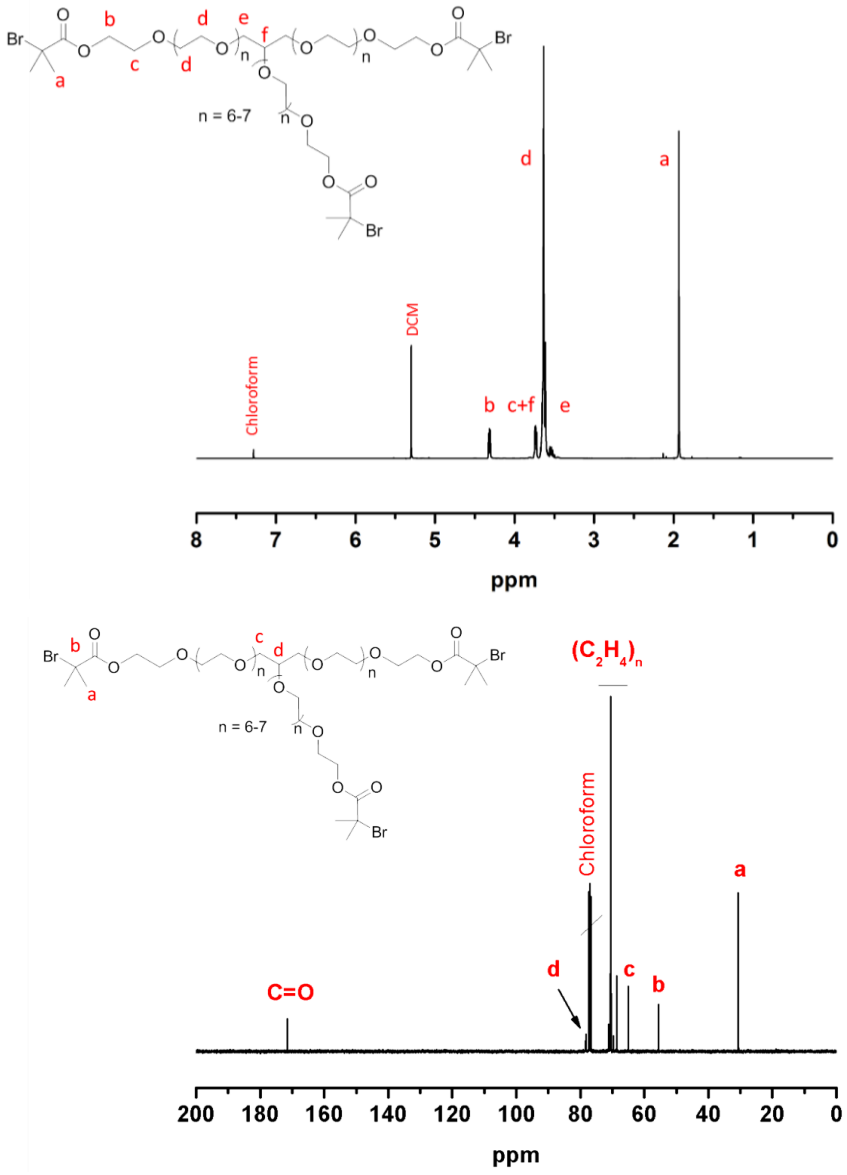

Figure 2.2: ^{1}H NMR (top) and ^{13}C NMR (bottom) spectrum of Gly-Br_3 initiator, after modification of glycerol ethoxylate, with corresponding peak assignments.

A water soluble 3-arm star initiator for the synthesis of multiblock star polymers is reported for the first time (**Scheme 2.2**).[26] Therefore, the reaction conditions (*i.e.* [CuBr] : [Ligand] : [Initiator]) were systematically varied to optimize the aqueous SET-LRP of NIPAM (**Table 2.1**).

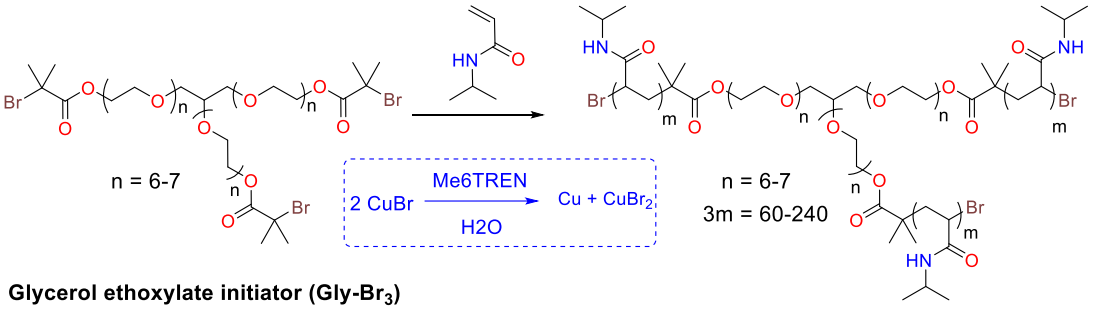

Scheme 2.2: Schematic representation of the polymerization of NIPAM *via* aqueous SET-LRP.

Table 2.1: Summary of the results obtained from the optimization reactions for the polymerization of NIPAM ([M]:[I] = 60), under various reaction conditions.

Entry	[I]:[CuBr]:[Me$_6$TREN]	ρ^a (%)	$M_{n,theo}$ (g/mol)	$M_{n,SEC}{}^b$ (g/mol)	$Đ^b$	Temp. (°C)
R01	1 : 0.8 : 0.4	38	3600	6000	1.12	25
R02	1 : 1.2 : 1.2	100	8300	11900	1.41	25
R03	1 : 1.8 : 1.2	100	8300	12700	1.14	25
R04	1 : 1.8 : 1.8	100	8300	15800	1.48	25
R05	1 : 2.4 : 1.2	100	6400	8800	1.30	25
R06	1 : 2.4 : 2.4	79	8300	15900	1.29	25
R07	1 : 1.2 : 1.2	100	8300	12300	1.13	0
R08	1 : 1.8 : 1.2	100	8300	10500	1.10	0
R09	1 : 1.8 : 1.8	100	8300	17100	1.24	0
R10	1 : 2.4 : 1.2	37	3600	5400	1.07	0
R11	1 : 2.4 : 2.4	100	8300	15900	1.30	0

[a] Conversion calculated from ^{1}H NMR. [b] DMF eluent, linear PMMA standards.

The reactions were carried out either at 25°C or at 0°C, as the temperature has a critical effect on the disproportionation of CuBr.[27] Initially, homopolymerization of NIPAM was carried out using the ratio of [NIPAM]:[Gly-Br$_3$]:[CuBr]:[Me$_6$TREN]= 60:1:0.8:0.4, which are established ratios for high DP$_n$ polymerizations using monofunctional initiators (See section 2.4.4. for the SEC traces and ^{1}H NMR spectra).[19]

The obtained low conversions were attributed to insufficient amount of *in situ* generated Cu(0), thus the CuBr concentration was increased and the Me_6TREN concentration adjusted accordingly. It was found that the ratio of [I]:[CuBr]:[Me_6TREN]= 1:1.8:1.2 was the most suitable for the SET-LRP of NIPAM due to very low polydispersity and $M_{n,SEC}$ being closest to theoretical number average molecular weights ($M_{n,theo}$) (**Table 2.1, R08**). Although no difference was observed when carrying out the reactions at 25°C or at 0°C using the ratio above (**R03** and **R08** respectively), all further reactions were carried out at 0°C to avoid possible termination events by the hydrolysis of the terminal bromine prior to further chain extensions. To demonstrate the applicability of these ratios to a range of monomer repeating units, star polymers with relatively high molecular weights were targeted (**Table 2.2, P1-P7**, DP_n = 60-240). Even at DP_n = 240, quantitative conversion was reached in less than 30 minutes.

Table 2.2: Summary of the results obtained for 3-arm star shaped PNIPAM, while increasing DP under same reaction conditions.

Entry	[NIPAM] / [Gly-Br_3]	ρ^a (%)	$M_{n,theo}$ (g/mol)	$M_{n,SEC}{}^b$ (g/mol)	$Đ^b$	$T_{cp}{}^c$ (°C)
P1	60	100	8300	9000	1.11	49
P2	90	100	11600	11700	1.09	46
P3	120	100	15000	14400	1.08	43
P4	150	100	18400	16600	1.07	40
P5	180	100	21800	19900	1.11	40
P6	210	100	25200	21400	1.09	39
P7	240	100	28600	25100	1.10	39

[a] Conversion calculated from ^{1}H NMR. [b] DMF eluent, linear PMMA standards. [c] T_{cp}: Cloud point temperature. Cloud point calculated from the 50% transmittance point in the heating cycle using 1 mg.mL^{-1} sample concentration.

Contrary to what has been reported in the literature, maintaining good control over the molecular weight distribution ($Đ < 1.11$) was possible without the need of DP_n dependent adjustment of the ratios (**Figure 2.3**).[28] In addition, all polymers were assessed *via* SEC, which showed that the differences between measured and theoretical molar mass were becoming more pronounced. This is most probably due to the difference in the linear hydrodynamic volume increase with higher molar mass between linear PMMA calibration standards used and star shaped PNIPAM.

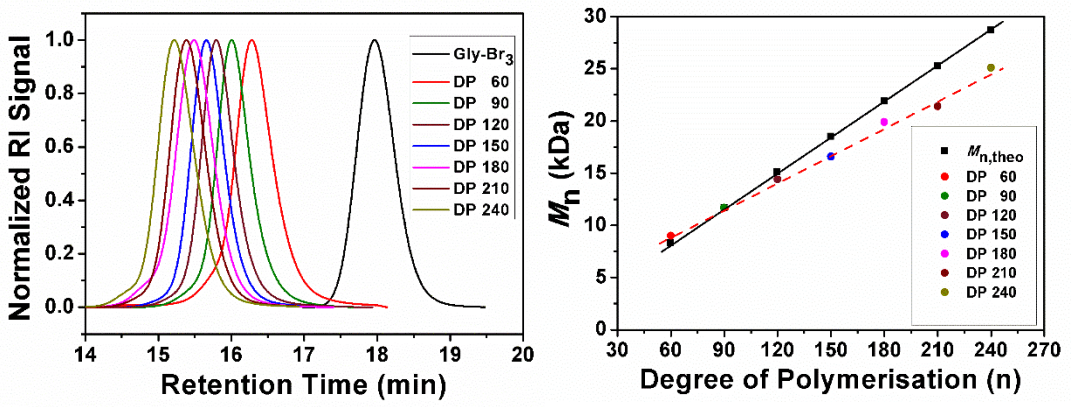

Figure 2.3: Overview of the results obtained for the homopolymers of NIPAM (P1-P7). SEC traces of 3-arm star shaped poly(NIPAM) with varying DP (left) and the comparison of $M_{n,theo}$ and $M_{n,SEC}$ (right). [M]:[I]:[CuBr]:[Me_6TREN] = [60]:[1]:[1.8]:[1.2].

Furthermore, the cloud points (T_{cp}) of 3-arm star-shaped PNIPAM with increasing DP_n was measured *via* UV/Vis spectroscopy. No hysteresis was observed for **P1-P7** and all polymer samples redissolved fully upon cooling (**Figure 2.4**). The cloud points were found to be in the range of 39 to 49°C (**Table 2.2**), decreasing with increasing chain lengths The LCST of PNIPAM homopolymer is usually reported to be around 32°C and the difference of 8-10°C could be due to the effect of hydrophilic core, which additionally has around 20 ethyleneglycol units.[29,30] For higher molecular weight stars ($DP_n \geq 150$), all cloud points observed were at elevated human body temperatures (*e.g.* fever temperature 38-42°C). It appears that the effect of the hydrophilic core is less significant in cloud point depression for high DP_n stars compared to smaller stars. This being another advantage of using a hydrophilic core, these PNIPAM polymers can also be used as an amphiphilic star polymer with a hydrophilic core.

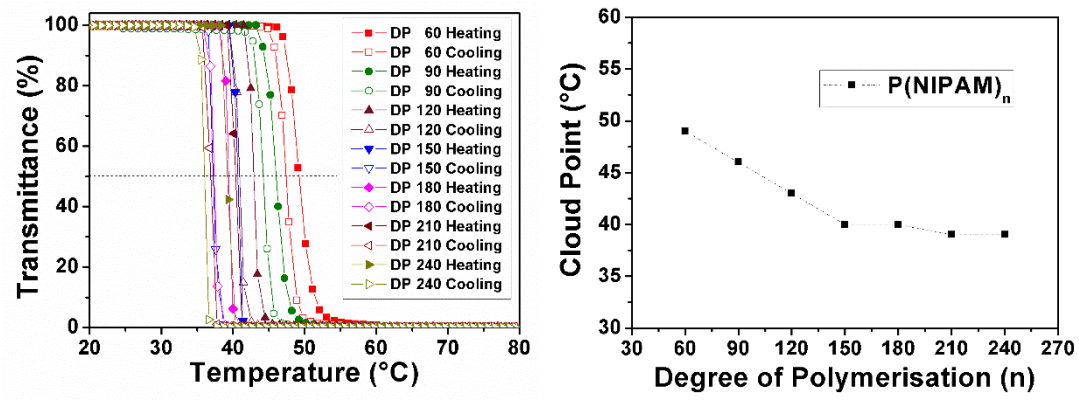

Figure 2.4: Turbidity curves of aqueous solutions of P1-P7 in water (c = 1 mg.mL^{-1}) (left) and dependence of the cloud point temperature (T_{cp}) of P1-P7 on the degree of polymerization (right)

To investigate the efficiency of this approach for the preparation of multi-block copolymers, the first block p(NIPAM)$_{60}$ was chain extended with twice as much acrylamide, equivalent to DP 120. Full conversion was reached within less than 30 minutes, with excellent control for p(NIPAM)$_{60}$-p(NIPAM)$_{120}$ (**Figure 2.5**, **P8**, $M_{n,SEC}$ = 24200 g.mol^{-1}, $Đ$ = 1.11). As predicted, no unwanted termination reactions were observed on the low or high molecular weight region of the SEC spectrum, indicating very high retention of the active end groups and no occurrence of star-star coupling. To assess the limits of applicability of this approach, two more chain extensions were carried out with aliquots of *N*,*N*,-dimethyl acrylamide (DMA, 120 eq.) (**Figure 2.5**, **P9**, $M_{n,SEC}$ = 24900 g.mol^{-1}, $Đ$ = 1.14) and *N*-hydroxyethyl acrylamide (HEAm, 120 eq.) (**Figure 2.5**, **P10**, $M_{n,SEC}$ = 23700 g.mol^{-1}, $Đ$ = 1.14), where in both cases full conversion was reached within 30 minutes with excellent control over the diblock star formation. The conversions for each block was monitored *via* ^{1}H NMR. After the polymerization of every block, samples were taken and conversions calculated to be 100%. This was confirmed by the disappearance of the signals for the vinyl protons in the 5.5-7.5 ppm range (**Figure 2.6,** zoomed in regions).

P8)

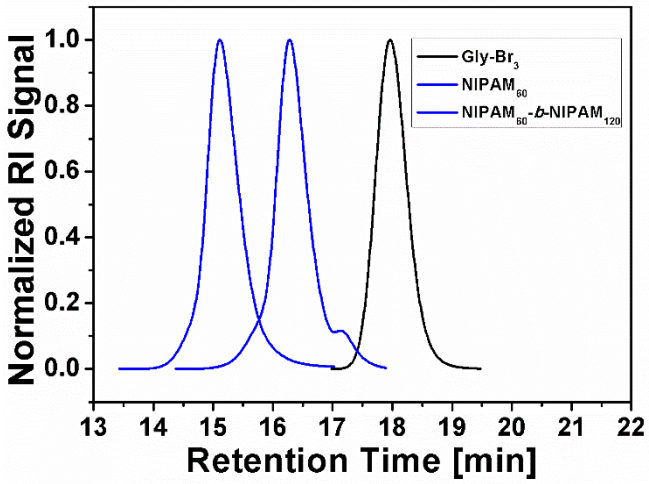

P9)

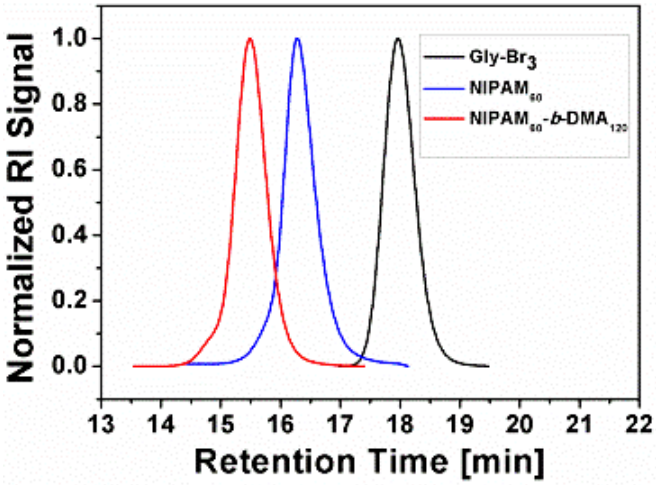

P10)

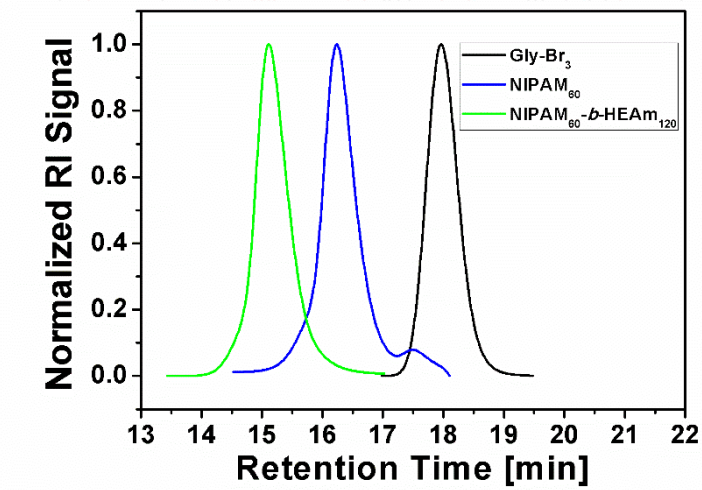

Figure 2.5: SEC traces of the 3-arm star **P8)** p(NIPAM)$_{60}$-*b*-p(NIPAM)$_{120}$, **P9)** p(NIPAM)$_{60}$-*b*-p(DMA)$_{120}$ and **P10)** p(NIPAM)$_{60}$-*b*-p(HEAm)$_{120}$.

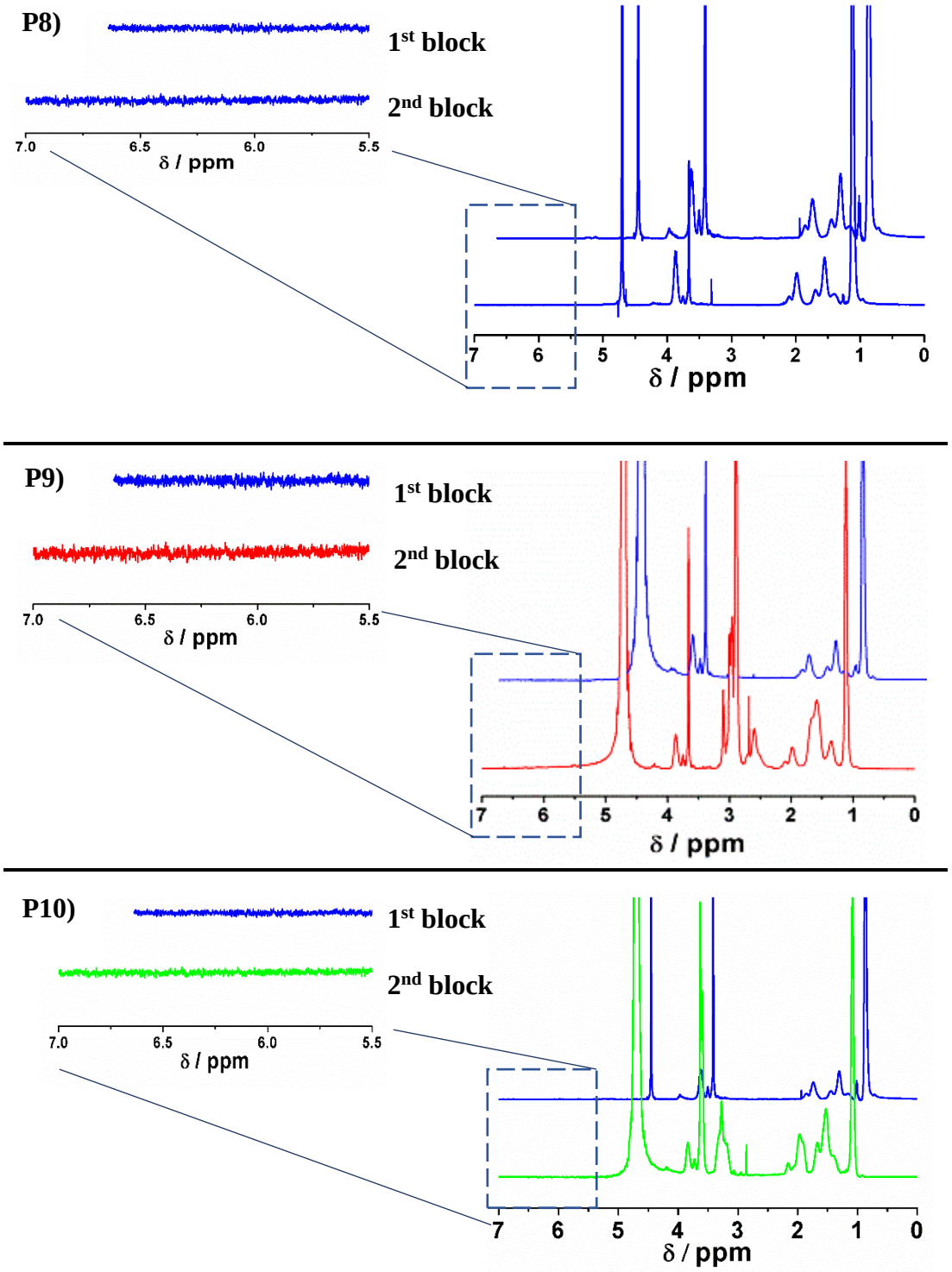

Figure 2.6: Synthesis of **P8)** p(NIPAM)$_{60}$-*b*-p(NIPAM)$_{120}$, **P9)** p(NIPAM)$_{60}$-*b*-p(DMA)$_{120}$ and **P10)** p(NIPAM)$_{60}$-*b*-p(HEAm)$_{120}$. ^{1}H NMR spectra of on the right, with the region between 5.5-7.0 ppm zoomed in to show the disappearance of the vinyl bonds (*i.e.* full conversion). Upper trace in overlaid spectrum shows full conversion of the first block (NIPAM, 60 eq.), lower trace in overlaid spectrum shows full conversion of the monomer from the second block (NIPAM, DMA and HEAm respectively).

A summary of the obtained SEC results for the polymers is presented in the table below (**Table 2.3**).

Table 2.3: Overview of the SEC results obtained for the 3-arm diblock star copolymers P8, P9 and P10

Entry	Polymer	ρ^{a} (%)	$M_{n,theo}$ (g/mol)	$M_{n,SEC}{}^{b}$ (g/mol)	$Đ^{b}$
P0	Gly-Br_3	n/a	1450	1900	1.04
P8	p(NIPAM)$_{60}$-*b*-p(NIPAM)$_{120}$	100	21800	24200	1.11
P9	p(NIPAM)$_{60}$-*b*-p(DMA)$_{120}$	100	20100	24900	1.14
P10	p(NIPAM)$_{60}$-*b*-p(HEAm)$_{120}$	100	22100	23700	1.14

[a] Conversion calculated from ^{1}H NMR. [b] DMF eluent, linear PMMA standards.

Based on the encouraging results obtained for diblock copolymerizations, the multi-block copolymerizations was performed in order to investigate the limits of this system. For this purpose, aliquots of NIPAM, DMA and HEAm (each 60 eq.) were injected alternatingly and a pentablock 3-arm star-shaped polymer was obtained (**Scheme 2.3**).

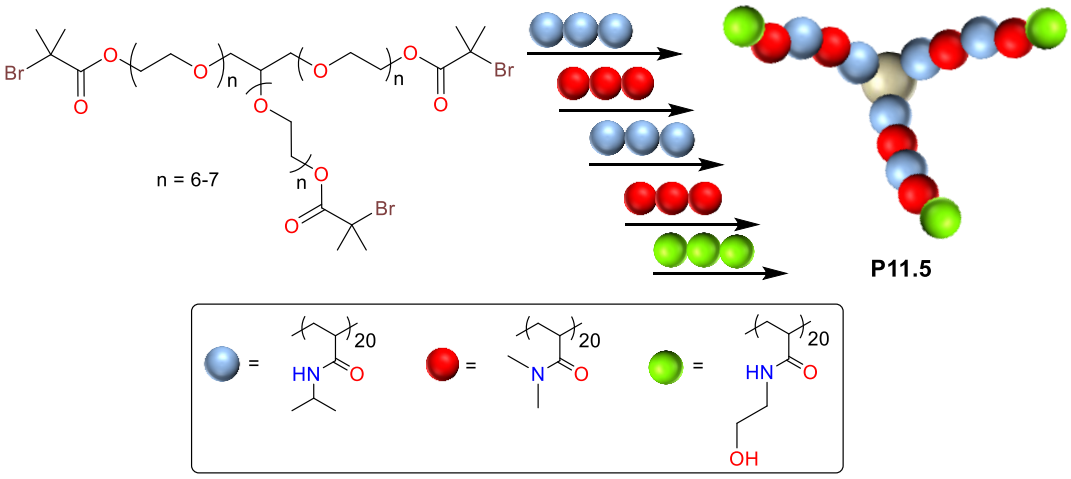

Scheme 2.3: Schematic representation of the polymerization of the sequence controlled 3-arm pentablock star shaped polymer P11.5; p(NIPAM)$_{60}$-*b*-p(DMA)$_{60}$-*b*-p(NIPAM)$_{60}$-*b*-p(DMA)$_{60}$-*b*-p(NIPAM)$_{60}$.

Initially, at high monomer concentrations the rate of propagation was high enough that the substitution of the chain end was found to be negligible. After reaching complete monomer conversion, prolonged reaction times may cause the loss of bromine end

groups due to possible side reactions, such as hydrolysis or coupling with the amine-based ligand.[31] In order to retain high chain end fidelity, conversion of each chain extension was monitored closely, to chain extend with the next block before monomer concentration reached zero, ideally at ρ≥95%. This procedure was carried out for each block until the desired core-first pentablock star polymer (**P11.5**, $M_{n,SEC}$ = 29700 g.mol^{-1}, $Đ$ = 1.14) was obtained *via* iterative chain extension (**Figure 2.7**).

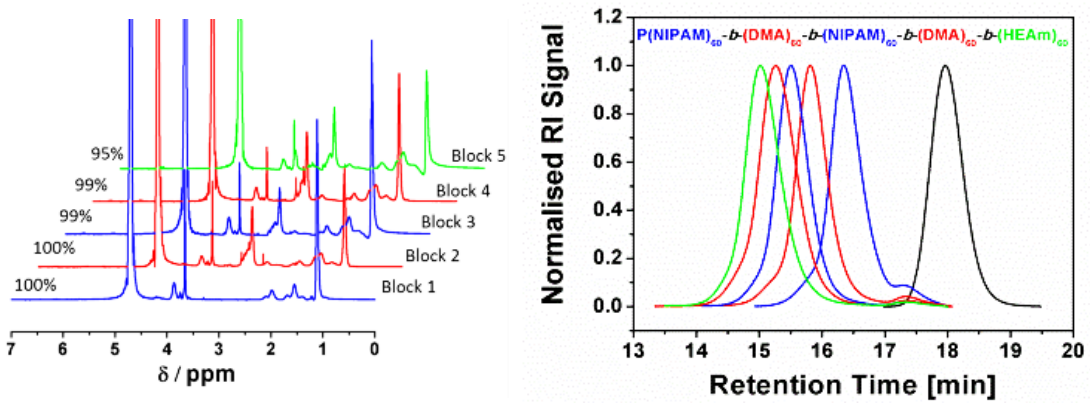

Figure 2.7: ^{1}H NMR spectra for pentablock star copolymer P11.5 composed of NIPAM, DMA and HEAm recorded in D_2O, showing quantitative conversion for every block (left) and SEC traces obtained, showing the evolution of molecular weight with increasing number of blocks (right). [M]:[I]:[CuBr]:[Me_6TREN] = [60]:[1]:[1.8]:[1.2].

The multi-block copolymerization was initiated using the 3-arm water soluble glycerol initiator (**Table 2.4, P0**). The first block of 20 repeating units of NIPAM per arm has been polymerized in 9 minutes (**P11.1**). Following the first block, 20 repeating units of DMA per arm has been reacted in only 5 minutes due to the higher propagation rate constant of DMA in comparison to NIPAM (**P11.2**)[32]. These two steps were repeated to get p(NIPAM)$_{60}$-*b*-p(DMA)$_{60}$-*b*-p(NIPAM)$_{60}$-*b*-p(DMA)$_{60}$ tetra-block copolymer (**P11.4**). Finally, the fifth block has been polymerized using 20 repeating units of PHEAm per arm (**P11.5**). As the total polymer chain length increased, a general trend of increase in the reaction time required for the consecutive block was observed. This can be due the decrease in initiator concentration or increase in $CuBr_2$ concentration per initiator as a result of termination reactions.[33]

Table 2.4: Overview of the obtained results for each block of P11.

Entry	ρ[a] (%)	$M_{n,theo}$ (g/mol)	$M_{n,SEC}$[b] (g/mol)	$Đ$[b]	Time per step[c] and total time (min)
P0	n/a	1450	1900	1.04	-
P11.1	100	8200	8100	1.14	9 (9)
P11.2	100	14100	14400	1.10	5 (14)
P11.3	99	20900	19200	1.10	13 (27)
P11.4	99	28600	24000	1.14	12 (39)
P11.5	95	35500	29700	1.14	45 (84)

[a] Conversion calculated from ^{1}H NMR. [b] DMF eluent, linear PMMA standards. [c] cumulative times stated in parenthesis.

Despite this, every block has reached to full conversion already in less than 15 minutes, except for the fifth block reaching 95% conversion in 45 minutes according to ^{1}H NMR measurement. Nevertheless, no significant side reaction or unreacted initiator was observed according to SEC spectra.

2.3. Conclusions

In conclusion, an aqueous polymerization technique has been investigated and by employing optimized reaction conditions, thermoresponsive core-first 3-arm star shaped polymers (**P1**-**P7**) and sequence controlled multi-block core-first 3-arm star shaped polymers based on acrylamides (**P8**-**P11**) utilizing a hydrophilic initiator have been reported for the first time. Core-first star shaped polymers can be synthesized *via* iterative chain extension up to a pentablock star, within a very short time period. Furthermore by systematically probing the optimum conditions for the polymerization, it was shown that costly and time consuming purification steps in between block copolymerizations can be avoided. Kinetic investigations have shown to be useful to obtain high chain end fidelity to retain and give excellent control over the molecular weight distribution. Importantly, the reactions were carried out in water; a "green", safe and cheaper alternative to organic solvents. This method can be easily up-scaled and be potentially utilized as a drug-delivery vehicle in biomedical applications.

2.4. Experimental

2.4.1. Materials

N-Isopropylacrylamide (NIPAM, 97%) was recrystallized from *n*-Hexane and stored at 4°C. 2-Hydroxyethyl acrylamide (HEAm, 97%) and *N*,*N*-Dimethylacrylamide (DMA, 99%) were passed over a short column of basic aluminium oxide to remove the inhibitor prior to use. Glycerol ethoxylate (Mn ≈ 1000 g/mol), α-Bromoisobutyryl bromide (BIBB, 98%) and Triethylamine (TEA, ≥99%) were also purchased from Sigma-Aldrich and used as received. All other chemicals and solvents were purchased from Sigma-Aldrich (UK) at the highest purity available and used as received unless stated otherwise. Used for the disproportionation and reaction solvent; water (H2O, HiPerSolv Chromanorm for HPLC) was purchased from VWR International (UK).

Tris(2-(dimethylamino)ethyl)amine (Me_6TREN) was synthesized according to literature procedures and stored at 4°C prior to use.[34,35] Copper(I) bromide (CuBr, 98%, Sigma-Aldrich) was purified by stirring in acetic acid overnight and washing with copious amounts of ethanol before drying under vacuum at 40°C overnight to constant weight.

2.4.2. Instruments and analysis

Proton nuclear magnetic resonance (^{1}H NMR) spectra were recorded on a Bruker AV-III 400 using D_2O at 303 K unless stated otherwise. Full monomer conversion was shown by the disappearance of the vinyl protons (H_2C=CH-CO–) (≈6.5-5.5 ppm). Otherwise, monomer conversion for NIPAM, HEAm and DMA was determined, comparing the integral of vinyl protons with isopropyl (–CH(CH_3)$_2$) (≈3.90-3.50 ppm), ethyl (NH(–CH_2–) (≈3.3 ppm) and dimethyl protons (–N(CH_3)$_2$) (≈3.0 ppm) respectively. All samples taken were immediately diluted with D_2O for analysis.

Size exclusion chromatography (SEC) measurements were conducted on an Agilent 1260 infinity system operating in DMF with 5mM NH_4BF_4 and equipped with refractive index and variable wavelength detector, 2 PLgel 5 μm mixed-C columns (300×7.5mm), a PLgel 5 mm guard column (50x7.5mm) and an autosampler. The instrument was calibrated with linear poly(methyl methacrylate) standards in range of 550-46890 g/mol. All samples were passed through neutral aluminium oxide to

remove any catalyst residues and filtered with a 0.2 μm Nylon 6,6 filter before analysis.

Turbidity measurements were performed on a Cary 100 UV-Vis spectrophotometer (Agilent) at a wavelength of 500 nm. Solutions of polymers were prepared in water (HPLC grade) at a concentration of 1 $mg \cdot mL^{-1}$ and stirred until fully dissolved. The samples were thermostatted at 20°C for 15 minutes prior to measurement. The transmittance was measured between 20°C and 80°C at a rate of $1°C \cdot min^{-1}$ in a heating and cooling cycle. The cloud points reported were determined as the 50% transmittance point during the heating cycle.

Matrix assisted laser desorption/ionisation – time of flight mass spectroscopy (MALDI-ToF MS) was performed using a Bruker Daltonics Autoflex MALDI-ToF mass spectrometer, equipped with a nitrogen laser at 337 nm with positive ion ToF detection. Polymer samples were measured as follows; solutions in THF of trans-2-[3-(4-*tert*-Butylphenyl)-2-methyl-2-propenylidene]malononitrile (DCTB, ≥98%) as matrix (30 $mg \cdot mL^{-1}$), potassium trifluoroacetate (KTFA) as cationisation agent (10 $mg \cdot mL^{-1}$) and sample (10 $mg \cdot mL^{-1}$) were mixed together in a 9:1:1 volume ratio for a total volume of 75 μL. 2 μL of the mixture was applied to the target plate. Spectra were recorded in reflectron mode and the mass spectrometer was calibrated with a peptide mixture up to 6000 Da.

All reactions were carried out using standard Schlenk techniques under inert atmosphere of oxygen-free argon.

2.4.3. Synthesis

Initiator Synthesis

In a round bottom flask, glycerol ethoxylate (26.4 mL) and TEA (22.35 mL) were stirred in dry THF (250 mL) and cooled down to 0°C in an ice-bath. A mixture of BIBB (16.7 mL) and THF (50 mL) were added dropwise over a period of an hour under argon. The mixture was then allowed to warm up to ambient temperature and stirred overnight. The precipitated salt was removed via filtration and washed with 30 mL of THF. The filtrate was collected an concentrated in vacuo, precipitated twice in hexane, dissolved in DCM and passed over a column of basic aluminium oxide to remove any impurities to yield a viscous off-white oil. (Yield = 29.0 mL, 78%).

$M_{n,MALDI}$ = 1456,1 Da, calculated for $[C_{55}H_{103}O_{26}Br_3+K^+]$ = 1455.392 Da.

$M_{n,SEC}$ = 1900 g·mol-1, ($Đ$ = 1.04).

^{1}H NMR (CDCl3, 400 MHz) δ: 4.32 (*t*, 6H), 3.76-3.71 (*m*, 7H), 3.69-3.58 (*broad*, 72H), 3.58-3.48 (*m*, 4H), 1.96 (*s*, 18H) ppm.

^{13}C NMR (CDCl3, 400 MHz) δ: 171.49, 78.30, 70.90-70.34, 68.65, 65.02, 55.62, 30.67 ppm.

Optimisation reactions for aqueous SET-LRP of star PNIPAM (R1-R11):

To a Schlenk tube fitted with a magnetic stirrer bar, different amounts of CuBr was weighed in and deoxygenated for 20 minutes **(Table 2.5).** The Schlenk tube was sealed with a rubber septum under a positive Argon pressure and lowered into an ice bath or oil bath set to 25°C. Then, respective amounts of Me_6TREN was added into a sealed vial with 2.5 mL of H_2O and deoxygenated for 15 minutes (Vial 1). Next, Vial 1 was transferred into the Schlenk tube with a degassed syringe and left for disproportionation for 30 minutes at 0°C or 25°C. Similarly in another vial (Vial 2), NIPAM (447 mg) and Gly-Br_3 (125 mg) were dissolved in 2 mL of H_2O under stirring and deoxygenated with Argon for 15 minutes. Vial 2 was then transferred with a degassed syringe into the Schlenk tube to start the polymerization. The transfer of Vial 2 defines t_0.

Table 2.5: Amounts of CuBr and Me_6TREN used in each reaction for **R01-R11**.

Entry	[M]:[I]:[CuBr]:[Me_6TREN]	CuBr [mg]	Me_6TREN [µL]	Temperature [°C]
R01	60 : 1 : 0.8 : 0.4	10	7	25
R02	60 : 1 : 1.2 : 1.2	11	21	25
R03	60 : 1 : 1.8 : 1.2	17	21	25
R04	60 : 1 : 1.8 : 1.8	17	32	25
R05	60 : 1 : 2.4 : 1.2	22	21	25
R06	60 : 1 : 2.4 : 2.4	22	42	25
R07	60 : 1 : 1.2 : 1.2	11	21	0
R08	60 : 1 : 1.8 : 1.2	17	21	0
R09	60 : 1 : 1.8 : 1.8	17	32	0
R10	60 : 1 : 2.4 : 1.2	22	21	0
R11	60 : 1 : 2.4 : 2.4	30	42	0

Aqueous SET-LRP of star PNIPAM with increasing DP_n (P1-P7):

In a typical reaction, CuBr (15 mg) was weighed into a Schlenk tube and fitted with a stirrer bar and deoxygenated with Argon for 20 minutes. The Schlenk tube was sealed with a rubber septum under a positive pressure of Argon and lowered into an ice bath. In the meanwhile, Me_6TREN (21 µL) was added to a vial with 2.5 mL of H_2O and sealed and degassed for 15 minutes (Vial 1) in an ice bath. Vial 1 was then transferred with a degassed syringe into the Schlenk tube and allowed to disproportionate for 30 minutes. In another vial (Vial 2), NIPAM (DP_n = 60-240) and Gly-Br_3 (125 mg, 1900 g·mol^{-1}) were dissolved in H_2O under stirring and deoxygenated with Argon for 20 minutes at 0°C **(Table 2.6)**. Vial 2 was then transferred with a degassed syringe into the Schlenk tube to start the polymerization. The transfer of Vial 2 defines t_0.

Table 2.6: Amounts of NIPAM used to obtain polymers **P1** to **P7** with increasing DP_n.

Entry	DP_n	NIPAM (g)	H_2O[a] (mL)
P1	60	0.447	2.0
P2	90	0.670	3.0
P3	120	0.893	4.0
P4	150	1.117	7.0
P5	180	1.340	7.5
P6	210	1.563	9.0
P7	240	1.787	9.0

[a] Indicates the amount of water used to dissolve NIPAM and Gly-Br_3 only prior to addition into a Schlenk tube.

Aqueous SET-LRP of the sequence controlled star polymers (P8-P11)

The polymerizations were carried out as described for the synthesis of star PNIPAM.

CuBr (15 mg) was weighed into a Schlenk tube and carefully fitted with a stirrer bar and deoxygenated with Argon for 20 minutes. The Schlenk tube was slowly sealed with a rubber septum under a positive pressure of Argon and lowered into an ice bath. In the meanwhile, Me_6TREN (21 µL) was added to a vial with 2.5 mL of H_2O and sealed and degassed for 15 minutes (Vial 1) in an ice bath. Vial 1 was then transferred with a degassed syringe into the Schlenk tube and allowed to disproportionate for 30 minutes at 0°C. In another vial (Vial 2), NIPAM (0.447 g, 4mmol) and Gly-Br_3 (125 mg, 1900 $g \cdot mol^{-1}$) were dissolved in 2 mL of H_2O under stirring and deoxygenated with Argon for 20 minutes at 0°C. Vial 2 was then transferred with a degassed syringe into the Schlenk tube to start the polymerization of the first $PNIPAM_{60}$ block. Once desired conversion was reached, the monomer for the next block was added to the Schlenk tube containing the polymer, as described for Vial 2 above in the following amounts (**Table 2.7**) to obtain **P8-P10** and the pentablock copolymer **P11**:

Table 2.7: Amounts of monomer and H_2O used for the chain extensions to obtain polymers **P8-P11**.

Entry	Monomer	DP_n	Amount	H_2O[a] [mL]
P8	NIPAM	120	894 mg	4.0
P9	DMA	120	814 µL	4.0
P10	HEAm	120	820 µL	4.0
P11.2	DMA	60	407 µL	2.0
P11.3	NIPAM	60	447 mg	2.0
P11.4	DMA	60	407 µL	2.0
P11.5	HEAm	60	410 µL	2.0

[a] Indicates the amount of water used to dissolve the monomer prior to addition into the Schlenk tube.

Before every chain extension, the monomer consumption for the previous block was monitored by sampling every 3 or 5 minutes to determine full conversion. Once this was done, a new reaction was started from beginning, where this time the successive block was investigated, until the desired polymer was obtained. Chain extensions were carried out at a conversion ≥95% (by ^{1}H NMR).

2.4.4. Characterization

The following SEC traces and ^{1}H NMR spectra were obtained after 60 minutes of reaction time for **R1-R11**.

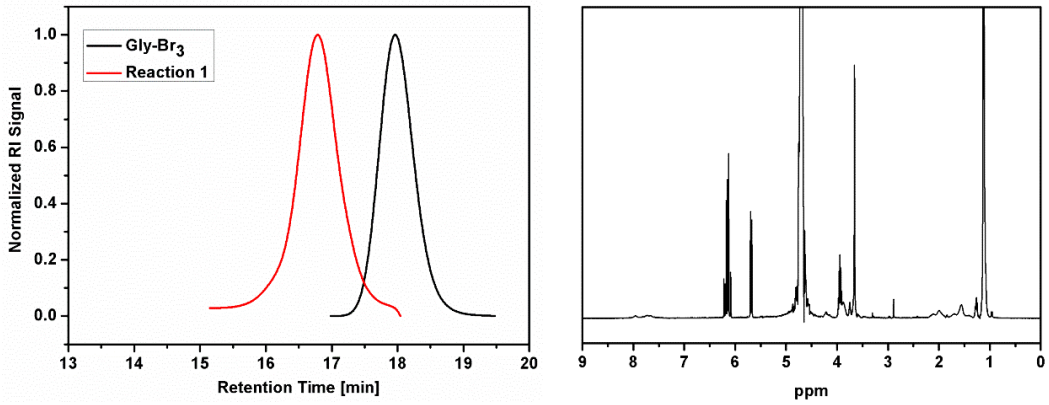

Figure 2.8: SEC trace (left) and ^{1}H NMR spectrum (right) obtained from reaction 1 (**R1**) showing an $M_{n,SEC}$ = 6000 g·mol^{-1}, $Đ$ = 1.12 and 38% conversion.

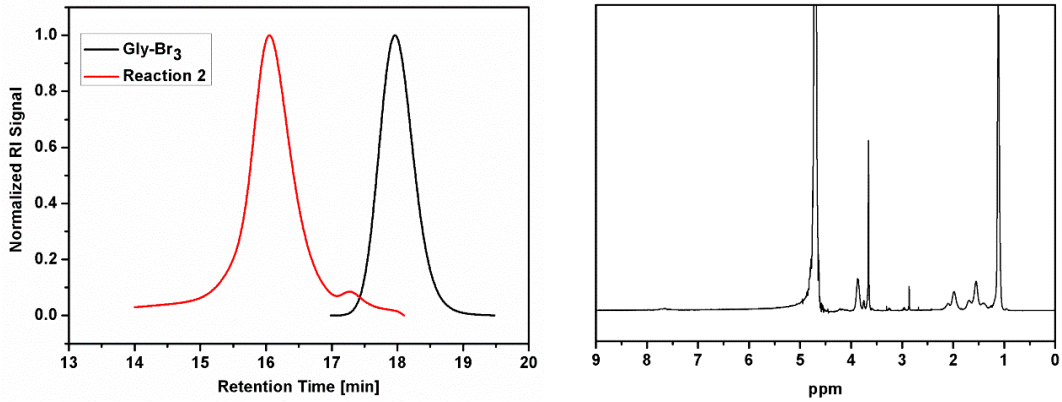

Figure 2.9: SEC trace (left) and ^{1}H NMR spectrum (right) obtained from reaction 2 (**R2**) showing an $M_{n,SEC}$ = 11900 g·mol^{-1}, $Đ$ = 1.41 and 100% conversion.

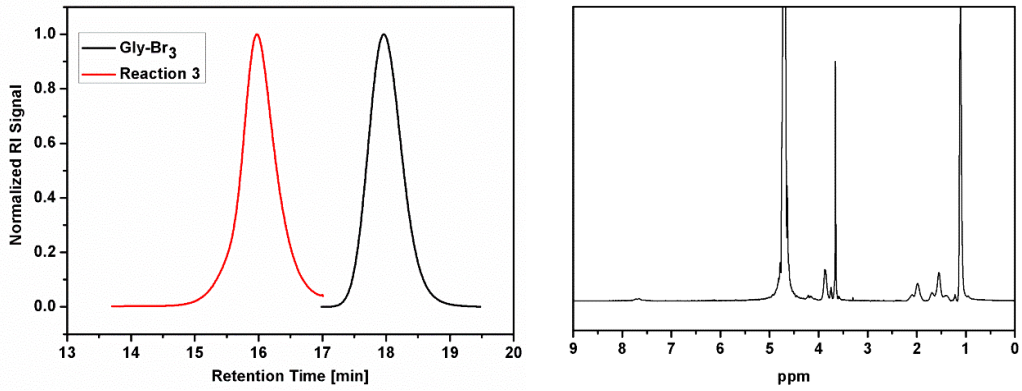

Figure 2.10: SEC trace (left) and ^{1}H NMR spectrum (right) obtained from reaction 3 (**R3**) showing an $M_{n,SEC}$ = 12700 g·mol^{-1}, $Đ$ = 1.14 and 100% conversion.

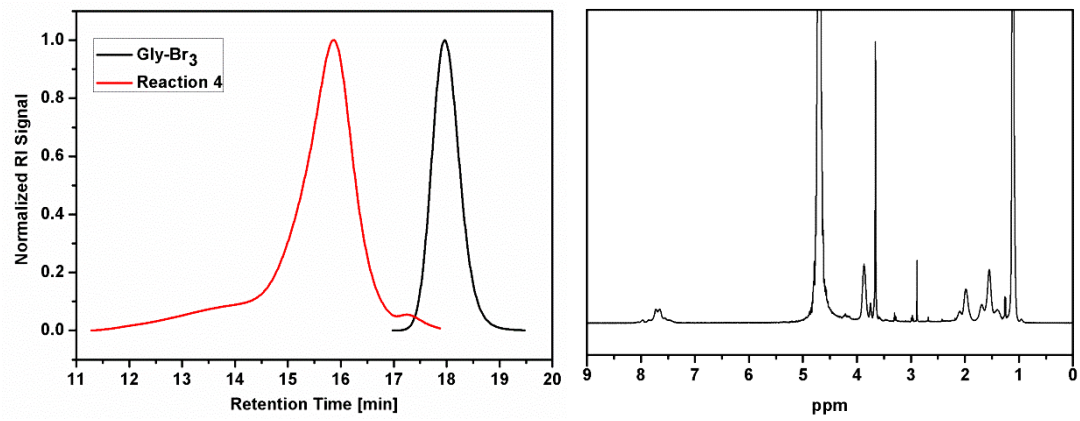

Figure 2.11: SEC trace (left) and ^{1}H NMR spectrum (right) obtained from reaction 4 (**R4**) showing an $M_{n,SEC}$ = 15800 g·mol^{-1}, $Đ$ = 1.48 and 100% conversion.

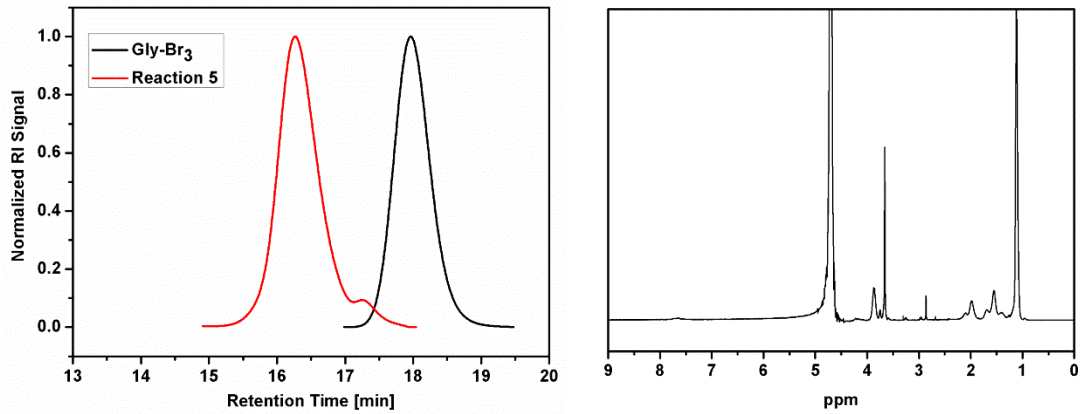

Figure 2.12: SEC trace (left) and ^{1}H NMR spectrum (right) obtained from reaction 5 (**R5**) showing an $M_{n,SEC}$ = 8800 g·mol^{-1}, $Đ$ = 1.30 and 100% conversion.

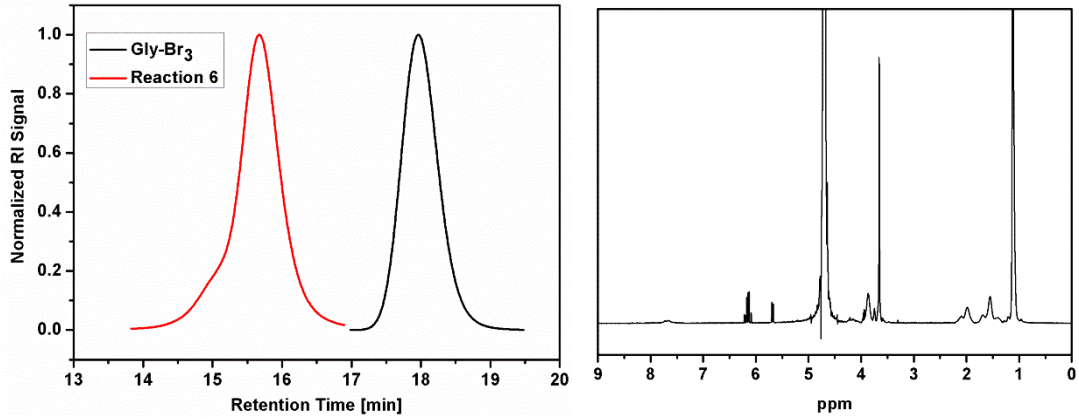

Figure 2.13: SEC trace (left) and ^{1}H NMR spectrum (right) obtained from reaction 6 (**R6**) showing an $M_{n,SEC}$ = 15900 g·mol^{-1}, $Đ$ = 1.29 and 79% conversion.

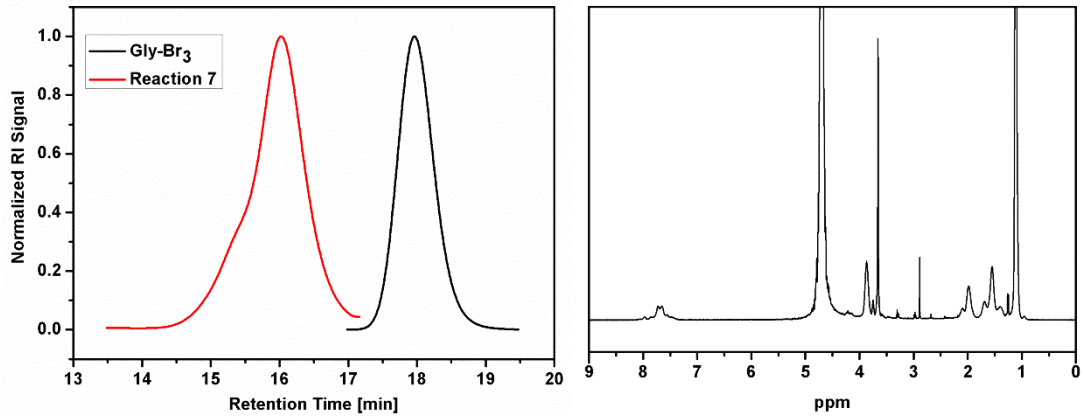

Figure 2.14: SEC trace (left) and ^{1}H NMR spectrum (right) obtained from reaction 7 (**R7**) showing an $M_{n,SEC}$ = 12300 g·mol^{-1}, $Đ$ = 1.13 and 100% conversion.

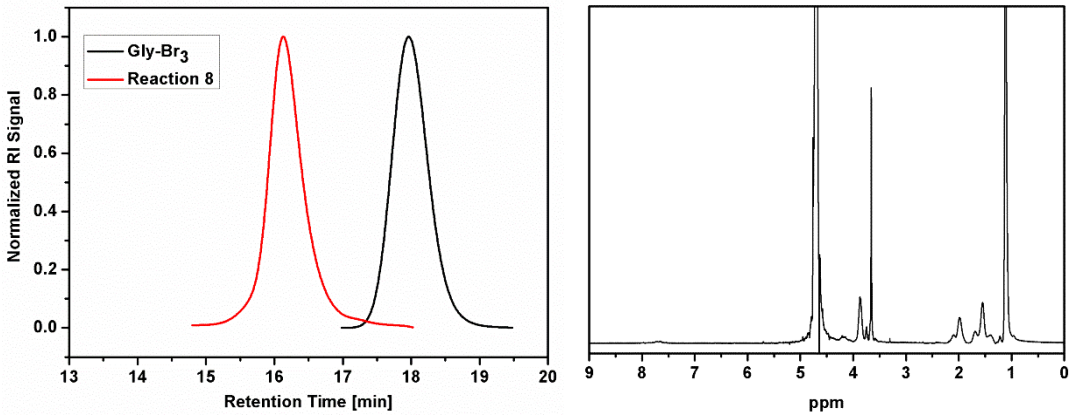

Figure 2.15: SEC trace (left) and ^{1}H NMR spectrum (right) obtained from reaction 8 (**R8**) showing an $M_{n,SEC}$ = 10500 g·mol^{-1}, $Đ$ = 1.10 and 100% conversion.

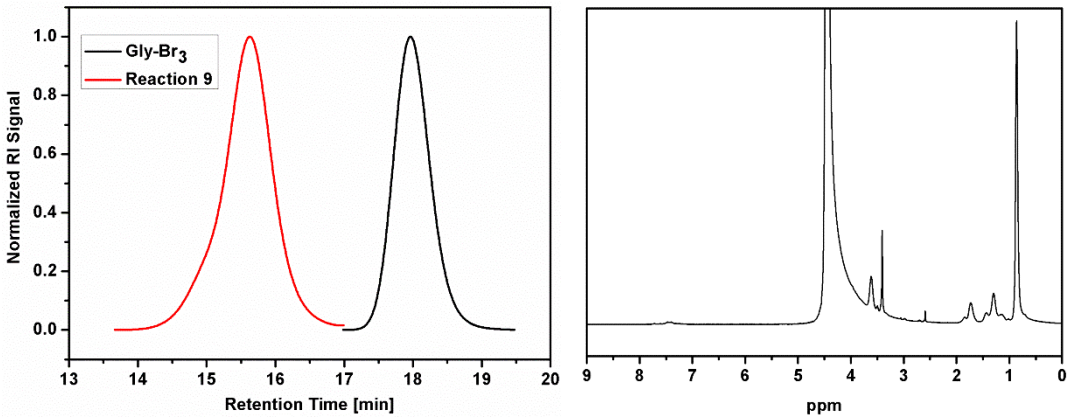

Figure 2.16: SEC trace (left) and ^{1}H NMR spectrum (right) obtained from reaction 9 (**R9**) showing an $M_{n,SEC}$ = 17100 g·mol^{-1}, $Đ$ = 1.24 and 100% conversion.

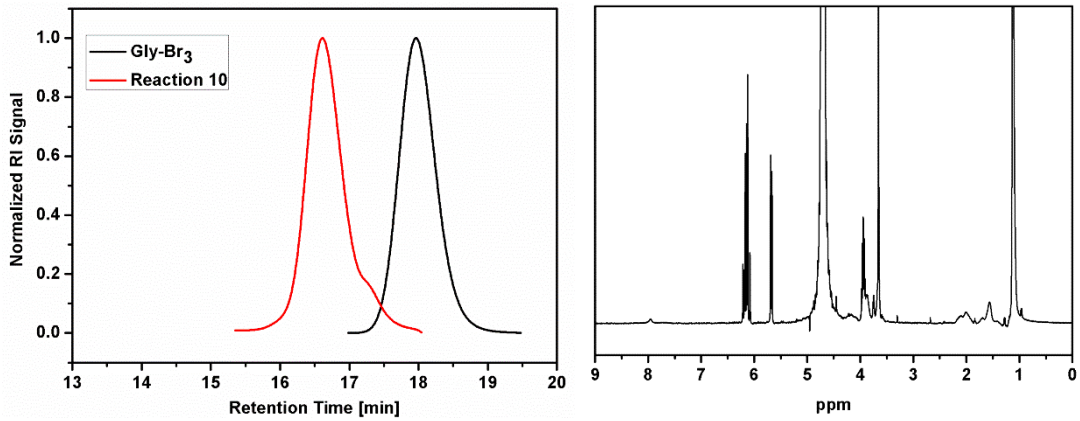

Figure 2.17: SEC trace (left) and ^{1}H NMR spectrum (right) obtained from reaction 10 (**R10**) showing an $M_{n,SEC}$ = 5400 g·mol^{-1}, $Đ$ = 1.07 and 37% conversion.

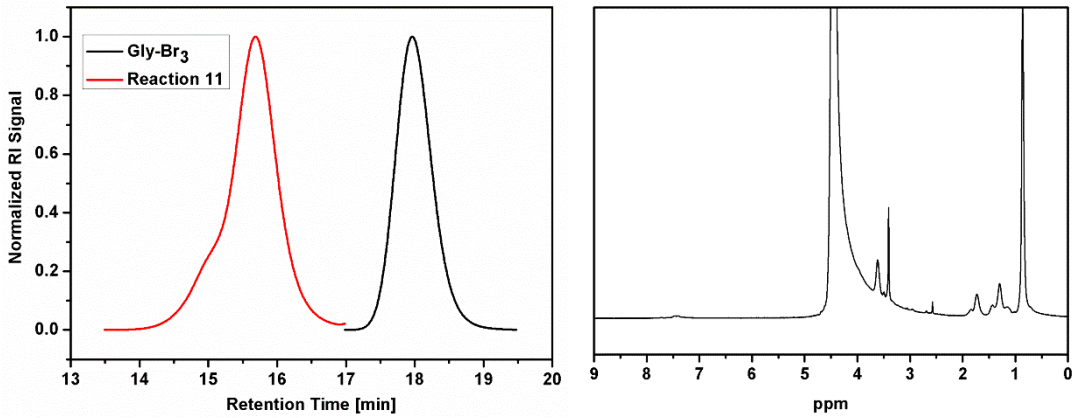

Figure 2.18: SEC trace (left) and ^{1}H NMR spectrum (right) obtained from reaction 11 (**R11**) showing an $M_{n,SEC}$ = 15900 g·mol^{-1}, $Đ$ = 1.30 and 100% conversion.

2.5. References

1. I. Cobo, M. Li, B. S. Sumerlin and S. Perrier, *Nat. Mater.*, 2015, **14**, 143-159.
2. B. Lewandowski, G. De Bo, J. W. Ward, M. Papmeyer, S. Kuschel, M. J. Aldegunde, P. M. E. Gramlich, D. Heckmann, S. M. Goldup, D. M. D'Souza, A. E. Fernandes and D. A. Leigh, *Science*, 2013, **339**, 189-193.
3. J.-F. Lutz, M. Ouchi, D. R. Liu and M. Sawamoto, *Science*, 2013, **341**, 628.
4. H. Colquhoun and J.-F. Lutz, *Nat. Chem.*, 2014, **6**, 455-456.
5. S. Pearson, H. Lu and M. H. Stenzel, *Macromolecules*, 2015, **48**, 1065-1076.
6. F. Zhang, S. Zhang, S. F. Pollack, R. Li, A. M. Gonzalez, J. Fan, J. Zou, S. E. Leininger, A. Pavia-Sanders, R. Johnson, L. D. Nelson, J. E. Raymond, M. Elsabahy, D. M. P. Hughes, M. W. Lenox, T. P. Gustafson and K. L. Wooley, *J. Am. Chem. Soc.*, 2015, **137**, 2056-2066.
7. Y. Chen, M. S. Lord, A. Piloni and M. H. Stenzel, *Macromolecules*, 2015, **48**, 346-357.
8. Q. Zhang, L. Su, J. Collins, G. Chen, R. Wallis, D. A. Mitchell, D. M. Haddleton and C. R. Becer, *J. Am. Chem. Soc.*, 2014, **136**, 4325-4332.
9. M. E. Fox, F. C. Szoka and J. M. J. Frechet, *Acc. Chem. Res.*, 2009, **42**, 1141-1151.
10. W. Shi, A. L. Hamilton, K. T. Delaney, G. H. Fredrickson, E. J. Kramer, C. Ntaras, A. Avgeropoulos and N. A. Lynd, *J. Am. Chem. Soc.*, 2015, **137**, 6160-6163.
11. H. Gao, S. Ohno and K. Matyjaszewski, *J. Am. Chem. Soc.*, 2006, **128**, 15111-15113.
12. T. G. McKenzie, E. H. H. Wong, Q. Fu, S. J. Lam, D. E. Dunstan and G. G. Qiao, *Macromolecules*, 2014, **47**, 7869-7877.
13. Q. Zhang, G.-Z. Li, C. R. Becer and D. M. Haddleton, *Chem. Commun.*, 2012, **48**, 8063-8065.
14. K. Kempe, A. Krieg, C. R. Becer and U. S. Schubert, *Chem. Soc. Rev.*, 2012, **41**, 176-191.
15. S. Harrisson and J. Nicolas, *ACS Macro Lett.*, 2014, **3**, 643-647.
16. S. Sinnwell, M. Lammens, M. H. Stenzel, F. E. Du Prez and C. Barner-Kowollik, *J. Polym. Sci. Part A: Polym. Chem.*, 2009, **47**, 2207-2213.
17. A. H. Soeriyadi, C. Boyer, F. Nystroem, P. B. Zetterlund and M. R. Whittaker, *J. Am. Chem. Soc.*, 2011, **133**, 11128-11131.
18. C. Boyer, A. H. Soeriyadi, P. B. Zetterlund and M. R. Whittaker, *Macromolecules*, 2011, **44**, 8028-8033.
19. Q. Zhang, P. Wilson, Z. Li, R. McHale, J. Godfrey, A. Anastasaki, C. Waldron and D. M. Haddleton, *J. Am. Chem. Soc.*, 2013, **135**, 7355-7363.
20. Q. Zhang, P. Wilson, A. Anastasaki, R. McHale and D. M. Haddleton, *ACS Macro Lett.*, 2014, **3**, 491-495.
21. W. Zhang, W. Zhang, Z. Zhang, Z. Cheng, Y. Tu, Y. Qiu and X. Zhu, *J. Polym. Sci. Part A: Polym. Chem.*, 2010, **48**, 4268-4278.
22. S. Paillet, A. Roncin, G. Clisson, G. Pembouong, L. Billon, C. Derail and M. Save, *J. Polym. Sci. Part A: Polym. Chem.*, 2012, **50**, 2967-2979.
23. C. Boyer, A. Derveaux, P. B. Zetterlund and M. R. Whittaker, *Polym. Chem.*, 2012, **3**, 117-123.

24. C. Waldron, A. Anastasaki, R. McHale, P. Wilson, Z. Li, T. Smith and D. M. Haddleton, *Polym. Chem.*, 2014, **5**, 892-898.
25. E. H. H. Wong, A. Blencowe and G. G. Qiao, *Polym. Chem.*, 2013, **4**, 4562-4565.
26. R. Aksakal, M. Resmini and C. R. Becer, *Polym. Chem.*, 2016, **7**, 171-175.
27. S. R. Samanta, V. Nikolaou, S. Keller, M. J. Monteiro, D. A. Wilson, D. M. Haddleton and V. Percec, *Polym. Chem.*, 2015, **6**, 2084-2097.
28. A. Anastasaki, A. J. Haddleton, Q. Zhang, A. Simula, M. Droesbeke, P. Wilson and D. M. Haddleton, *Macromol. Rapid Commun.*, 2014, **35**, 965-970.
29. C. Weber, T. Neuwirth, K. Kempe, B. Ozkahraman, E. Tamahkar, H. Mert, C. R. Becer and U. S. Schubert, *Macromolecules*, 2012, **45**, 20-27.
30. C. R. Becer, S. Hahn, M. W. M. Fijten, H. M. L. Thijs, R. Hoogenboom and U. S. Schubert, *J. Polym. Sci. Part A: Polym. Chem.*, 2008, **46**, 7138-7147.
31. A. Anastasaki, C. Waldron, P. Wilson, R. McHale and D. M. Haddleton, *Polym. Chem.*, 2013, **4**, 2672-2675.
32. N. H. Nguyen, B. M. Rosen and V. Percec, *J. Polym. Sci. Part A: Polym. Chem.*, 2010, **48**, 1752-1763.
33. F. Alsubaie, A. Anastasaki, P. Wilson and D. M. Haddleton, *Polym. Chem.*, 2015, **6**, 406-417.
34. M. Ciampolini and N. Nardi, *Inorg. Chem.*, 1966, **5**, 41-44.
35. J. Queffelec, S. G. Gaynor and K. Matyjaszewski, *Macromolecules*, 2000, **33**, 8629-8639.

Chapter 3

SET-LRP of acrylates mediated by a 1 penny copper coin

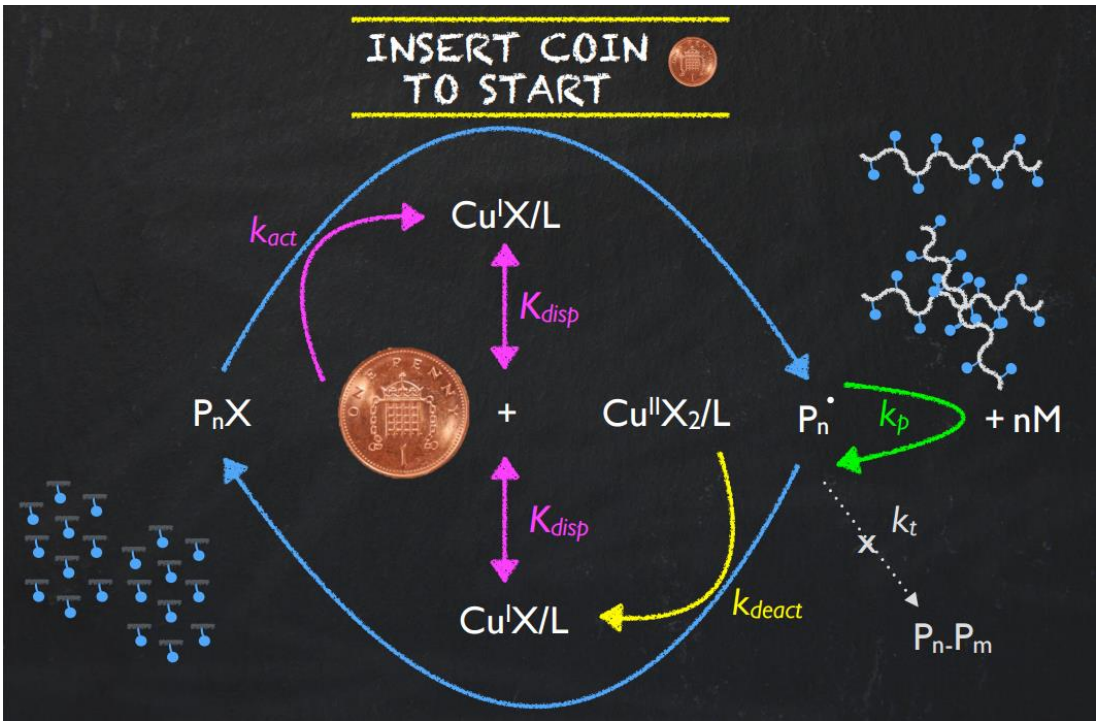

A British 1 penny coin (1 p) was used to catalyze the polymerization of a selection of hydrophobic and hydrophilic acrylate monomers using linear and star shaped initiators to obtain polymers even in 50 gram scale with low dispersity values (Đ = 1.05 - 1.11). When compared with Cu wire systems, no induction period was observed, hence demonstrating an economic and easily accessible catalyst for SET-LRP acrylates.

Parts of this chapter have been published;

R. Aksakal, M. Resmini and C.R. Becer, *Polym. Chem*., 2016, **7**, 6564 – 6569.

3.1. Introduction

The ability to control chemical composition and architecture is a key priority in polymer synthesis, to obtain materials with the specific characteristics for desired applications. In the last two decades, several robust controlled radical polymerization (CRP) techniques have been developed, that enable the synthesis of well-defined polymers, with excellent control over chain length, dispersity and composition. Among the most established CRP methods reversible addition-fragmentation chain transfer (RAFT) polymerization,[1,2] nitroxide mediated polymerization (NMP),[3,4] atom transfer radical polymerization (ATRP)[5-7] and more recently, single electron transfer living radical polymerization (SET-LRP)[8,9] are the four major techniques that have been widely investigated. SET-LRP, in particular, is a versatile method that allows excellent control over the polydispersity (*Đ*) with high chain end fidelity, even at high monomer conversions (ρ). Unlike the activation step in ATRP with Cu(I)X (X = Br or Cl), the mechanism proposed for SET-LRP, requires the disproportionation of Cu(I)X to Cu(0) and Cu(II)X_2, in a polar solvent (*i.e.* DMSO, H_2O or alcohols), and an *N*-donor ligand (*i.e.* Me_6TREN or PMDETA).[10,11] Despite various hypotheses, the detailed mechanism of SET-LRP is yet to be fully understood.[12-15] Detailed optimization of reaction conditions and the choice of catalyst system are essential requirements in order to obtain the desired polymer. Many reports have already identified the importance of the ligand[16] choice and the deactivator concentration,[17] effect of solvent,[18] initiator type,[19-22] and other additives[23] as essential parameters to be considered. The choice of metal used as a catalyst in the polymerisation is also crucial. In comparison to other zero valent metals, Cu is the most widely used catalyst,[24] obtained from various sources and in different formats. Elegant examples describe the successful use of Cu powder,[25] Cu pellets,[26] Cu tubing,[27,28] Cu plate,[29] Cu wire[30] and in situ generated Cu(0) particles under aqueous SET-LRP conditions. In aqueous SET-LRP, the pre-disproportionation of Cu(I)Br in water in the presence of Me_6TREN[15,31] results in highly active, in situ generated Cu(0) particles, which provided the shortest polymerization periods. By employing this system, multi-block copolymers of various acrylamides were synthesized within 3.5 hours.[32] Our group has also recently demonstrated the first example of synthesis of star shaped penta-block copolymers *via* aqueous SET-LRP, completed in just under 90 minutes.[33] On the other hand, especially in the case of Cu wire, pellets and plate, the pre-activation

of the Cu surface plays a crucial role for the reactivity and outcome of the polymerization.[34] For pre-activation, typically HCl or hydrazine is employed to remove Cu oxides from the surface, which increases the polymerization rate and minimizes the induction period. Interestingly, there are conflicting reports in the literature regarding the mechanistic explanation that justifies the presence of an induction period.[35,36] Nevertheless, an attempt was made to investigate the influence of a new type of copper source, namely a 1 penny coin. It was hypothesized that using a penny coin for typical conditions would help to shine light on the understanding of the role of the copper catalyst for SET-LRP on well investigated monomers such as methyl acrylate, ethyl acrylate, di(ethyleneglycol) ethyl ether acrylate and oligo(ethylene glycol) acrylate. SET-LRP of these monomers were initiated with a linear and four-arm initiator in order to establish a comparison on the reactivity behavior.

3.2. Results and Discussion

In this work, findings on the polymerization of various hydrophilic and hydrophobic acrylates using a British 1 penny coin as an alternative and readily available copper source are presented. A linear (ethyl-2-bromo isobutyrate, EBiB) and a 4-arm star initiator (PE-Br$_4$) have been utilized to carry out kinetic investigation on the SET-LRP of methyl acrylate (MA), ethyl acrylate (EA), di(ethyleneglycol) ethyl ether acrylate (eDEGA) and oligo(ethylene glycol) methyl ether acrylate (OEGA) (**Scheme 3.1**). The polymers were obtained with very good control over dispersity ($Đ$ < 1.11) and in close agreement between theoretical and experimental molecular weight. Moreover, the feasibility of using a coin as a copper source for the polymerization of EA has been demonstrated for different chain lengths (DP_n = 20–80) as well as presented the SET-LRP of EA in relatively large scale (50 g).

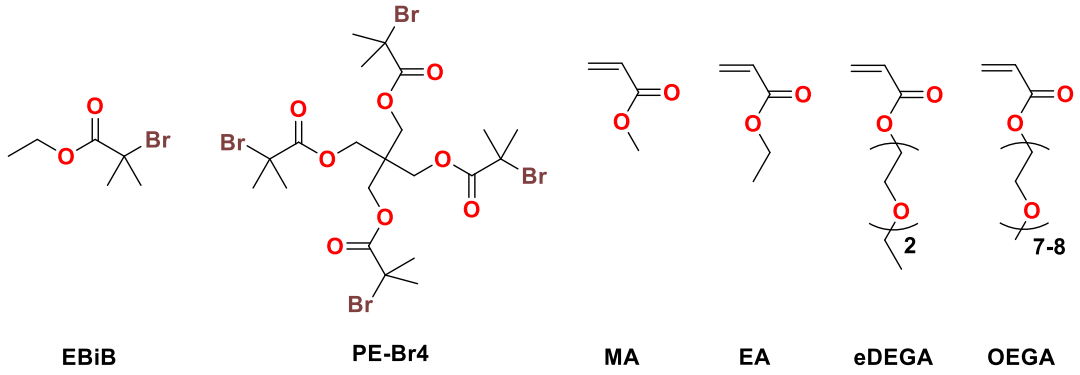

Scheme 3.1: Initiators and monomers used in this work.

In order to avoid star–star coupling in later reactions, initial polymerizations of MA initiated by PE-Br$_4$ were carried out at different monomer concentrations (*i.e.* 1:1, 1:4 and 1:10 *v/v* monomer:solvent). When a MA:DMSO ratio of 1:1 (*v/v*) was used, significant side products derived from coupling reactions were observed in the SEC traces, despite a relatively low MWD ($M_{n,SEC}$ = 4200 g·mol^{-1}, $Đ$ = 1.18). The amount of coupling was at minimum when either ratios of 1:4 or 1:10 (*v/v*) were used. However, the conversion of the latter was determined to be 87% by ^{1}H NMR spectroscopy, whereas the ratio of 1:4 resulted in a conversion of 97% already after 3 h. The obtained SEC traces are presented in **Figure 3.1**. Based on these results, the monomer:solvent ratio was kept at 1:4 (*v/v*) for the following reactions and the polymerization kinetics were investigated for up to 3 hours.

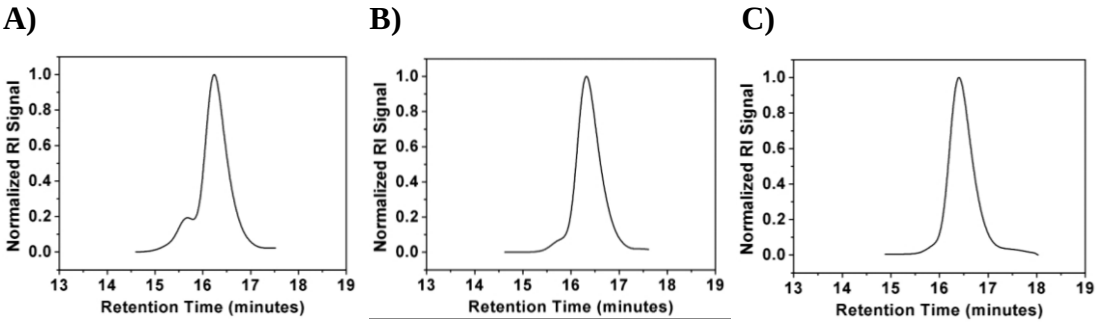

Figure 3.1: SEC traces obtained from the SET-LRP of MA_{40} in; **A)** monomer:DMSO = 1:1 (*v/v*): $M_{n,SEC}$ = 4200 g·mol^{-1}, $Đ$ = 1.18, ρ = 97% **B)** monomer:DMSO = 1:4 (*v/v*): $M_{n,SEC}$ = 4000 g·mol^{-1}, $Đ$ = 1.18, ρ = 97% **C)** monomer:DMSO = 1:10 (*v/v*): $M_{n,SEC}$ = 3600 g.mol^{-1}, $Đ$ = 1.18, ρ = 87%.

Using the suitable reaction conditions determined in the control reactions with MA, a series of hydrophobic and hydrophilic monomers were polymerized using a linear and 4-arm star shaped initiator. An overview of the obtained polymers (**P1**-**P8**) can be found in **Table 3.1**.

Table 3.1: Polymers obtained in this study using linear EBiB and 4-arm PE-Br_4 initiators under the same SET-LRP conditions [M]:[I]:[$CuBr_2$]:[Me_6TREN] = 20:1:0.1:0.19 at 25°C in DMSO for 3 h.

Polymer	Initiator	Monomer (DP_n = 20)	ρ (%)	$M_{n,theo}$ (g·mol^{-1})	$M_{n,SEC}$[c] (g·mol^{-1})	$Đ$[c]	$\Delta m_{Cu(0)}$ (mg)
P1	EBiB	MA	97[a]	1900	2000	1.10	6.5
P2	EBiB	EA	99[b]	2200	2600	1.10	7.1
P3	EBiB	eDEGA	98[b]	3900	4500	1.11	7.6
P4	EBiB	$OEGA_{480}$	93[a]	9200	9200	1.07	8.1
P5	PE-Br_4	MA	98[a]	2400	1600	1.07	7.9
P6	PE-Br_4	EA	99[b]	2700	2600	1.08	7.5
P7	PE-Br_4	eDEGA	97[b]	4400	4400	1.09	7.6
P8	PE-Br_4	$OEGA_{480}$	80[a]	8400	8300	1.06	7.5

[a]Conversion was measured by ^{1}H NMR spectroscopy. [b]Conversion was measured by GC. [c]THF (TEA, 2% *v/v*) eluent, linear p(MMA) standards.

For all reactions, the mass change of the copper coin, between before and after the polymerizations was also noted. The importance and relevance of the mass change will be discussed later in this section.

The SET-LRP kinetics for **P1–P4**, which are catalysed by 1 p coin at 25 °C in DMSO are shown in **Figure 3.2**. The reactions were initiated with the linear initiator (EBiB), whereas all molar ratios were kept constant at [Monomer]:[EBiB]:[Me_6TREN]:[$CuBr_2$]=20:1:0.19:0.1.

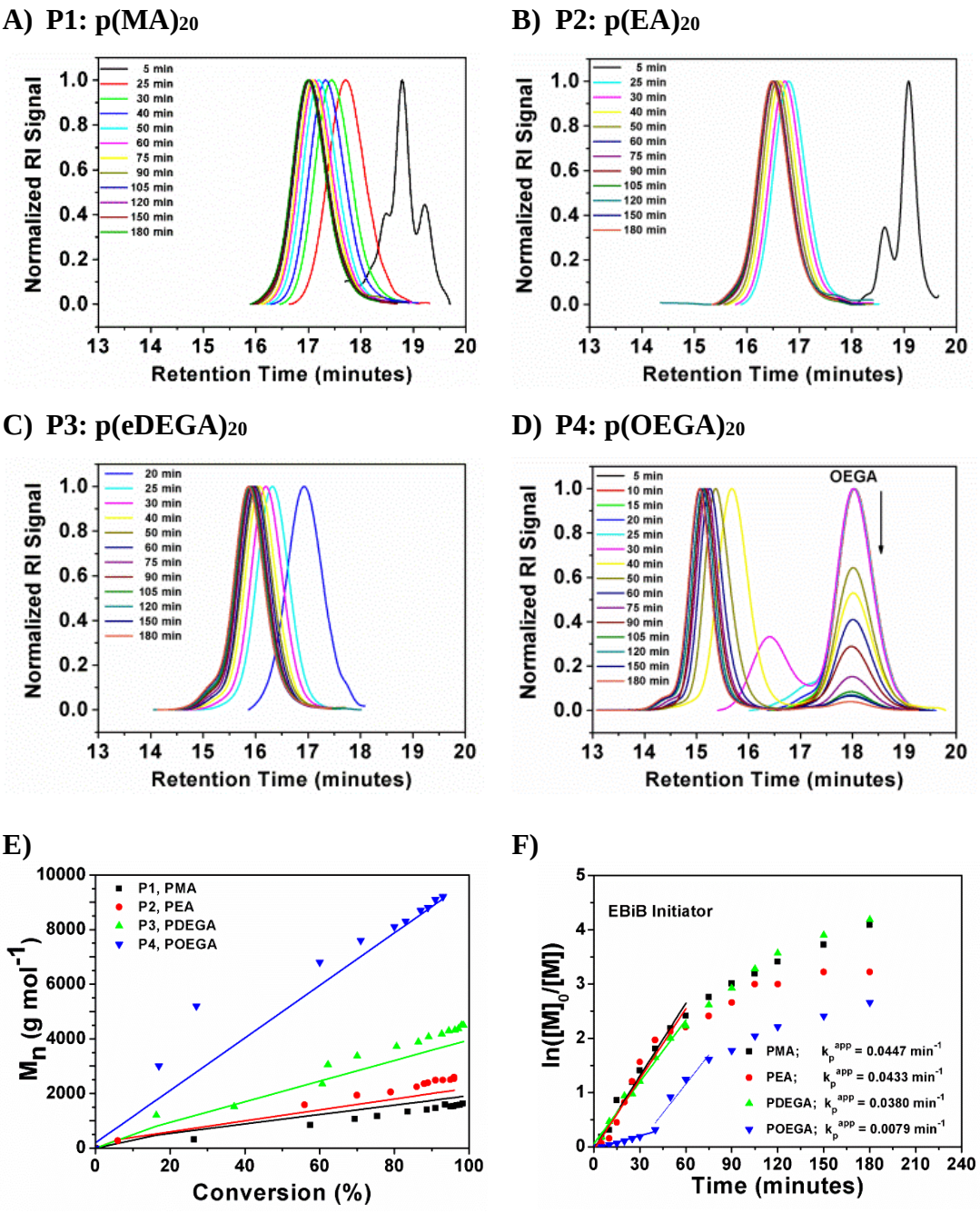

Figure 3.2: A general overview of the characterization of the obtained polymers are displayed above. SEC traces of the obtained polymers **A) P1, B) P2, C) P3** and **D) P4** using EBiB as initiator. **E)** M_n *vs.* conversion plot for **P1-P4**. Coloured symbols represent M_n obtained from SEC; straight lines represent theoretical M_n calculated from corresponding conversions **F)** Ln($[M]_0/[M]$) vs. time plot for **P1-P4** with the corresponding k_p^{app} values obtained from the initial linear increase.

The obtained SEC traces show no bimolecular coupling or early termination for the hydrophobic monomers MA and EA (**Figure 3.2**, **A** and **B** respectively), whereas little termination from bimolecular coupling was evident for the hydrophilic monomers eDEGA and OEGA (**C** and **D** respectively), which indicates a higher retention in chain end fidelity for the polymerization of MA and EA. As a representative example, the chain end fidelity of **P1** was characterized *via* MALDI-ToF MS and ^{1}H NMR spectroscopy (**Figure 3.3**). A secondary distribution, which was attributed to the –OH terminated species of p(MA)$_{17}$, indicating the presence of a certain loss in chain end functionality is present.

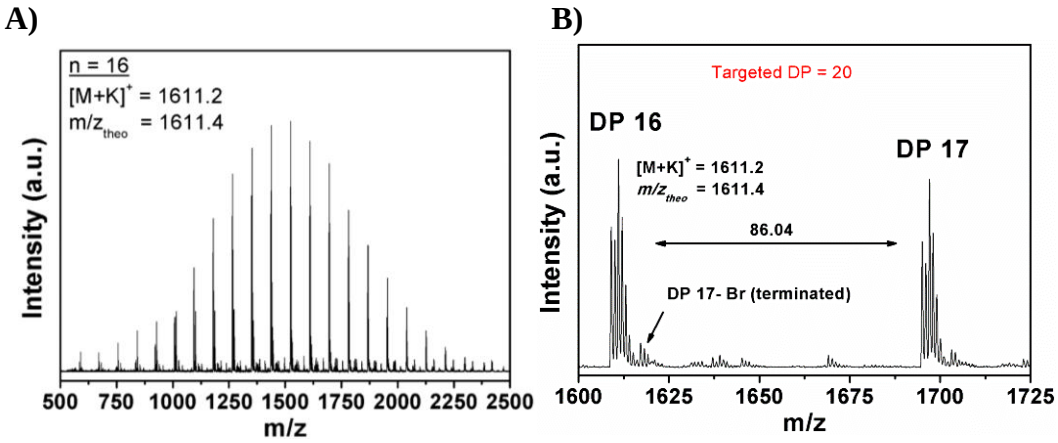

Figure 3.3: A) MALDI-ToF MS spectrum of **P1** in full scale **B)** MALDI-ToF MS spectrum displaying peaks for the secondary distribution of **P1** p(MA)$_{20}$. $M_{n,SEC}$ = 2000 g·mol^{-1}, $Đ$ = 1.10, ρ = 97%.

In order to characterize to what extend the chain end fidelity is retained, the polymer was isolated *via* precipitation and subjected to ^{1}H NMR spectroscopy. By comparing the broad signal of –C*H*–Br (ω-terminus) between 4.09–4.00 ppm and CH$_3$–C*H*$_2$–O (initiator) between 3.92–3.80 ppm, the end group fidelity was calculated to be 81% (**Figure 3.4**). It is known that the end group fidelity can still be improved even further by varying the ligand and/or CuBr$_2$ concentration in such SET-LRP systems.

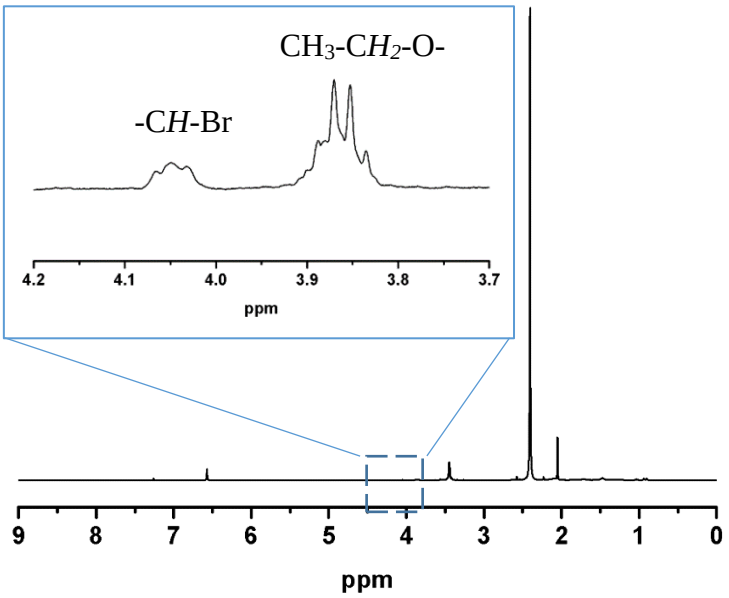

Figure 3.4: Full ^{1}H NMR spectrum of **P1** used to determine 81% chain end fidelity from the comparison of C*H*-Br (*ω*-terminus) integral between 4.09-4.00 ppm and CH_3–C*H*$_2$–O– (initiator) integral between 3.92-3.80 ppm.

The semi-logarithmic kinetic plot of the polymerizations is presented in **Figure 3.2**, **F**. The initial linear increase in the first 60 minutes for **P1, P2** and **P3** show similar apparent rate constants (k_p^{app}) with no evidence of an induction period.

On the other hand, a significant de*via*tion from the general trend was observed for **P4** in the first 30 minutes (ρ = 17%), which was attributed to the known induction period of $(OEGA)_n$ monomers, bearing long side chains.[37] The second linear regime for **P4** between 30-60 minutes, relates to the overall values obtained for **P1**–**P3** in the first hour. After an hour of reaction period, all polymerization reactions tend to display a second linear regime, in which the rate constant decreases until quantitative conversion is reached. This is due to the low concentration of the monomer left at later stages of the polymerization. **P4** follows a similar trend as **P1**–**P3**, after the induction period. Although very good control over the MWDs was maintained, high molecular weight shoulders have become evident in the obtained SEC traces for **P3** and **P4** (**Figure 3.2**, SEC traces **C**–**D**). Moreover, the data indicates that as bimolecular termination takes place, the active chain end concentration decreases, thus effectively leading to a higher ligand and $CuBr_2$ to dormant species ratio, which in turn slows down the reaction (*i.e.* persistent radical effect).[38] Nevertheless, all polymerizations reached almost quantitative conversions within 3 hours, regardless of the monomers chosen.

The increase in molecular weight (M_n) with higher conversion (**Figure 3.2**, **E**) shows a similar trend to the semi-logarithmic kinetic plot. Up to a conversion of about 30%, the experimental M_n values measured for **P4** are not in agreement with the theoretical values $M_{n,theo}$ (**Figure 3.2**). This is attributed to difference in the hydrodynamic volume of p(OEGA) in comparison to p(MMA) standards. For all other values a linear evolution of M_n with respect to monomer conversion was observed within very close approximation to the theoretical values.

Similarly to the case with the linear initiator, when a branched initiator was utilized the same molar ratios of [Monomer]:[PE-Br_4]:[Me_6TREN]:[$CuBr_2$] = 20:1:0.19:0.1 were used. Here only the amount of the initiator was varied, in order to keep the concentration of the monomer and catalyst system to solvent constant. **Figure 3.8** shows the obtained SEC traces for the polymers **P5-P8**. All polymerizations reached quantitative conversions, whereas a conversion of 80% for **P8** was obtained ($M_{n,SEC}$ = 8300 g·mol^{-1}, $Đ$ = 1.06) in 3 hours. By using a four-arm star initiator for **P5-P8**, the effective ligand concentration per initiating site has been decreased to a fourth. Although comparable k_p^{app} values could not be obtained from the Ln($[M]_0$/[M]) vs. time plot (**P5-P8**, **Figure 3.5**), a significantly slower conversion was observed for the first 30 minutes, when compared to the linear **P1-P4** polymerizations.

Contrary to the trend observed with the linear initiator where a decrease in the polymerization rate occurs (**Figure 3.2**, **F**), monomer consumption tends to speed up after 30 minutes for **P5–P8**. The increase in rate for **P5–P7** is significantly more evident than the increase for **P8**, which can be explained with the induction time for OEGA. Furthermore, the evolutions of the molecular weights obtained from SEC analysis are found to be in excellent agreement with the theoretical molecular weights (**Figure 3.5**). For instance, with the exception of polymer **P8**, all molecular weights during the polymerization follow a linear trend whilst growing. For **P8**, a rapid increase in M_n is observed up to 12% monomer consumption ($M_{n,SEC}$ = 3300 g·mol^{-1}, $Đ$ = 1.05), which is followed by a slower linear increase up to 80% conversion. Nevertheless the MWD remains low throughout the polymerization, which can be taken as a reliable indication that good control is maintained, with no apparent coupling reactions taking place.

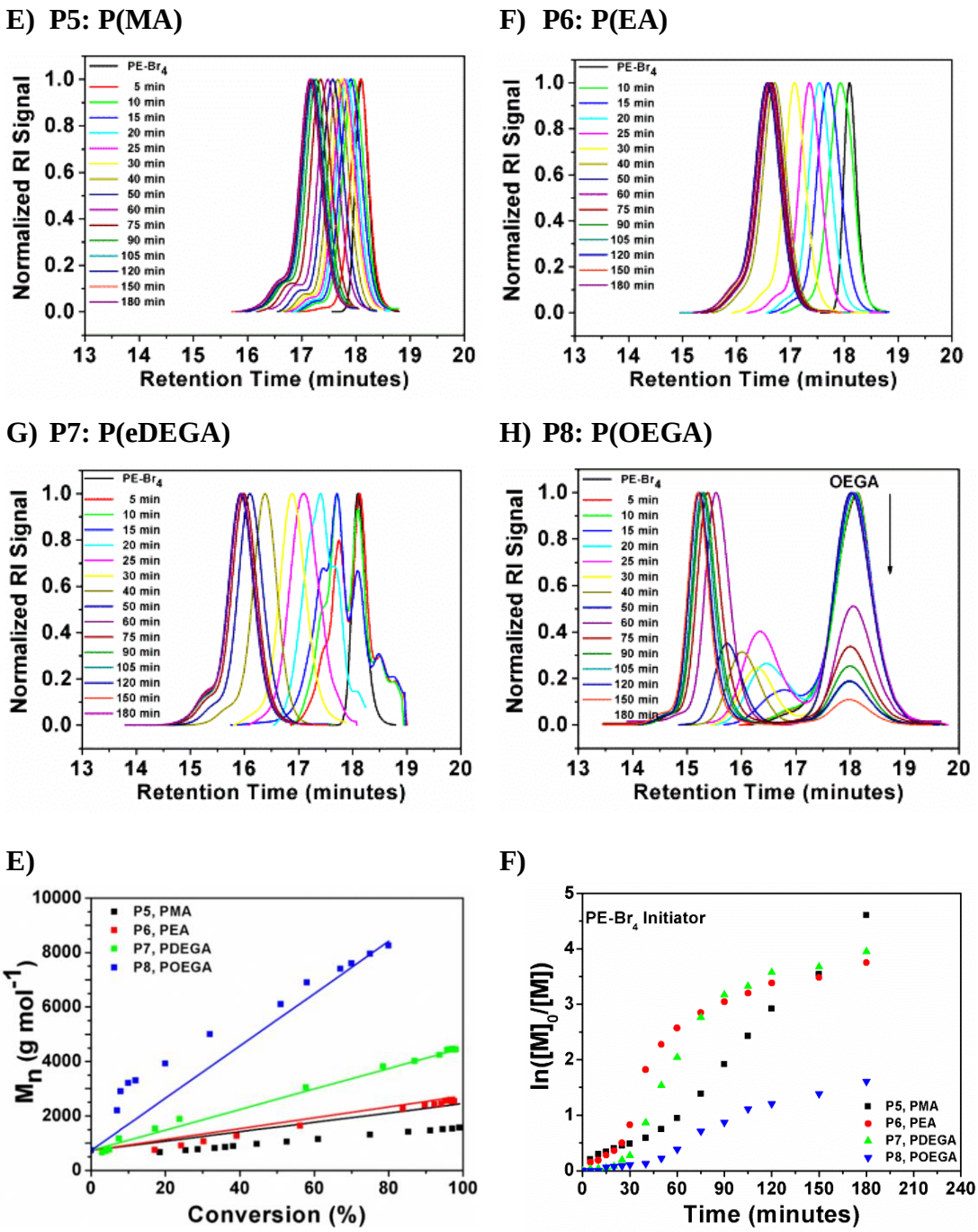

Figure 3.5: A general overview of the characterization of the obtained polymers are displayed above. SEC traces of the obtained polymers **A)** P5, **B)** P6, **C)** P7 and **D)** P8 using the PE-Br$_4$ initiator. **E)** M_n *vs.* conversion plot for **P5-P8**. Coloured symbols represent M_n obtained from SEC; straight lines represent theoretical M_n calculated from corresponding conversions **F)** Ln([M]$_0$/[M]) vs. time plot for **P5-P8** with the corresponding k_p^{app} values obtained from the initial linear increase.

Furthermore, EA was polymerized using EBiB at DP$_n$ = 40 and 80 (**P9** and **P10**, respectively) under the same conditions. Good control was retained over polymerization ($Đ$ = 1.07 and 1.10 respectively) even at higher DP$_n$ and negligible

amount of coupling reactions were observed (**Figure 3.6**). However, it was evident that the amount of coupling reactions increased with increasing DP, whereas no early termination was presedent during the course of the reaction. Kinetic investigation of the polymerizations shows identical behaviour to **P2** (DP_n = 20). Polymerization rate of the monomer tends to be slow for the initial 15 minutes but displays a rapid increase until 30 minutes, with a decline in rate until quantitative conversion is reached. In summary, it is observed that the polymerization rate is not DP_n dependent. Although negligible, the amount of side reactions (coupling) tend to increase with increasing DP_n.

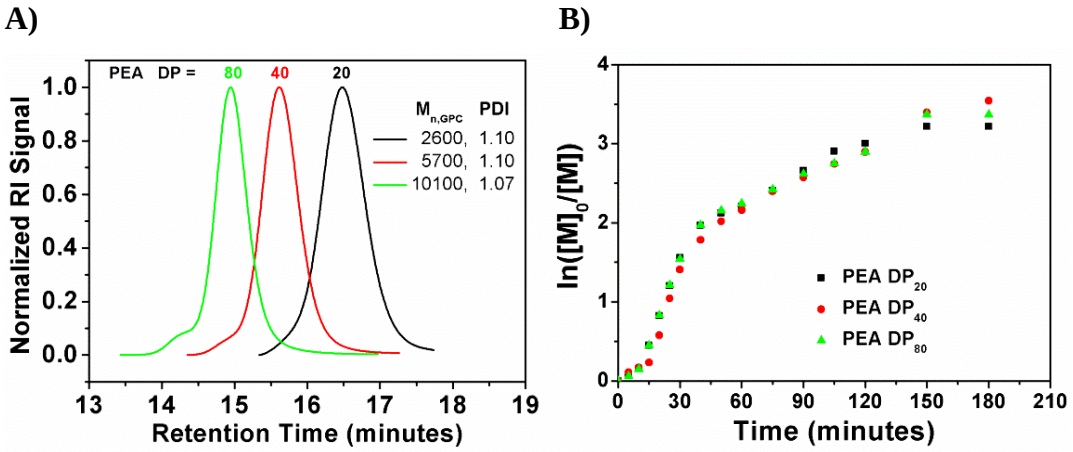

Figure 3.6: Polymerization kinetics of the obtained PEA polymers. **A)** SEC traces of PEA at different DP_n, **P2** = DP_{20}, **P9** = DP_{40} and **P10** = DP_{80}. **B)** Semi-logarithmic kinetic plot for **P2, P9** and **P10** obtained *via* 1 penny mediated SET-LRP using EBiB as initiator.

Finally, an attempt was done to obtain a polymer on large scale by polymerizing EA (DP_n = 80) on a 50 g monomer scale (**P11**) using a single 1p coin. Within 3 hours, monomer conversion has already reached to 90% ($M_{n,SEC}$ = 7400 g·mol^{-1}, $Đ$ = 1.06). At this point, the polymerization was allowed to proceed for 16 hours to reach to full conversion (**Figure 3.7**, $M_{n,SEC}$ = 8300 g·mol^{-1}, $Đ$ = 1.06, ρ = 100%).

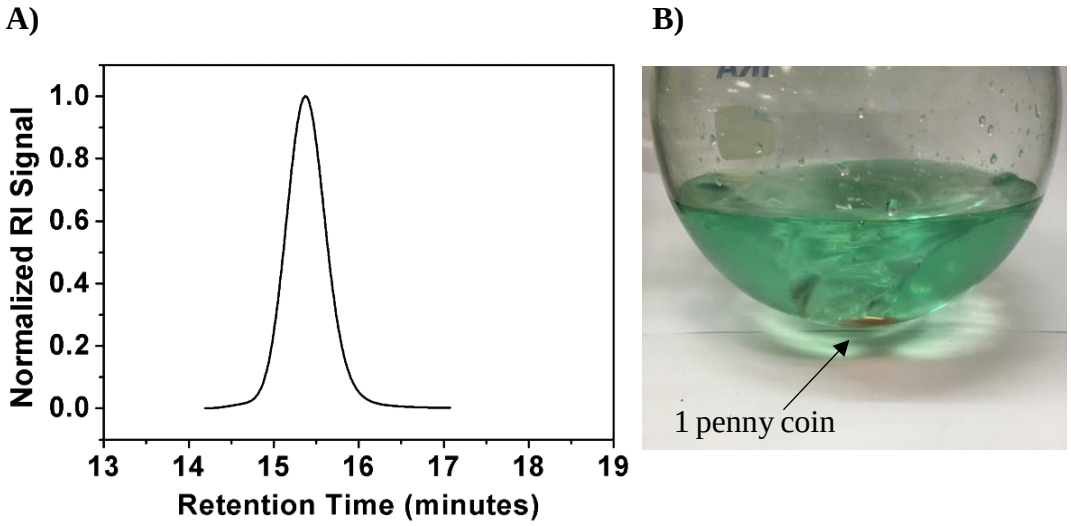

Figure 3.7: A) SEC trace obtained from the SET-LRP of PEA_{80} (**P11**) at 50 g scale. $M_{n,SEC}$ = 8300 g·mol^{-1}, $Đ$ = 1.06, ρ = 100%. **B)** Picture of the flask containing the polymerization mixture, before it was terminated by exposing to air and further bubbling with air for 1 minute.

When compared to **P10 (**with same DP_n, however small scale), an obvious difference in coupling was observed. The large scale polymerization **P11** displayed no coupling reaction, whereas some coupling was observed for **P10.** Due to this, although dispersities were similar, **P11** displayed a smaller hydrodynamic volume, which was reflected in a difference of *ca.* 2000 g·mol^{-1} in M_n, attributed to the coin surface to solvent volume ratio.

As mentioned earlier, the weight change of the copper coin was monitored for each polymerization reaction, by noting the differences in mass of the copper coin at t = 0 and right after the polymerization was stopped at t = 3 h. Before pre-activation, the copper coin was immersed into a beaker containing HCl (2–3 times), then thoroughly washed with deionised H_2O and acetone before drying under nitrogen. The initial weights of the Cu coins were found to be around 3.500 and 3.600 g. After this, the coins were pre-activated as usual (see experimental). When the polymerizations were allowed to react for 3 hours and terminated, the Cu coins were immediately removed from the reaction medium and rinsed with acetone and dried under nitrogen, prior to weighing. Negligible mass losses in comparison to the initial weight of the Cu coins were obtained. The mass changes were found to be between 6.5 and 8.1 mg ($\Delta m_{coin} < 0.2\%$) and are listed above in **Table 3.1**. Interestingly, when one of our initial attempts to polymerize eDEGA with EBiB failed due to an issue with the Schlenk line, it was observed that only a mass change of 1.7 mg took place at a

monomer conversion of 7% in 3 h (**Figure 8**), indicating that Cu is only consumed when SET-LRP occurs.

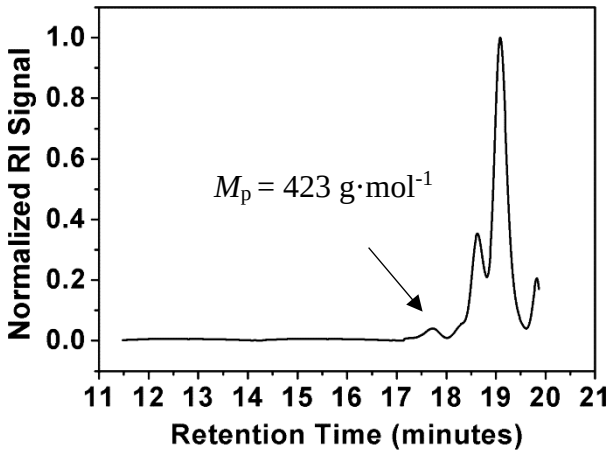

Figure 8: Normalised RI signal, obtained for the failed polymerization of eDEGA. No high molecular weight species was detected, in agreement with the low conversion (ρ = 7%).

It should be noted that there are two different types of 1 p coins in circulation (as of 2017). From their first issue in 1971 until 1992, the composition of a 1 p coin consisted of 97% Cu, 2.5% Zn and 0.5% Sn. Hereafter, Cu plated steel coins were introduced (94% mild steel from Fe, C and Mn, and 6% Cu).[39] It was found that both coins can be used equally, providing almost identical polymerization results (**Figure 3.9**).

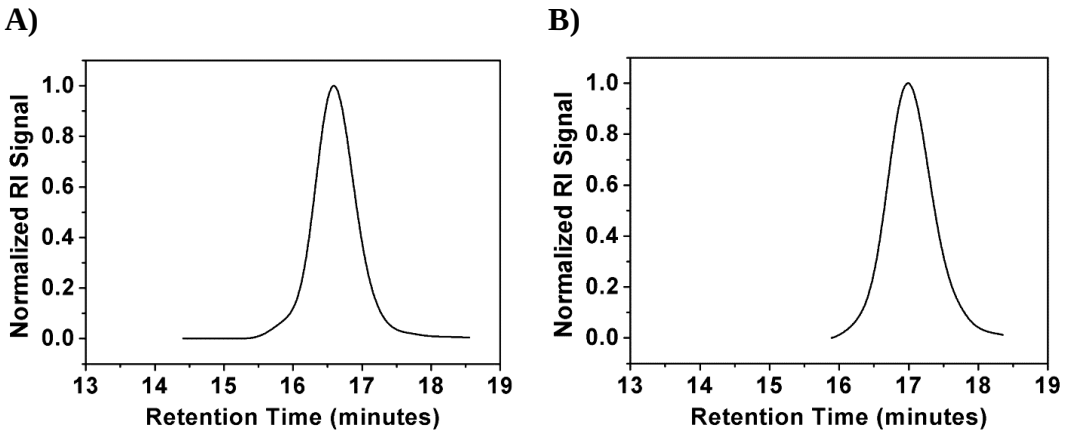

Figure 3.9: Comparison of the obtained SEC traces for p(MA)$_{20}$. **A)** mediated *via* 1 penny coin dated 1986 ($M_{n,SEC}$ = 2200 g·mol^{-1}, $Đ$ = 1.10, ρ = 100%). **B)** mediated *via* 1 penny coin dated 2015 ($M_{n,SEC}$ = 2000 g·mol^{-1}, $Đ$ = 1.10, ρ = 100%)

As identical polymerization results were obtained for different coins, it was speculated that this might be due to the equal surface area of the coins, although the compositions are different. For comparison purposes a Cu wire is used with the same surface area to that of a coin. The total surface area of a standard British 1 p coin (diameter = 20.3 mm, thickness = 1.65 mm) equals to that of a cylindrical copper wire (9.58 cm, 0.25 mm diameter, **Eq. 1**).

$$A_{cylinder} = 2\pi r^2 + 2\pi rh \qquad \textbf{Eq. 1}$$

Therefore, EA was polymerized with EBiB using a 9.6 cm (diameter = 0.25 mm, P12) Cu wire under the same polymerization conditions as for **P2**. Then the effect of a shorter (5 cm in length) Cu wire (**P13**) for comparison was investigated, as this is a widely employed standard Cu wire length in the literature. As expected, induction periods of 25 and 40 minutes, were observed for **P12** and **P13** respectively.34 Nicolas et al. attributed this initial slow rate of polymerization to autocatalysis by studying the initiator conversion, which is however not applicable for this study as only the monomer concentration was monitored.35 On the contrary, when a coin with the same surface area was employed the kinetics for **P2** provided already a conversion of 6% in 5 minutes, with a further linear increase in the kinetic plot. In order to investigate if the acceleration in the polymerization was due to the uneven surface of the Cu coin, an extra long (20 cm in length) Cu wire (**P14**) was utilized. However, an induction period of 20 minutes was also observed, which indicates that a higher surface area of Cu is not the main reason for eliminating the induction period.

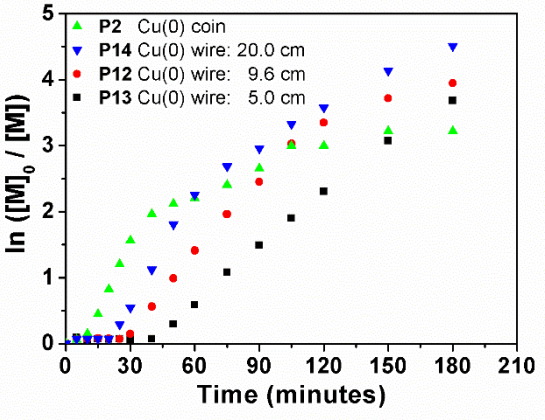

Figure 3.10: Ln($[M]_0/[M]$) vs. time plot for **P2**, **P12**, **P13** and **P14** obtained *via* copper mediated SET-LRP using EBiB as initiator.

3.3. Conclusion

In conclusion, a series of well defined polymers were obtained *via* 1 penny coin catalyzed SET-LRP of MA, EA, DEGA and OEGA using both a linear (EBiB) and a 4-arm star initiator (PE-Br_4). All obtained polymers were characterized in detail *via* SEC, ^{1}H NMR and MALDI-ToF MS techniques. Although some of the polymers displayed minor bimolecular termination to some extent, linear $p(MA)_{20}$ and $p(EA)_{20}$ displayed no coupling reactions at all ($Đ$ = 1.10). Furthermore, in order to demonstrate the scope of this protocol, the polymerization of EA at various degrees of polymerizations (DP_n = 20, 40 and 80) was shown as well as the synthesis $p(EA)_{80}$ at a relatively large scale (50 g) with excellent control over MWD and in good agreement between theoretical and experimental molecular weight. Furthermore, a Cu wire with an equal surface area was used for polymerization to demonstrate a comparison to a more widely used system in the literature. The obtained results indicate that, a Cu coin can be utilized as a cheap, convenient and readily available alternative source to Cu wire for Cu(0) mediated polymerizations of acrylates.

3.4. Experimental

3.4.1. Materials

Monomers (MA, EA, eDEGA, $OEGA_{480}$), α-Bromoisobutyryl bromide (BIBB, 98%), Triethylamine (TEA, ≥99%), DMSO and other chemicals were obtained from Sigma Aldrich at highest purity available. The 1 penny coins were used as received from the Royal Mint. All monomers were passed over a short column of basic aluminium oxide to remove the inhibitor prior to use.

Tris(2-(dimethylamino)ethyl)amine (Me_6TREN) and $PE\text{-}Br_4$ initiator were synthesized according to literature procedures and stored at 4°C prior to use.

Conversion was calculated by comparing the change of the monomer:mesitylene integrals ratio of a desired time, with the monomer:mesitylene integrals ratio of the t = 0 sample taken 5 minutes prior to polymerization initiation with a degassed syringe.

The authors declare that no financial interest was gained from this work. Defacing or destroying British currency was under no circumstance intended or was expected in any procedure described. The 1 penny coins were used only for research purposes. The coin retains throughout every stage of experimentation its original condition. Pictures before and after the HCl wash; and after the polymerization are depicted below, displaying no visible damage (**Figure 3.11**).

Figure 3.11: A) British 1 penny before HCl wash (dirty), **B)** British 1 penny after HCl wash (clean and shiny) and **C)** British 1 penny after polymerization was stopped (still clean and shiny). Neither **B)** nor **C)** shows any macroscopic physical damage, defacing or destruction to the coin.

3.4.2. Instruments and analysis

Proton nuclear magnetic resonance (^{1}H NMR) spectra were recorded on a Bruker AV III 400 in $CDCl_3$ at 303 K. All samples taken were immediately diluted with $CDCl_3$ for analysis. Conversions were calculated by the comparison integrals of the respective vinyl peaks of the monomers and the integral of mesitylene (5% v/v) which was added prior to the start of polymerization.

Gas chromatography - flame ionisation detection (GC-FID) analysis was performed using Agilent Technologies 7820A. An Agilent J&W HP-5 capillary column of 30 m x 0.320 mm, film thickness 0.25 μm was used. The oven temperature was programmed as follows: 40 °C (hold for 1 minute) increase at 30 °C min^{-1} to 300 °C (hold for 2.5 minutes). The injector was operated at 250 °C and the FID was operated at 320 °C. Nitrogen was used as carrier gas at a flow rate of 6.5 mL min^{-1} and a split ratio of 1:1 was applied. Data was processed using OpenLab CDS ChemStation Edition, version C.01.05. Conversions were obtained by comparing the integral of the monomer with mesitylene.

Gel permeation chromatography (SEC) measurements were conducted on an Agilent 1260 infinity system operating in THF with TEA (2% v/v) at 1 ml/min flow rate and equipped with refractive index detector and variable wavelength detector, 2 PLgel 5 μm mixed-C columns (300×7.5mm), a PLgel 5 mm guard column (50x7.5mm) and an autosampler. The instrument was calibrated with linear narrow poly(methyl methacrylate) standards in range of 550 to 46890 g·mol^{-1}. All samples were passed through basic aluminium oxide to remove any catalyst residues and filtered using 0.2 μm Nylon 66 filters before analysis.

MALDI-ToF MS was performed using a Bruker Daltonics Autoflex MALDI-ToF mass spectrometer, equipped with a nitrogen laser at 337 nm with positive ion ToF detection. Polymer samples were measured as follows; solutions in THF of trans-2-[3-(4-tert-Butylphenyl)-2-methyl-2-propenylidene] malononitrile (DCTB, ≥98%) as matrix (30 mg·mL^{-1}), potassium trifluoroacetate (KTFA) as cationisation agent (10 mg·mL^{-1}) and sample (10 mg·mL^{-1}) were mixed together in a 9:1:1 volume ratio for a total volume of 75 μL. 2 μL of the mixture was applied to the target plate. Spectra were recorded in reflectron mode and the mass spectrometer was calibrated with a peptide mixture up to 6000 Da.

3.4.3. Synthesis

Synthesis of Pentaerythritol tetrakis(2-bromoisobutyrate) (PE-Br$_4$)

Into a 500 mL round-bottom flask, 100 mL of THF (dried over $MgSO_4$ and filtered prior to addition), 12 g (0.12 mol) of triethylamine (TEA) and 3.7 g (27 mmol) of pentaerythritol (PE) were successively added and placed in an ice bath to be cooled down to 0°C. Then, a solution containing 26 g (0.12 mol) of α-bromoisobutyryl bromide (BiBB) and 40 mL dry THF was prepared and added dropwise under moderate stirring. The mixture was allowed to heat up to room temperature and stirred overnight. The mixture was transferred into a 1 L separatory funnel containing 300 mL of ether and successively extracted with 200 mL of H_2O, 200 mL of saturated aqueous $NaHCO_3$ (3 times) and 200 mL of H_2O. The organic phase was dried over $MgSO_4$ and filtered and dried *in vacuo*. The crude product was redissolved and passed through a silica column using EtOAc:Hexane (1:9, *v/v*) as eluent. The eluent was removed and a white powder was obtained by crystallizing twice from diethyl ether (11.2 g, 57%).
^{1}H NMR ($CDCl_3$, 400 MHz) δ: 4.33 (*s*, 8H, C-C*H*$_2$-O), 1.94 (*s*, 24H, C-(C*H*$_3$)$_2$-Br) ppm

Experimental Procedures

SET-LRP conditions for polymers P1-P10

For a typical polymerization, $CuBr_2$ (9.2 mg, 0.04 mmol), DMSO, Me_6TREN (21 µL, 0.076 mmol), monomer (20 equiv.), mesitylene (2.5%, *v/v*) and initiator (1 equiv.) were added to a Schlenk tube containing a stirrer bar. The Schlenk tube was subsequently sealed with a rubber septum, lowered into an oil bath set to 25 °C and degassed with argon for 30 minutes. At the same time, a copper coin was pre-activated in 10 mL HCl (conc. 37%) for 20 minutes, then washed with deionised water and acetone and dried under argon. The activated copper coin was then transferred to the Schlenk tube containing the polymerization mixture to start the reaction (the addition of the copper coin defines t = 0). The exact amounts of DMSO, monomer and initiator used are given in the following table (Table 2).

Table 2: Overview of the amounts used for the polymerization of **P1-P13.**

Polymer	Initiator	Monomer	DMSO
	EBiB		
P1 $p(MA)_{20}$	61 µL	0.75 mL	3.0 mL
P2 $p(EA)_{20}$	61 µL	0.90 mL	3.6 mL
P3 $p(DEGA)_{20}$	61 µL	1.50 mL	6.0 mL
P4 $p(OEGA)_{20}$	61 µL	3.70 mL	14.6 mL
	PE-Br_4		
P5 $p(MA)_{20}$	304.6 mg	0.75 mL	3.0 mL
P6 $p(EA)_{20}$	304.6 mg	0.90 mL	3.6 mL
P7 $p(DEGA)_{20}$	304.6 mg	1.50 mL	6.0 mL
P8 $p(OEGA)_{20}$	304.6 mg	3.70 mL	14.6 mL
	EBiB		
P9 $p(EA)_{40}$	61 µL	1.50 mL	6.0 mL
P10 $p(EA)_{80}$	61 µL	3.00 mL	12.0 mL
	EBiB		
P11 $p(EA)_{80}$ (50 g)	3.40 mL	50 mL	200 mL
	EBiB		
P12 $p(EA)_{20}$	61 µL	0.90 mL	3.6 mL
P13 $p(EA)_{20}$	61 µL	0.90 mL	3.6 mL

SET-LRP conditions for polymer P11

A 200 mL DMSO containing round-bottom flask was fitted with a stirrer bar and sealed to be degassed with argon overnight at 25 °C. The next day, $CuBr_2$ (92 mg, 0.4 mmol), Me_6TREN (210 µL, 0.76 mmol), ethyl acrylate (50 mL, 458 mmol), mesitlyene (5 mL) and initiator (1.01 mL, 5.73 mmol) were subsequently added under a positive flow of argon. The mixture was degassed for further 2 hours. At the same time, a copper coin was pre-activated in 10 mL HCl (conc. 37%) for 20 minutes, then washed with deionised water and acetone and dried under argon. The activated copper coin was then transferred to the round-bottom flask containing the polymerization mixture to start the reaction (the addition of the copper coin defines t = 0).

SET-LRP conditions for polymers P12-P13

The polymerization was carried out as described above in section **3.1** for **P2** with identical amounts of materials used. However, instead of a copper coin, wires of 5 cm and 9.6 cm were used. The activation of the copper wires and the polymerization initiation is as described above.

Kinetic Experiments of P1-P8

Table 3: Results obtained from kinetic experiments for **P1.**

Time (min)	$M_{n,theo}$ (g·mol^{-1})	$M_{n,SEC}$ (g·mol^{-1})	$Đ$	ρ (%)
5	480	-	-	16
10	690	-	-	28
20	1200	840	1.12	58
25	1400	1100	1.11	70
30	1500	1200	1.11	76
40	1700	1300	1.10	84
50	1800	1400	1.11	89
60	1800	1500	1.10	92
75	1800	1600	1.10	94
90	1800	1600	1.11	95
105	1900	1700	1.12	96
120	1900	1800	1.11	96
150	1900	1900	1.11	97
180	1900	2000	1.10	97

Table 4: Results obtained from kinetic experiments for **P2.**

Time (min)	$M_{n,theo}$ (g·mol^{-1})	$M_{n,SEC}$ (g·mol^{-1})	$Đ$	ρ (%)
5	500	-	-	18
10	600	-	-	25
15	700	-	-	27
20	800	1600	1.10	33
25	800	1900	1.09	35
30	800	2000	1.09	37
40	1000	2200	1.09	44
50	1100	2400	1.09	51
60	1200	2400	1.09	60
75	1500	2500	1.09	75
90	1700	2500	1.10	85
105	1800	2500	1.09	91
120	1900	2500	1.12	95
150	2100	2500	1.10	97
180	2200	2600	1.10	99

Table 5: Results obtained from kinetic experiments for **P3.**

Time (min)	$M_{n,theo}$ (g·mol^{-1})	$M_{n,SEC}$ (g·mol^{-1})	$Đ$	ρ (%)
5	800	-	-	16
10	1600	-	-	37
20	2500	1700	1.10	61
25	2500	3000	1.10	65
30	2800	3400	1.10	70
40	3200	3700	1.10	80
50	3400	3900	1.10	86
60	3600	4100	1.08	89
75	3700	4200	1.10	92
90	3800	4300	1.10	94
105	3800	4300	1.11	96
120	3900	4400	1.12	97
150	3900	4500	1.11	98
180	3900	4500	1.11	98

Table 6: Results obtained from kinetic experiments for **P4.**

Time (min)	$M_{n,theo}$ (g·mol^{-1})	$M_{n,SEC}$ (g·mol^{-1})	$Đ$	ρ (%)
5	0	-	-	0
10	480	-	-	3
15	770	-	-	6
20	1200	-	-	10
25	1500	-	-	14
30	1800	3000	1.08	17
40	2800	5200	1.12	27
50	6000	6800	1.06	60
60	7000	7600	1.06	71
75	7900	8100	1.07	80
90	8200	8300	1.06	83
105	8500	8700	1.07	87
120	8700	8800	1.07	89
150	8900	9100	1.07	91
180	9200	9200	1.07	93

Table 7: Results obtained from kinetic experiments for **P5.**

Time (min)	$M_{n,theo}$ (g·mol^{-1})	$M_{n,SEC}$ (g·mol^{-1})	$Đ$	ρ (%)
5	1000	700	1.03	18
10	1200	800	1.05	25
15	1200	800	1.05	27
20	1300	800	1.05	33
25	1300	900	1.05	35
30	1400	900	1.06	38
40	1500	1000	1.06	44
50	1600	1100	1.06	51
60	1800	1200	1.06	60
75	2000	1300	1.06	75
90	2200	1400	1.06	85
105	2300	1500	1.06	91
120	2300	1500	1.07	95
150	2400	1500	1.07	97
180	2400	1600	1.07	98

Table 8: Results obtained from kinetic experiments for **P6.**

Time (min)	$M_{n,theo}$ (g·mol^{-1})	$M_{n,SEC}$ (g·mol^{-1})	$Đ$	ρ (%)
5	1000	700	1.03	15
10	1100	700	1.05	17
15	1200	900	1.06	24
20	1500	1100	1.05	40
25	1600	1300	1.06	45
30	1900	1600	1.06	56
40	2200	2300	1.07	74
50	2500	2400	1.06	90
60	2600	2400	1.06	92
75	2600	2400	1.07	94
90	2600	2600	1.08	95
105	2700	2600	1.08	96
120	2700	2600	1.08	97
150	2700	2600	1.07	97
180	2700	2600	1.08	99

Table 9: Results obtained from kinetic experiments for **P7**.

Time (min)	$M_{n,theo}$ (g·mol^{-1})	$M_{n,SEC}$ (g·mol^{-1})	$Đ$	ρ (%)
5	900	-	-	3
10	900	-	-	4
15	900	-	-	5
20	1000	1200	1.09	8
25	1400	1500	1.07	17
30	1600	1900	1.07	24
40	2900	3000	1.07	57
50	3700	3800	1.08	79
60	4000	4000	1.09	87
75	4300	4200	1.09	94
90	4300	4400	1.09	96
105	4400	4400	1.09	96
120	4400	4400	1.09	97
150	4400	4400	1.09	97
180	4400	4400	1.09	97

Table 10: Results obtained from kinetic experiments for **P8.**

Time (min)	$M_{n,theo}$ (g·mol^{-1})	$M_{n,SEC}$ (g·mol^{-1})	$Đ$	ρ (%)
5	0	-	-	0
10	0	-	-	0
15	1300	-	-	6
20	1400	2200	-	7
25	1500	2900	-	8
30	1700	3200	-	10
40	1900	3300	1.05	12
50	2700	3900	1.06	20
60	3800	5000	1.05	32
75	5600	6100	1.06	51
90	6300	6900	1.06	58
105	7200	7400	1.06	67
120	7500	7600	1.06	70
150	7900	8000	1.05	75
180	8400	8300	1.06	80

3.5. References

1. G. Moad, E. Rizzardo and S. H. Thang, *Aust. J. Chem.*, 2012, **65**, 985-1076.
2. D. J. Keddie, *Chem. Soc. Rev.*, 2014, **43**, 496-505.
3. C. J. Hawker, A. W. Bosman and E. Harth, *Chem. Rev.*, 2001, **101**, 3661-3688.
4. J. Nicolas, Y. Guillaneuf, C. Lefay, D. Bertin, D. Gigmes and B. Charleux, *Prog. Polym. Sci.*, 2013, **38**, 63-235.
5. J. S. Wang and K. Matyjaszewski, *J. Am. Chem. Soc.*, 1995, **117**, 5614-5615.
6. K. Matyjaszewski, *Macromolecules*, 2012, **45**, 4015-4039.
7. M. Kato, M. Kamigaito, M. Sawamoto and T. Higashimura, *Macromolecules*, 1995, **28**, 1721-1723.
8. V. Percec, A. V. Popov, E. Ramirez-Castillo, M. Monteiro, B. Barboiu, O. Weichold, A. D. Asandei and C. M. Mitchell, *J. Am. Chem. Soc.*, 2002, **124**, 4940-4941.
9. V. Percec, T. Guliashvili, J. S. Ladislaw, A. Wistrand, A. Stjerndahl, M. J. Sienkowska, M. J. Monteiro and S. Sahoo, *J. Am. Chem. Soc.*, 2006, **128**, 14156-14165.
10. B. M. Rosen and V. Percec, *Chem. Rev.*, 2009, **109**, 5069-5119.
11. N. Zhang, S. R. Samanta, B. M. Rosen and V. Percec, *Chem. Rev.*, 2014, **114**, 5848-5958.
12. D. Konkolewicz, Y. Wang, M. Zhong, P. Krys, A. A. Isse, A. Gennaro and K. Matyjaszewski, *Macromolecules*, 2013, **46**, 8749-8772.
13. D. Konkolewicz, Y. Wang, P. Krys, M. Zhong, A. A. Isse, A. Gennaro and K. Matyjaszewski, *Polym. Chem.*, 2014, **5**, 4396-4417.
14. F. Alsubaie, A. Anastaski, V. Nikolaou, A. Simula, G. Nurumbetov, P. Wilson, K. Kempe and D. M. Haddleton, *Macromolecules*, 2015, **48**, 5517-5525.
15. F. Alsubaie, A. Anastasaki, V. Nikolaou, A. Simula, G. Nurumbetov, P. Wilson, K. Kempe and D. M. Haddleton, *Macromolecules*, 2015, **48**, 6421-6432.
16. A. Anastasaki, C. Waldron, P. Wilson, R. McHale and D. M. Haddleton, *Polym. Chem.*, 2013, **4**, 2672-2675.
17. W. Ding, C. Lv, Y. Sun, H. Luan, T. Yu and G. Qu, *Polym. Bull.*, 2011, **67**, 1499-1505.
18. A. Anastasaki, C. Waldron, P. Wilson, C. Boyer, P. B. Zetterlund, M. R. Whittaker and D. Haddleton, *ACS Macro Lett.*, 2013, **2**, 896-900.
19. A. Anastasaki, A. J. Haddleton, Q. Zhang, A. Simula, M. Droesbeke, P. Wilson and D. M. Haddleton, *Macromol. Rapid Commun.*, 2014, **35**, 965-970.
20. N. H. Nguyen, J. Kulis, H.-J. Sun, Z. Jia, B. Van Beusekom, M. E. Levere, D. A. Wilson, M. J. Monteiro and V. Percec, *Polym. Chem.*, 2013, **4**, 144-155.
21. L. Voorhaar, S. Wallyn, F. E. Du Prez and R. Hoogenboom, *Polym. Chem.*, 2014, **5**, 4268-4276.
22. S. Fleischmann and V. Percec, *J. Polym. Sci. Part A: Polym. Chem.*, 2010, **48**, 2236-2242.
23. M. Gavrilov, T. J. Zerk, P. V. Bernhardt, V. Percec and M. J. Monteiro, *Polym. Chem.*, 2016, **7**, 933-939.
24. A. Anastasaki, V. Nikolaou and D. M. Haddleton, *Polym. Chem.*, 2016, **7**, 1002-1026.

25. G. Lligadas, B. M. Rosen, C. A. Bell, M. J. Monteiro and V. Percec, *Macromolecules*, 2008, **41**, 8365-8371.
26. M. E. Levere, I. Willoughby, S. O'Donohue, A. de Cuendias, A. J. Grice, C. Fidge, C. R. Becer and D. M. Haddleton, *Polym. Chem.*, 2010, **1**, 1086-1094.
27. N. Chan, M. F. Cunningham and R. A. Hutchinson, *Macromol. Rapid Commun.*, 2011, **32**, 604-609.
28. J. A. Burns, C. Houben, A. Anastasaki, C. Waldron, A. A. Lapkin and D. M. Haddleton, *Polym. Chem.*, 2013, **4**, 4809-4813.
29. T. Zhang, Y. Du, F. Mueller, I. Amin and R. Jordan, *Polym. Chem.*, 2015, **6**, 2726-2733.
30. A. H. Soeriyadi, C. Boyer, F. Nystroem, P. B. Zetterlund and M. R. Whittaker, *J. Am. Chem. Soc.*, 2011, **133**, 11128-11131.
31. Q. Zhang, P. Wilson, Z. Li, R. McHale, J. Godfrey, A. Anastasaki, C. Waldron and D. M. Haddleton, *J. Am. Chem. Soc.*, 2013, **135**, 7355-7363.
32. F. Alsubaie, A. Anastasaki, P. Wilson and D. M. Haddleton, *Polym. Chem.*, 2015, **6**, 406-417.
33. R. Aksakal, M. Resmini and C. R. Becer, *Polym. Chem.*, 2016, **7**, 171-175.
34. N. H. Nguyen and V. Percec, *J. Polym. Sci. Part A: Polym. Chem.*, 2010, **48**, 5109-5119.
35. Y. Gao, T. Zhao, D. Zhou, U. Greiser and W. Wang, *Chem. Commun.*, 2015, **51**, 14435-14438.
36. S. Harrisson, P. Couvreur and J. Nicolas, *Macromolecules*, 2012, **45**, 7388-7396.
37. A. Simula, G. Nurumbetov, A. Anastasaki, P. Wilson and D. M. Haddleton, *Eur. Polym. J.*, 2015, **62**, 294-303.
38. H. Fischer, *Chem. Rev.*, 2001, **101**, 3581-3610.
39. The Royal Mint, Coin Designs and Specifications, http://www.royalmint.com (accessed on 01.08.2016).

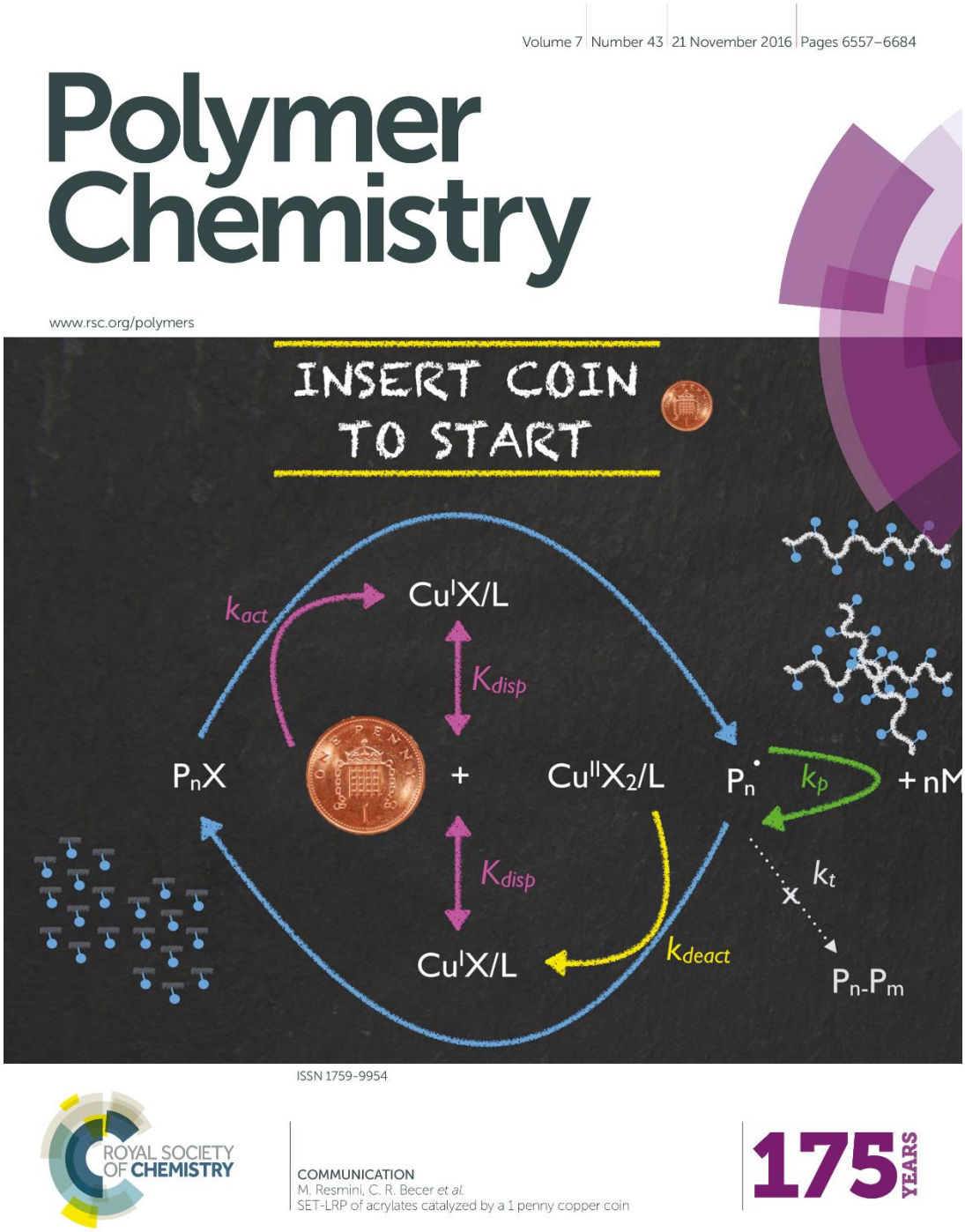

R. Aksakal, M. Resmini and C.R. Becer, *Polym. Chem.*, 2016, **7**, 6557 – 6557.

Chapter 5

Modification and polymerization of SET-LRP to obtain glycopolymers

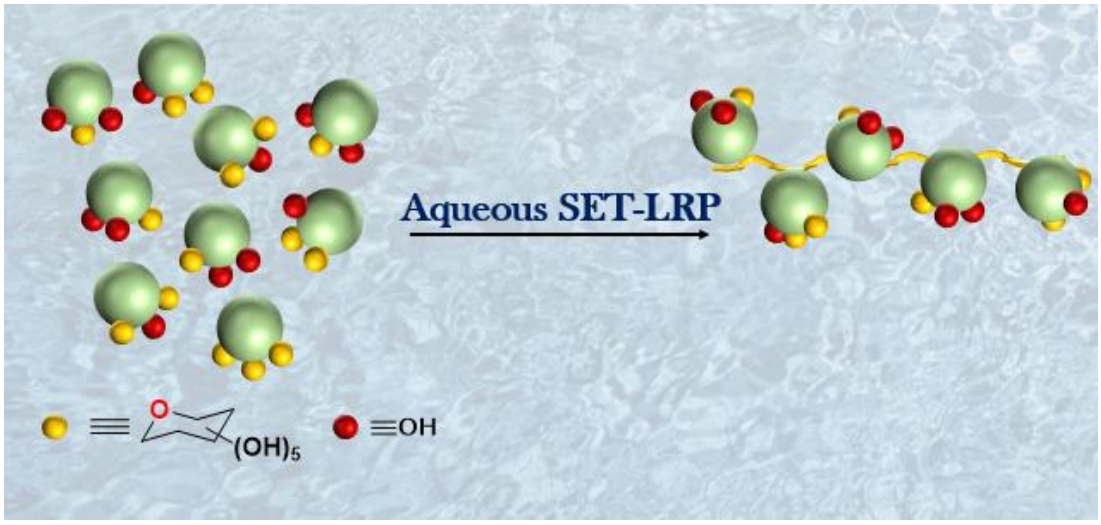

The glycosylation of an acrylamide with three hydroxyl functionalities (TRIS) is reported, allowing the regulation of the sugar density on the monomer. The method described is used to conjugate peracetylated carbohydrates on to hydroxyl functionalities of the monomer. Furthermore, the isolation of the mono substituted monomer and its deprotection is investigated. Subsequently, these monomers were polymerized via aqueous SET-LRP to give well-defined glycopolymers.

5.1. Introduction

Nature and biological systems bear the biggest collection of examples that scientists try to practice as a source of inspiration. Studying the functions of carbohydrates especially plays a pivotal role in understanding biological systems, as they are involved in many essential processes such as reproduction, signal transduction as well as recognition. This way, cells can be recognized by carbohydrate binding proteins, which act as receptors (lectins) for differentiation or infection on the cellular level. Taking advantage of this, polymers bearing carbohydrates can be prepared that allow to mimic some of these functionalities, the most prominent being recognition.[1,2]

To be able to modulate and increase recognition specificity precisely, their exact path of functioning needs to be fully understood. The recognition can be enhanced by multivalency, the so called "*cluster glycoside effect*".[3] Strength of glycopolymer binding by lectins is known to be dependent on a number of factors, such as polymer architecture, carbohydrate type, number of carbohydrates *etc*[4,5]. Glycopolymers can access multiple binding sites that can be regulated by chain length, which was observed by investigating the affinity between Concanavalin A (Con A) and mannose bearing polymers.[6] A similar trend in affinity was later observed between lactose glycopolymers and RCA120, which was attributed to the number of carbohydrate units on the polymer.[7]

Similar findings were reported by monodisperse polymers. Hartmann *et al.* have recently demonstrated the synthesis of a clickable alkyne functional backbone on solid phase.[8] Azide functional mannose was attached to the backbone, in which mono-, di- or tri- functional chains were obtained. These polymers were then subjected to binding studies with ConA, investigated with surface plasmon resonance (SPR). It was found that binding increased with number of carbohydrate units, but decreased with increased spacing inbetween. In addition, binding was highest when the spacing was similar to the distance between two binding sites of ConA.

Another possibility to regulate the affinity between glycopolymers and lectins can be achieved by control over the polymer structure.[9] Becer *et al.* synthesized a series of random copolymers based on mannose and galactose, in which their ratio was varied. The obtained polymers demonstrated that the interactions between a human dendritic

cell-associated lectin (DC-SIGN) and the viral envelope glycoprotein gp120, associated with the infection of cells with HIV, could be prevented.

The same group later reported the structural dependency of glycopolymer binding, in which the synthesis of star shaped *β*-Cyclodextrin (*β*-CD) based glycopolymers *via* SET-LRP was demonstrated.[10] The polymers exhibited strong binding to DC-SIGN according to SPR measurements, which was attributed to topology. The hydrophobic core of *β*-CD has been shown to further exhibit a high loading capacity of an anti-HIV drug, indicating a novel approach in HIV-therapeutic and drug delivery.

Next to the elegant examples above, the effect of morphology[11], distance of carbohydrate to the backbone[12] and thermoresponsiveness[13] are among others that have been reported to influence binding affinity.[5,14,15] However, the ability to vary the sugar density within a monomer and its influence has never been investigated. In the following, the synthesis of an acrylamide monomer with one, two or three carbohydrates is described and subsequently polymerized *via* aqueous SET-LRP. Varying the sugar density on a monomer would yield polymers which are equal in chain length, contain however different number of carbohydrates attached. This could be used as a novel strategy to alter the structure of the polymer, in order to for example influence binding properties of the polymer to lectins. Additionally, for polymerization techniques, which do not allow the synthesis of high DP glycopolymers, monomers with a higher sugar content could be used in order to compensate the molecular weight.

5.2. Results and Discussion

To be able to introduce more than one carbohydrate on a single monomer, *N*-[Tris(hydroxymethyl)methyl]acrylamide (TRIS) was employed, as the hydroxyl groups can be used as anchor points for sugars. A schematic representation is given below in **Scheme 5.1**.

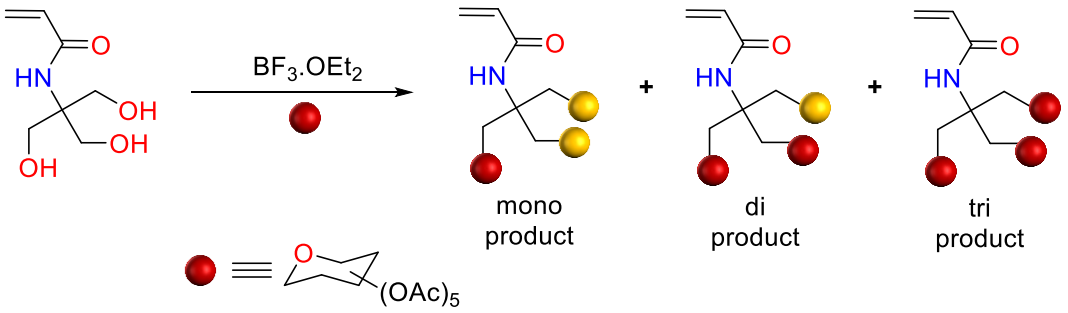

Scheme 5.1: Schematic representation of the synthesis route to obtain mono-, di- and tri-substituted mannose acrylamide.

5.2.1. Glycosylation of TRIS

Prior to the glycosylation of TRIS with $BF_3{\cdot}OEt_2$, mannose was per acetylated using a well-known procedure, with acetic anhydride and H_2SO_4.[15] The purified product was dissolved in cold DCM. Unlike reported, the solubility of TRIS was found to be mediocre in DCM. After being dispersed in DCM, the reaction vessel was sonicated to increase solubility, however full dissolution was not observed. Nevertheless, $BF_3{\cdot}OEt_2$ was added dropwise to the cold mixture. ESI-MS analysis of the crude mixture after 24 hours has shown masses of a mixture of three products present at *m/z* 506.22, 836.76 and 1166.16 corresponding to $[M+H]^+$ of the mono-, di- and tri-substituted products respectively. The crude mixture was washed with saturated Na_2CO_3, dried over $MgSO_4$ and dried *in vacuo*. However, although it was not possible to determine the percentage composition of individual monomers, an average number of carbohydrates per monomer was determined to be 1.1 using the acetyl groups between 2.25-1.75 ppm and vinyl groups between 5.75-5.55 ppm, indicating mostly the formation of the mono substituted product **Figure 5.1**. At this point the mixture was split into two equal halves for direct deacetylation and for further separation of the products.

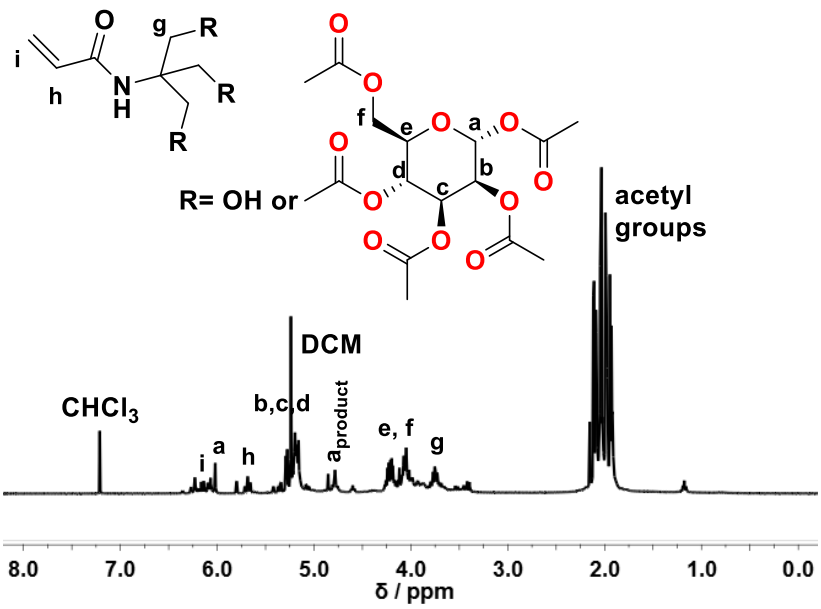

Figure 5.1: ^{1}H NMR spectrum of the crude product.

5.2.2. Direct deacetylation

The crude mixture was subjected to direct deacetylation using NaOMe for 3 hours prior to passing over a H^+ exchanged resin until neutrality.[16] Subsequently, the mixture was concentrated to dryness. The obtained ^{1}H NMR displays the disappearance of the acetyl groups between 2.25-1.75 ppm, indicating full deacetylation. Next, the crude mixture was used to be polymerized *via* standard aqueous SET-LRP conditions using [Sugar]:[I]:[CuBr]:[Me_6TREN] = 20:1:0.8:0.4, which will be discussed under the polymerization section **5.2.4**.

5.2.3. Monomer separation

The acetylated monomeric mixture was subjected to column chromatography to separate the mixture to its individual monomers using EtOAc:Hexanes 3:1. Thin layer chromatography (TLC) revealed four products. The products were identified to be mono- (R_f =0.15, $[M+H]^+$=506.22), di- (R_f =0.57, $[M+H]^+$= 836.76), tri- (R_f =0.72, $[M+H]^+$=1166.16) substituted products and unreacted peracetylated mannose (R_f =0.80) *via* preparative TLC and ESI-MS. Unfortunately, only the mono substituted product could be isolated from the rest, as the separation of the di and tri substituted products from the left over starting material remained challenging. Next, the monomer was deacetylated with NaOMe for three hours, after which all volatiles were removed

in vacuo. The obtained viscous monomer was then polymerized *via* aq. SET-LRP using the same conditions as described in the following section.

5.2.4. Polymerization reactions

Initially, the polymerization conditions were optimized for the homopolymerization of TRIS for DP_n=20 (**Scheme 2**). The conditions for the polymerization and obtained results are given below in **Table 5.1**.

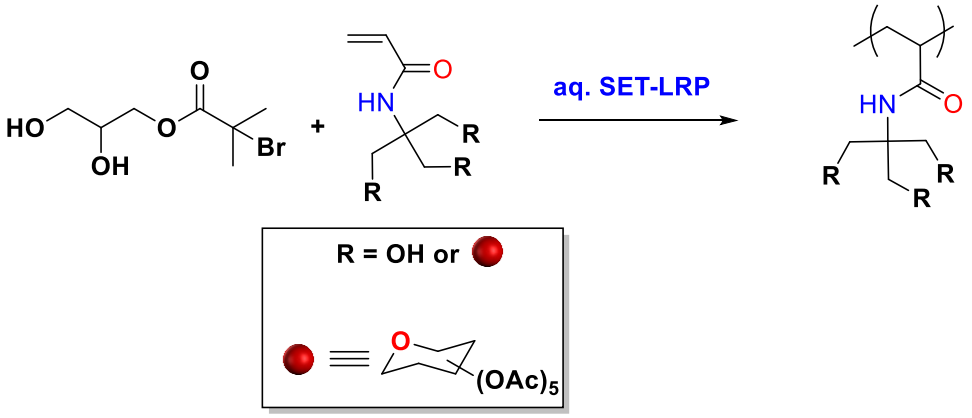

Scheme 2: Schematic representation of the polymerization of glycomonomers.

Table 5.1: Reaction conditions and obtained results for the SET-LRP of TRIS.

Entry	[TRIS]:[I]:[CuBr]:[Me$_6$TREN]	ρ^a (%)	$M_{n,theo}$ (g/mol)	$M_{n,SEC}{}^b$ (g/mol)	$Đ^b$	Temp. (°C)
P01	20 : 1 : 0.4 : 0.4	86	3100	3800	1.15	0
P02	20 : 1 : 0.8 : 0.4	94	3500	4600	1.12	0

[a] Conversion calculated from ^{1}H NMR. [b] DMF eluent, linear PMMA standards.

Fortunately, standard conditions of aqueous SET-LRP (**P01)** were not sufficient enough to obtain a well-defined homopolymer of TRIS at a monomer to initiator ratio of 20. Therefore, the [CuBr]:[I] ratio was increased and conditions for **P02** were used for further polymerizations as it was believed to offer better control over the polymerization next to yielding 94% monomer conversion. Obtained SEC traces and ^{1}H NMR spectra are given below in **Figure 5.2** and **Figure 5.3**.

A)

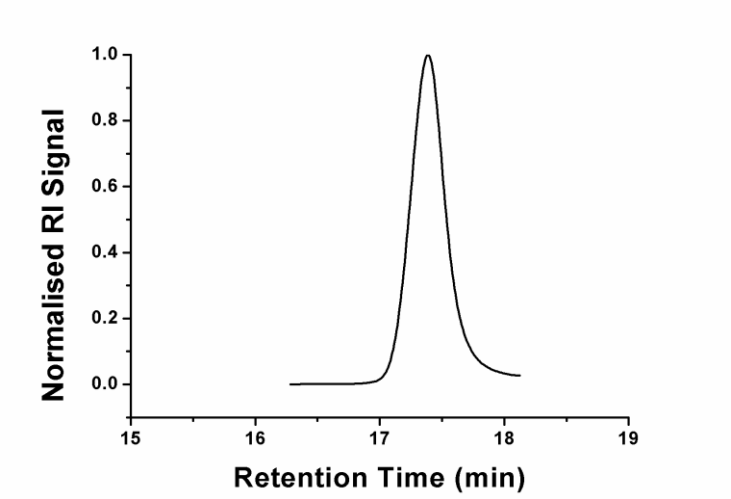

B)

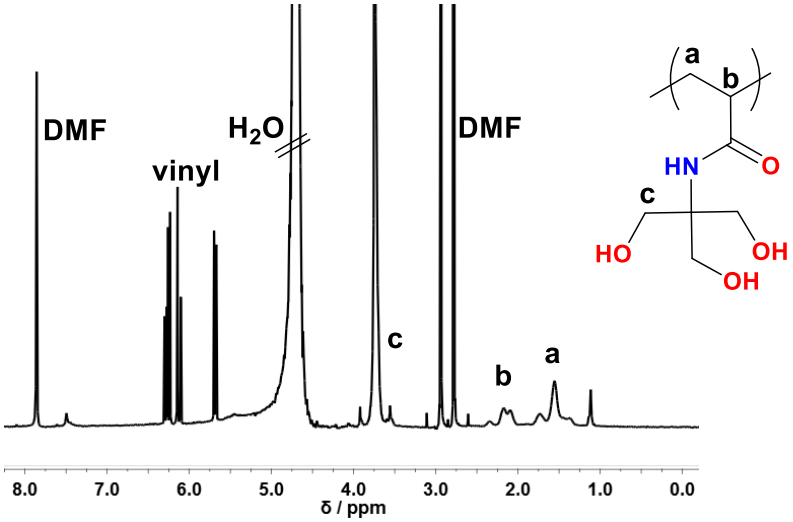

Figure 5.2: Obtained SEC trace (A) and ^{1}H NMR spectrum (B) for **P01**.

C)

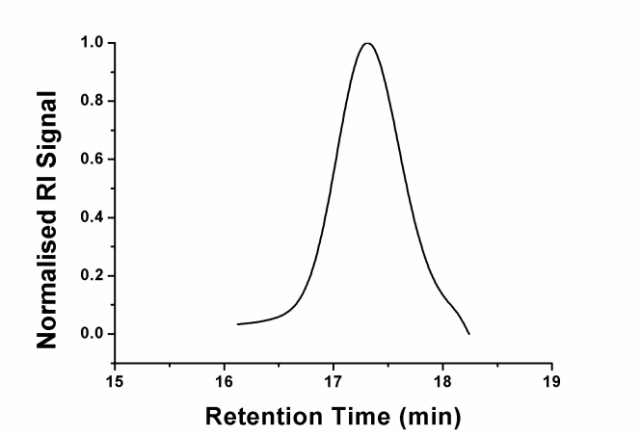

Figure 5.3: continued on next page

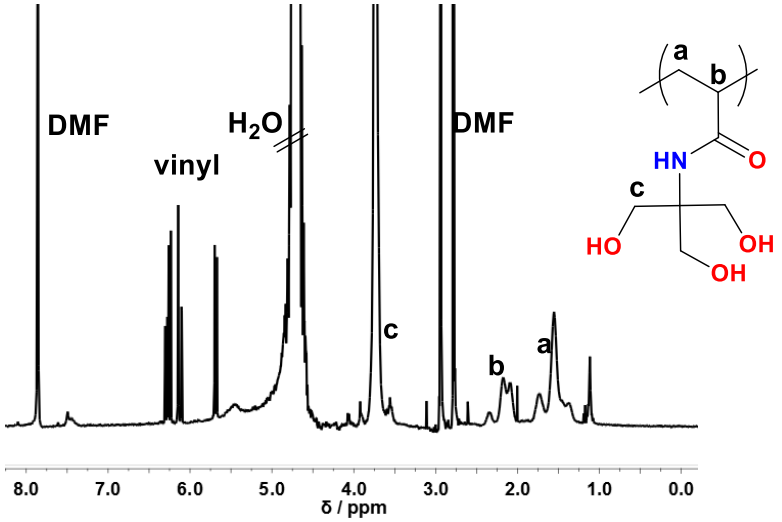

Figure 5.3: Obtained SEC trace (A) and ^{1}H NMR spectrum (B) for **P02**.

Finally, the mixture of the deprotected mono-, di- and tri substituted mannose acrylamide was polymerized. The obtained results are given below in **Figure 5.4** and **Table 5.2**.

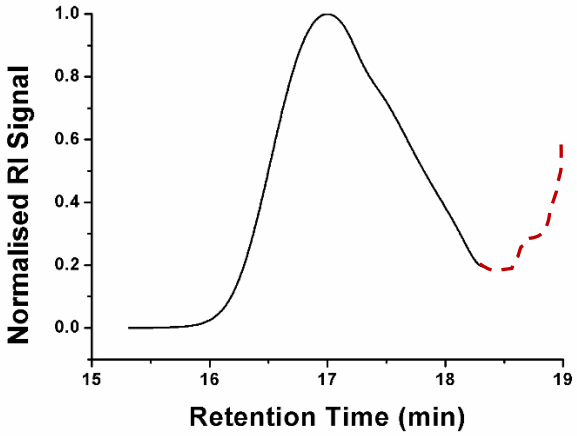

Figure 5.4: SEC trace obtained from the polymerization of the deprotected mix carbohydrate monomer (red dashed line shows instrumental artefact).

Table 5.2: Reaction conditions and obtained results for the SET-LRP of the mannose acrylamide mixture.

Entry	[Mix]:[I]:[CuBr]:[Me$_6$TREN]	ρ^{a} (%)	$M_{n,theo}$ (g/mol)	$M_{n,SEC}{}^{b}$ (g/mol)	$Đ^{b}$	Temp. (°C)
P03	20 : 1 : 0.8 : 0.4	93	6900	8100	1.24	0

[a] Conversion calculated from ^{1}H NMR. [b] DMF eluent, linear PMMA standards.

The polymerization of the mixture was carried out successfully, reaching 93% monomer conversion. Control over the polymerization was maintained yielding a polydispersity of 1.24, with the measured molecular weight being in near relation with the theoretical molecular weight of 1.1 mannose per monomer. Although a mixture of monomers are present, the reaction indicates that once separated, all monomers polymerize with the given reaction conditions, independent of the number of carbohydrates attached to TRIS.

Encouraged by the obtained results, the mono substituted mannose acrylamide was polymerized using the same conditions. The reaction conditions and obtained results are given below in**Table 5.3**.

Table 5.3: Reaction conditions and obtained results for the SET-LRP of the mannose acrylamide mixture.

Entry	[Mix]:[I]:[CuBr]:[Me_6TREN]	ρ^a (%)	$M_{n,theo}$ (g/mol)	$M_{n,SEC}{}^b$ (g/mol)	$Đ^b$	Temp. (°C)
P04	20 : 1 : 0.8 : 0.4	100	6500	7000	1.22	0

[a] Conversion calculated from ^{1}H NMR. [b] DMF eluent, linear PMMA standards.

The homopolymerization of the monomer yielded in 100% monomer conversion with a polydispersity of 1.22. The combined results of **P03** and **P04**, show that it is possible to polymerize the above described monomers employing aqueous SET-LRP under optimized conditions.

5.3. Conclusion

In conclusion, the synthesis of a new class of glycomonomer was shown, in which the number of carbohydrates can be varied between one, two of three. The polymerization of a mixture of the above mentioned monomers and the homopolymerization via aqueous SET-LRP of TRIS and mono substituted mannose acrylamide was shown under optimized conditions. It was found that polymerizations for a glycomonomer to initiator ratio of 20 can be carried out using [I]:[CuBr]:[Me_6TREN]=1:0.8:0.4 at 0°C, yielding well-defined polymers. The above reported synthesis and polymerizations are hoped to employed for the synthesis of more sophisticated glycopolymers, which can be employed to shine light on better understanding the interactions between these materials and their affinity to lectins.

5.4. Experimental

5.4.1. Materials

D-Mannose and acetic anhydride were purchased from Sigma-Aldrich and used as received. All other chemicals and solvents were purchased from Sigma-Aldrich (UK) at the highest purity available and used as received unless stated otherwise. Used for the disproportionation and reaction solvent; water (H_2O, HiPerSolv Chromanorm for HPLC) was purchased from VWR International (UK).

Water soluble initiator 2, 3-dihydroxypropyl 2-bromo-2-methylpropanoate was synthesized according to literature procedure.[17]

Tris(2-(dimethylamino)ethyl)amine (Me_6TREN) was synthesized according to literature procedures and stored at 4°C prior to use.[18,19] Copper(I) bromide (CuBr, 98%, Sigma-Aldrich) was purified by stirring in acetic acid overnight and washing with copious amounts of ethanol before drying under vacuum at 40°C overnight to constant weight.

5.4.2. Instruments and analysis

Proton nuclear magnetic resonance (^{1}H NMR) spectra were recorded on a Bruker AV-III 400 using D_2O at 303 K unless stated otherwise. Full monomer conversion was shown by the disappearance of the vinyl protons (H_2C=C*H*-CO–) (≈6.5-5.5 ppm). All samples taken were immediately diluted with D_2O for analysis.

Size exclusion chromatography (SEC) measurements were conducted on an Agilent 1260 infinity system operating in DMF with 5mM NH_4BF_4 and equipped with refractive index and variable wavelength detector, 2 PLgel 5 μm mixed-C columns (300×7.5mm), a PLgel 5 mm guard column (50x7.5mm) and an autosampler. The instrument was calibrated with linear poly(methyl methacrylate) standards in range of 550-46890 g/mol. All samples were passed through neutral aluminium oxide to remove any catalyst residues and filtered with a 0.2 μm Nylon 6,6 filter before analysis. All reactions were carried out using standard Schlenk techniques under inert atmosphere of oxygen-free argon.

5.2.5. Synthesis

1,2,3,4,6-penta-*o*-acetyl-D-mannose ($Man(OAc)_5$) (1)

$Man(OAc)_5$ was prepared according to a literature procedure. Sulfuric acid (3-4 drops) was added to a stirred mixture of acetic anhydride (100 mL, 1.03 mol) and D-mannose (20g, 0.108 mol) in an ice bath at 0°C. The mixture was kept in the ice bath for 1 hour, then allowed to warm up to room temperature and stirred for an additional 12 hours. The mixture was carefully poured into ice-cold water (300 mL) and extracted with CH_2Cl_2 (3x200 mL). The extract was washed with water, sat. aq. $NaHCO_3$ and brine. The organic phase was dried over $MgSO_4$ and the solvent evaporated under reduced pressure to afford mannose pentaacetate as an oily liquid, which solidified upon standing at room temperature. (Yield: 39 g, 88%)

^1H NMR (300 MHz, $CDCl_3$, δ): 6.01 (d, 1H, CH of sugar moiety), 5.31–5.29 (m, 2H, CH of sugar moiety), 5.20-5.18 (m, 1H, CH of sugar moiety), 4.26-4.19 (m, 2H, CH_2 of sugar moeity), 4.06-3.95 (m, 1H, CH of sugar moiety), 2.14, 2.11, 2.02, 1.99, 1.94 (s, 15 H, $COCH_3$).

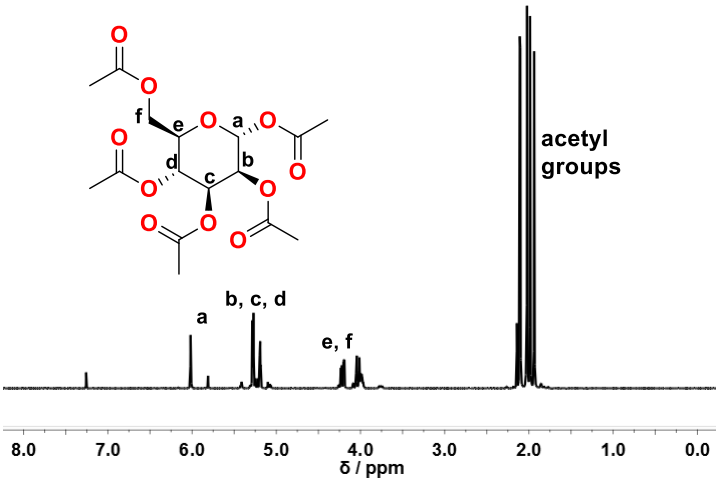

Figure 5.5: ^1H NMR spectrum of $Man(OAc)_5$.

Glycosylation of TRIS (AcManAm-Mix) (2)

In a 250 mL round bottom flask, TRIS (2 g, 11.4 mmol) and $Man(OAc)_5$ (11.14 g, 28.5 mmol) were dissolved in 100 mL DCM and cooled to 0°C under an atmosphere of nitrogen and fitted with a rubber septum. $BF_3{\cdot}OEt_2$ (14.1 mL, 114 mmol) was added

dropwise over a period of 1 hour with a degassed syringe. The mixture was kept at 0°C for an additional hour, was then allowed to warm up to room temperature and stirred for 16 hours. Next, insoluble were filtered and the organic phase washed with sat. aq. $NaHCO_3$ (4x100) until the pH reached 7. After a final wash with water (100 mL), the organic phase was dried over $MgSO_4$ and the solvent evaporated to dryness. (Yield 6.3 g of crude mixture)

^{1}H NMR (300 MHz, $CDCl_3$, δ): 6.38-6.03 (m, 2H, C*H*$_2$=CH-), 6.01 (d, 1H, CH of sugar moiety), 5.31–5.29 (m, 2H, CH of sugar moiety), 5.20-5.18 (m, 1H, CH of sugar moiety), 4.26-4.19 (m, 2H, CH_2 of sugar moeity), 4.06-3.95 (m, 1H, CH of sugar moiety), 2.14, 2.11, 2.02, 1.99, 1.94 (s, 15 H, $COCH_3$).

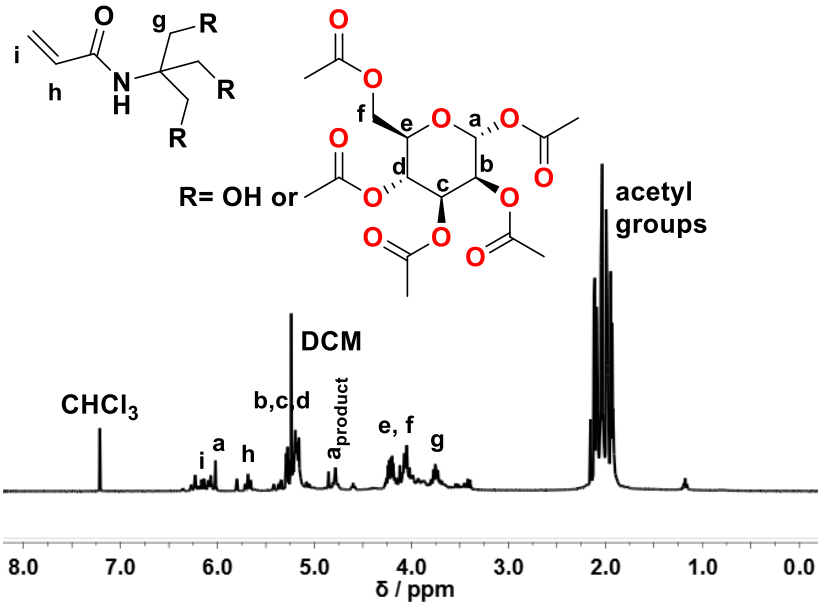

Figure 5.6: ^{1}H NMR spectrum of the crude product.

Synthesis of mono substituted TRIS glycomonomer (3)

2 g of a mixture of AcManAm-Mix was loaded on a silica column and eluted with EtOAc:Hexanes 3:1. The mono substituted product was collected and dried *in vacuo* to yield an oily liquid. (Yield 730 mg, R_f =0.15, $[M+H]^+$=506.22).

^{1}H NMR (300 MHz, $CDCl_3$, δ): 6.63 (s, 1H, OC*H*O of sugar moiety), 6.28-6.05 (m, 2H, C*H*$_2$=CH-), 5.75-5.63 (dd, 1H, CH_2=C*H)*, 5.28-5.11 (m, 2H, OH), 4.83-4.77 (m,

1H, CH of sugar moiety), 4.28-4.15 (m, 2H, CH of sugar moiety), 4.14-3.93 (m, 1H, CH of sugar moiety), 3.45 (s, 2H, CCH_2OH), 2.38-1.74 (m, 12H, $COCH_3$)

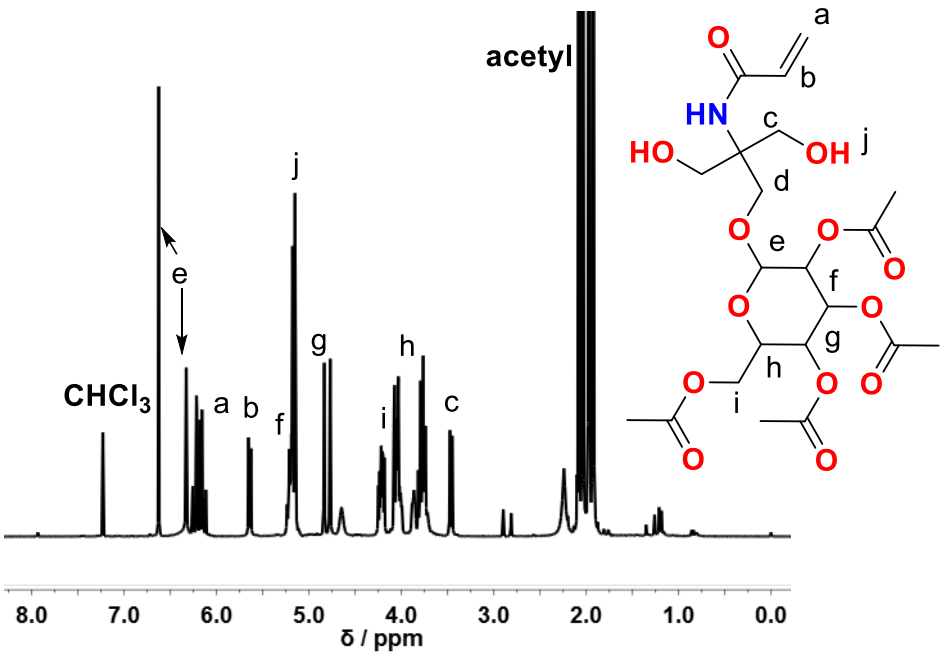

Figure 5.7: ^{1}H NMR spectrum of the crude product.

Polymerization reactions

In a typical reaction, CuBr (5 mg, 0.4 eq. or 10 mg 0.8 eq.) was weighed into a Schlenk tube and fitted with a stirrer bar and deoxygenated with Argon for 20 minutes. The Schlenk tube was sealed with a rubber septum under a positive pressure of Argon and lowered into an ice bath. In the meanwhile, Me_6TREN (9 µL, 0.4 eq.) was added to a vial with 2.5 mL of H_2O and sealed and degassed for 15 minutes (Vial 1) in an ice bath. Vial 1 was then transferred with a degassed syringe into the Schlenk tube and allowed to disproportionate for 30 minutes. In another vial (Vial 2), monomer (mono substituted: 588 mg, 20 eq., TRIS: 175.18 mg, 20 eq.) and initiator (21 mg, 1 eq.) were dissolved in H_2O under stirring and deoxygenated with Argon for 20 minutes at 0°C.***** Vial 2 was then transferred with a degassed syringe into the Schlenk tube to start the polymerization. The transfer of Vial 2 defines t_0.

*****For the SET-LRP of TRIS, 0.15 mL of DMF was added to Vial 2 as internal standard.

5.5. References

1. S. R. S. Ting, G. Chen and M. H. Stenzel, *Polym. Chem.*, 2010, **1**, 1392-1412.
2. L. L. Kiessling, J. E. Gestwicki and L. E. Strong, *Angew. Chem. Int. Ed.*, 2006, **45**, 2348-2368.
3. J. J. Lundquist and E. J. Toone, *Chem. Rev.*, 2002, **102**, 555-578.
4. M. A. Mees, C. Effenberg, D. Appelhans and R. Hoogenboom, *Biomacromolecules*, 2016, **17**, 4027-4036.
5. Y. Chen, M. S. Lord, A. Piloni and M. H. Stenzel, *Macromolecules*, 2015, **48**, 346-357.
6. J. E. Gestwicki, C. W. Cairo, L. E. Strong, K. A. Oetjen and L. L. Kiessling, *J. Am. Chem. Soc.*, 2002, **124**, 14922-14933.
7. Y. Miura, D. Koketsu and K. Kobayashi, *Polym. Adv. Technol.*, 2007, **18**, 647-651.
8. D. Ponader, F. Wojcik, F. Beceren-Braun, J. Dernedde and L. Hartmann, *Biomacromolecules*, 2012, **13**, 1845-1852.
9. Q. Zhang, J. Collins, A. Anastasaki, R. Wallis, D. A. Mitchell, C. R. Becer and D. M. Haddleton, *Angew. Chem. Int. Ed.*, 2013, **52**, 4435-4439.
10. Q. Zhang, L. Su, J. Collins, G. Chen, R. Wallis, D. A. Mitchell, D. M. Haddleton and C. R. Becer, *J. Am. Chem. Soc.*, 2014, **136**, 4325-4332.
11. A. Dag, J. Zhao and M. H. Stenzel, *ACS Macro Lett.*, 2015, **4**, 579-583.
12. S.-J. Richards, M. W. Jones, M. Hunaban, D. M. Haddleton and M. I. Gibson, *Angew. Chem. Int. Ed.*, 2012, **51**, 7812-7816.
13. Q. Zhang, P. Wilson, A. Anastasaki, R. McHale and D. M. Haddleton, *ACS Macro Lett.*, 2014, **3**, 491-495.
14. S. Sinnwell, M. Lammens, M. H. Stenzel, F. E. Du Prez and C. Barner-Kowollik, *J. Polym. Sci. Part A: Polym. Chem.*, 2009, **47**, 2207-2213.
15. S. Pearson, H. Lu and M. H. Stenzel, *Macromolecules*, 2015, **48**, 1065-1076.
16. S. G. Spain and N. R. Cameron, *Polym. Chem.*, 2011, **2**, 1552-1560.
17. S. Perrier, S. P. Armes, X. S. Wang, F. Malet and D. M. Haddleton, *J. Polym. Sci. Part A: Polym. Chem.*, 2001, **39**, 1696-1707.
18. M. Ciampolini and N. Nardi, *Inorg. Chem.*, 1966, **5**, 41-44.
19. J. Queffelec, S. G. Gaynor and K. Matyjaszewski, *Macromolecules*, 2000, **33**, 8629-8639.

Chapter 4

Graft shaped copolymers by combination of SET-LRP and cationic ring opening polymerization

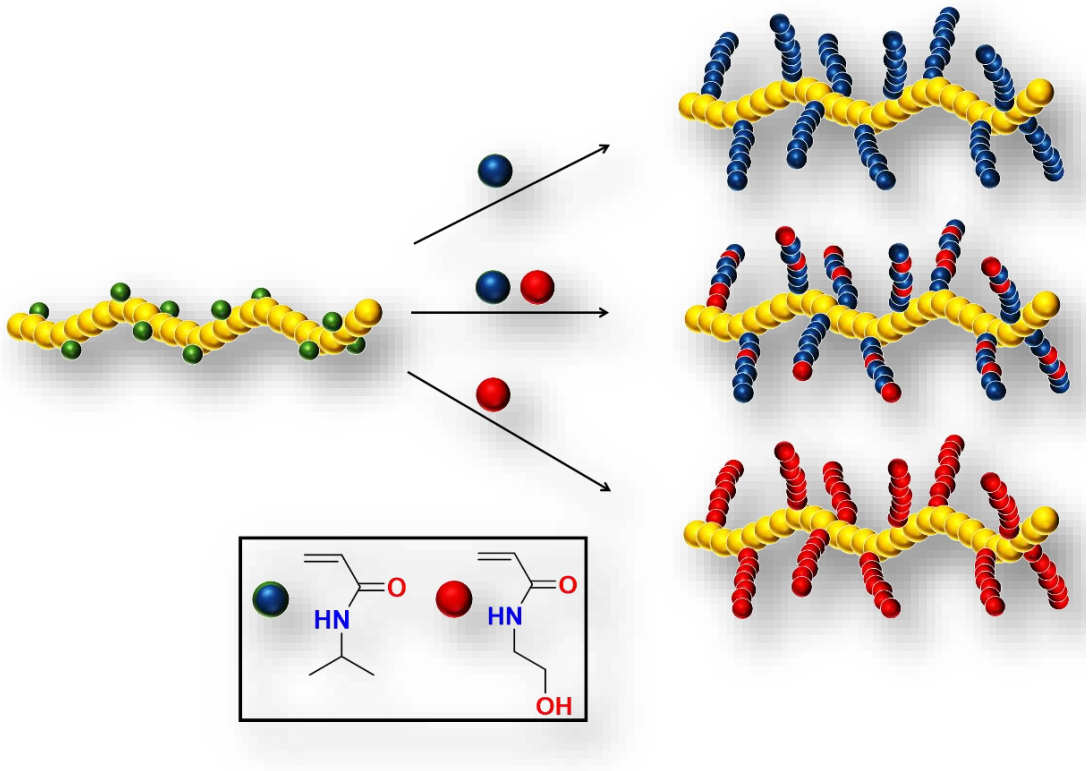

The synthesis of graft copolymers via SET-LRP in aqueous solution has been reported. This aqueous polymerization technique allows rapid and direct access to acrylamide based graft-shaped copolymers. To achieve this, Poly(2-Ethyl-2-Oxazoline) ($PEtOx_{100}$) was synthesized in a microwave reactor. Next, the hydrolysis of $PEtOx_{100}$ to Poly(ethylene imine) was investigated at various times, which subsequently was functionalized into an ATRP graft-initiator. The obtained initiator was then used to polymerize N-isopropylacrylamide and N-hydroxyethyl acrylamide via the "grafting from" method. Graft-shaped polymers of DP=200 with polydispersities below 1.33 were obtained as evidenced by SEC and ^1H NMR.

4.1. Introduction

Graft polymers have attracted considerable interest over the last decades as an important polymer structure, due to their diverse physical properties[1,2] and wide range of use in various applications, which include but are not limited to self-assembly,[3] drug delivery,[4] biomimetics[5,6] and coatings[7]. Synthetically graft polymers can be prepared *via* three methods.[6] The "*grafting through*" approach typically involves the direct polymerization of a long macromonomer, that later forms the side chain (*i.e.* oligo(ethylene glycol) acrylate).[8] This method gives access to fully grafted polymers, where the design can already be engineered at the monomeric level. For example, a macromonomer with the desired functionality can be synthesized that could later be conjugated to others giving additional properties. However, polymerization of macromonomers does not usually reach to full conversions and tend to be uncontrolled. Similarly, side chains can be directly attached to the polymeric backbone with coupling reactions (*i.e.* "click" reaction) *via* the "*grafting onto*" approach, which can possibly allow to obtain grafts with predefined number of side chains.[9] Typically, a large excess of side chains are necessary to ensure efficient coupling, which requires additional purification steps. Finally, the polymerization of the side chains initiated on the backbone is described as the "*grafting from"* method. This can be, for example, obtained by the polymerization of an initiating monomer (*i.e.* inimer), which can be used in an additional step to polymerize out the side chains.

All three methods provide certain advantages and disadvantages, which need to be assessed depending on the tolerance of concurring reactions, if present, and the polymerization system. To overcome this, more than one type of polymerization techniques can also be combined, in order to polymerize the backbone and the side chain.

SET-LRP is one of the recent polymerization techniques, that has started to emerge as a new tool in the synthesis of graft/branched polymers. As described in Chapter 1, SET-LRP can be vaguely categorized into two systems depending on the solvent as organic- or aqueous SET-LRP. Many elegant examples of report for the synthesis of graft polymers *via* organic SET-LRP already exist, yet the complete implementation of their synthesis into aqueous SET-LRP lacks in reports and is yet to be fully understood.

The inimer approach is a popular strategy, when it comes to organic or aqueous SET-LRP. Mostly, the inimer is polymerized with another technique to avoid random branching due to the presence of two or more initiating sites of the same nature. In the following, some of the key examples in the literature will be presented and the initial findings for the synthesis in the aqueous system will be reported.

For example, Matson *et al.* made use of a dithiocarbamate RAFT agent with a ROMP-active Z-group that was used to polymerize styrenic and acrylic oligomeric macromonomers (PDI < 1.08). Next, these macromonomers were polymerized *via* ROMP in a grafting through process to yield bottlebrush polymers. However, despite attempts to fully optimize the polymerization process, conversions were only as high as 90%. Nevertheless, obtained polymers were well-defined and of high molecular weights (PDI < 1.48, $M_{n,SEC}$ = 25–1250 kg·mol^{-1}).

Similarly, Huang *et al.* polymerized a 2-hydroxyethyl acrylate (HEA) based ATRP inimer *via* RAFT.[10] The well-defined RAFT polymer (PDI = 1.17) was then used to polymerise NIPAM in DMF *via* organic SET-LRP, to obtain well-defined PHEA-PNIPAM (PDI = 1.33). The polymerizations were stopped at 52% in order to avoid intermolecular coupling reactions between chains. Although, the polymers showed an LCST behavior (31°C or 32°C, depending on the polymer concentration), no sudden drop in transmittance was observed, as it gradually decreased over a range between 30°C to 50°C. However, an evident increase in hydrodynamic diameter from 20 nm to 390 nm was observed when the temperature was raised above the LCST determined *via* DLS.

The same group later reported a similar approach to obtain quaternized PDMAEA containing graft polymers *via* SET-LRP.[11] The same inimer was polymerized *via* RAFT, which was successively used as a macroinitiator to polymerize DMAEA. The self-hydrolysis in water was quantified and found to be 90% in 2 weeks. In addition, the tertiary amines were quaternized using MeI, which self-assembled into reversed micelles.

Very recently, another example was reported by Percec *et al.*, where various protected and unprotected monomers were polymerized *via* SET-LRP from a surface under UV light in a grafting from approach.[12]

Herein, it was hypothesized that poly(2-oxazolines) would be an excellent candidate as a precursor macromolecule due to its water solubility, which could be hydrolyzed to PEI, yielding an amine functionality that could be transformed into an initiating site. This would allow an easy and straight forward access to water soluble multi-arm initiators for aqueous SET-LRP polymerizations, in which the number of arms can be targeted. To investigate its function in SET-LRP, well investigated acrylamides were employed to be polymerized.

4.2. Results and Discussion

Implementing these into aqueous SET-LRP system tends to be challenging. The most important drawback is the limited range of water-soluble inimers, and macromonomers or backbones. The grafting from approach tends to be the most popular approach due to its simplicity. Many techniques can be employed to polymerize a water-soluble macroinitiator that bears multiple initiating sites.

Recently, Hoogenboom *et al.* reported the synthesis and microwave assisted acidic hydrolysis of PEtOx.[13] It was shown that the hydrolysis degree can be targeted to obtain PEtOx-*r*-PEI. As PEtOx is a well-investigated, easy to polymerize water soluble polymer,[14-17] it was proposed that secondary amines of the PEI segment could be used to functionalize into a macroinitiator. This would allow enough water solubility due to the PEtOx content, while the number of initiating sites could be targeted with hydrolysis (**Scheme 4.1**).

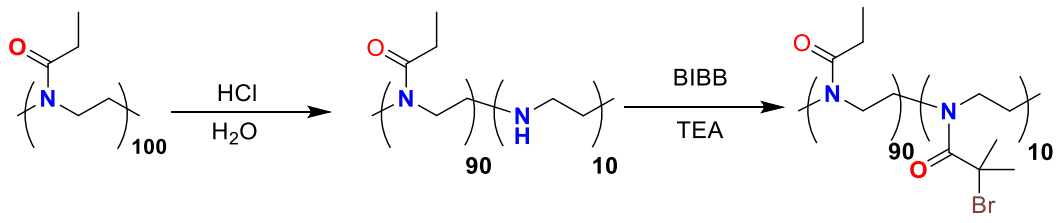

Scheme 4.1: Proposed route to obtain a water soluble graft macroinitiator for aq. SET-LRP.

For this purporse, methyl tosylate initiated PEtOx was synthesized under optimized conditions (*i.e.* 140°C, 15 min.), reaching full conversion, which was confirmed by the disappearance of the monomer peaks corresponding to -N-CH_2-CH_2-O- between 4.50 – 3.50 ppm (**P1**, **Figure 4.1**, $M_{n,SEC}$ = 15100 g·mol^{-1}, PDI = 1.15).[15,17]

Furthermore, the calculated integrals of the peaks were in excellent agreement with the final product.

Then, a series of small scale hydrolysis experiments were carried out ranging from 5 minutes to 60 minutes reaching 76% hydrolysis (**Figure 4.2**). The hydrolysis of PEtOx can be calculated from the ^{1}H NMR spectrum, where the ratio of the integrals corresponding to the PEtOx backbone (-C*H*$_2$-C*H*$_2$-) between 3.90 – 3.40 ppm (peak a) can be compared to the integrals corresponding to the PEI backbone (-NH-C*H*$_2$-C*H*$_2$-) between 2.90 – 2.65 ppm. Next, the hydrolysis was conducted on a larger scale, yielding only 10% hydrolysis according to ^{1}H NMR. The hydrolysis from a total volume of 3 mL to 13 mL showed a dramatic decrease in the hydrolysis. The obtained SEC trace of PEtOx$_{90}$-*r*-PEI$_{10}$ (**P2,** $M_{n,SEC}$ = 21100 g·mol^{-1}, PDI = 1.20) and the corresponding ^{1}H NMR spectrum of the polymer is given below (**Figure 4.3**). Interestingly, although the molecular weight is decreasing, a slight shift to higher retention time from **P1** to **P2** was observed, indicating a higher hydrodynamic volume.

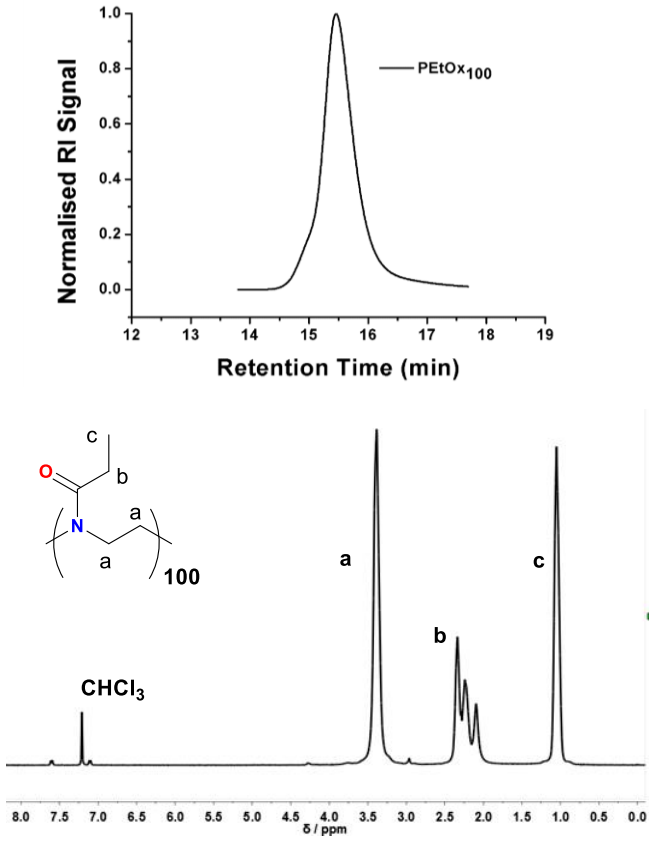

Figure 4.1: Obtained SEC trace from the synthesis of PEtOx$_{100}$ (**top**) and ^{1}H NMR spectrum showing 100% conversion $M_{n,SEC}$ = 15100 g·mol^{-1}, PDI = 1.15 (**bottom**).

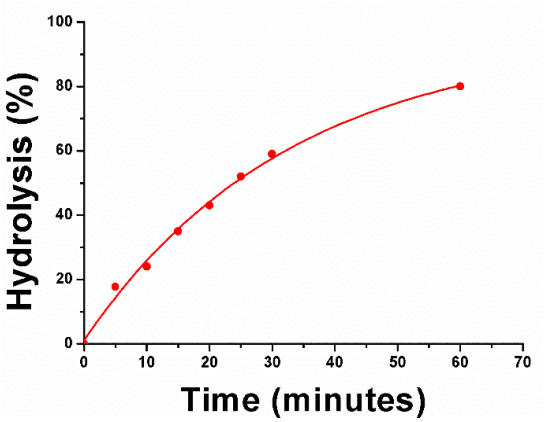

Time (minutes)	Hydrolysis (%)
5	18
10	24
15	35
20	43
25	52
30	59
60	76

Figure 4.2: Time dependent hydrolysis rate of PEtOx to PEtOx-*r*-PEI.

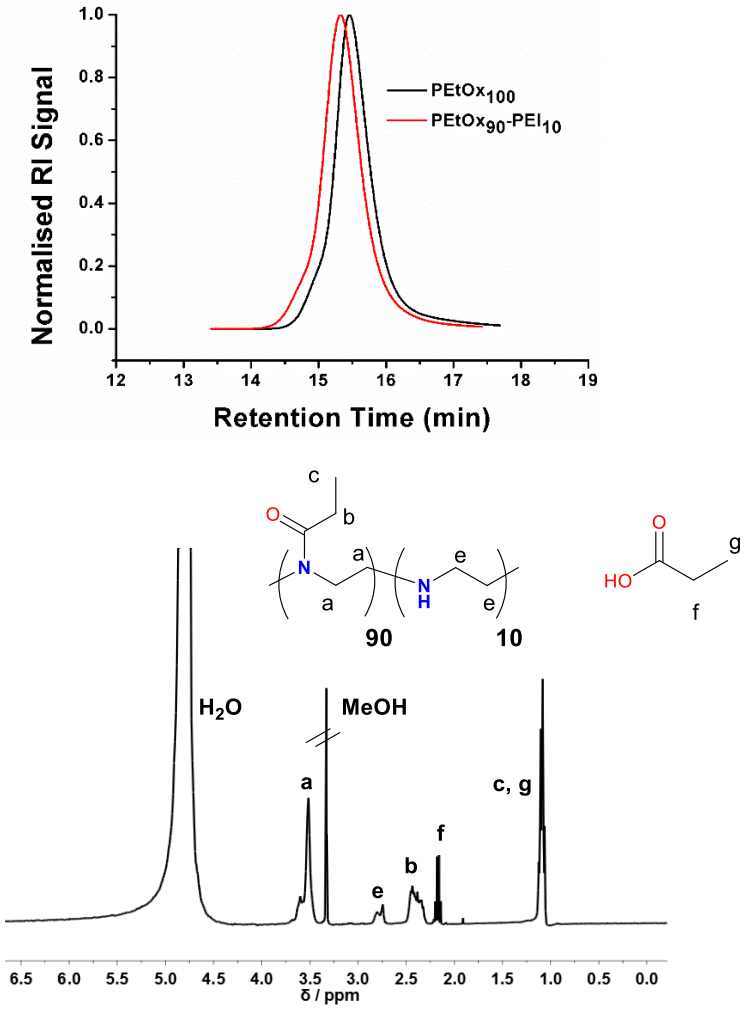

Figure 4.3: Overlaid SEC traces of $PEtOx_{100}$ and $PEtOx_{90}$-*r*-PEI_{10} (**top**) and ^{1}H NMR spectrum of the purified product $M_{n,SEC}$ = 21100 g·mol^{-1}, PDI = 1.20 (**bottom**).

In the last step, BIBB and TEA were used for the synthesis of the water soluble macroinitiator (**MI1**) (**P3,** $M_{n,SEC}$ = 10800 g·mol^{-1}, PDI = 1.19). The obtained SEC trace and ^{1}H NMR spectrum of the final product is given below (**Figure 4.4**.4).

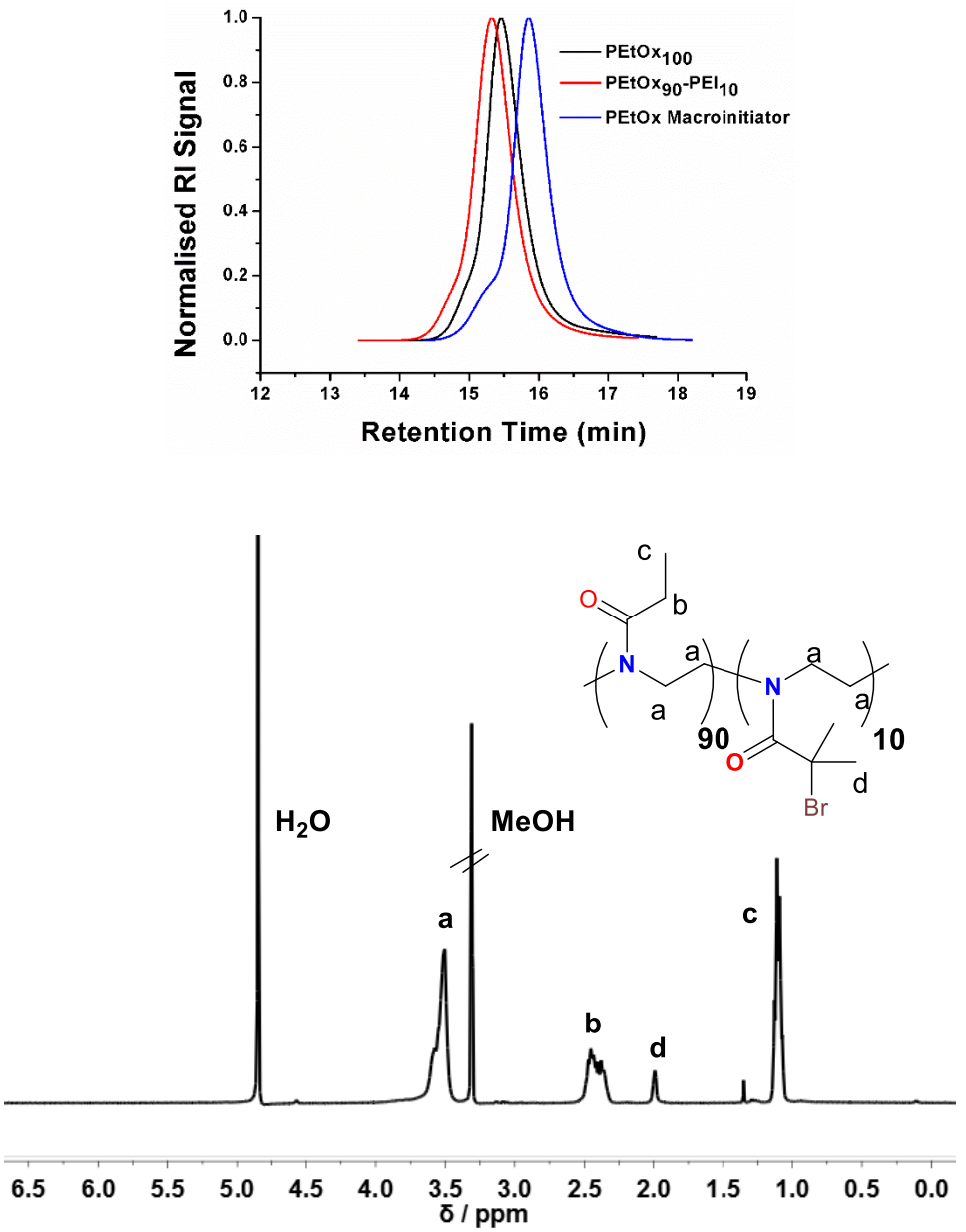

Figure 4.4: Overlaid SEC traces of $PEtOx_{100}$, $PEtOx_{90}$-*r*-PEI_{10} and PEtOx macroinitiator (**P3**) (**top**) and ^{1}H NMR spectrum of the purified product $M_{n,SEC}$ = 10800 g·mol^{-1}, PDI = 1.19 (**bottom**).

Due to the change in hydrodynamic volume from **P1** to **P2**, the initiator **P3** elutes at lower retention times, although the molecular weight increases, possibly due to the change in solubility. Pleasingly, when the integral at 2.00 ppm corresponding to the two methyl groups (Signal d, -(CH_3)$_2$-Br) of the initiating moiety was compared to the backbone signal between 3.90 – 3.40 ppm, the initiator ratio was found to be 10%, confirming the rate of hydrolysis. In addition, the disappearance of the PEI backbone

signal (-NH-CH_2-CH_2-) between 2.90 – 2.65 ppm, shows full substitution, confirming the number of initiating groups on the oxazoline backbone.

In the above, the synthesis of a hydrophilic ATRP macroinitiator starting from PEtOx is described. The chain length of PEtOx and the percentage hydrolysis can easily be targeted. This allows to tailor the hydrophilic *vs.* hydrophobic content of the macroinitiator, which can be obtained depending on the requirements. By maintaining a balance between the two, the possibility to selectively obtain well defined macroinitiators was shown.

In order to test the initiator in an aqueous SET-LRP system, a test polymerization of NIPAM was carried out using standard conditions for star shaped polymers described elsewhere, adjusted to a 10-arm initiator.[18] Hence, the SET-LRP of NIPAM was carried out using [NIPAM]:[MI1]:[CuBr]:[Me_6TREN] = 200:1:6:4. Later, polymerizations of HEAm and a random copolymer of NIPAM and HEAm was also polymerized.

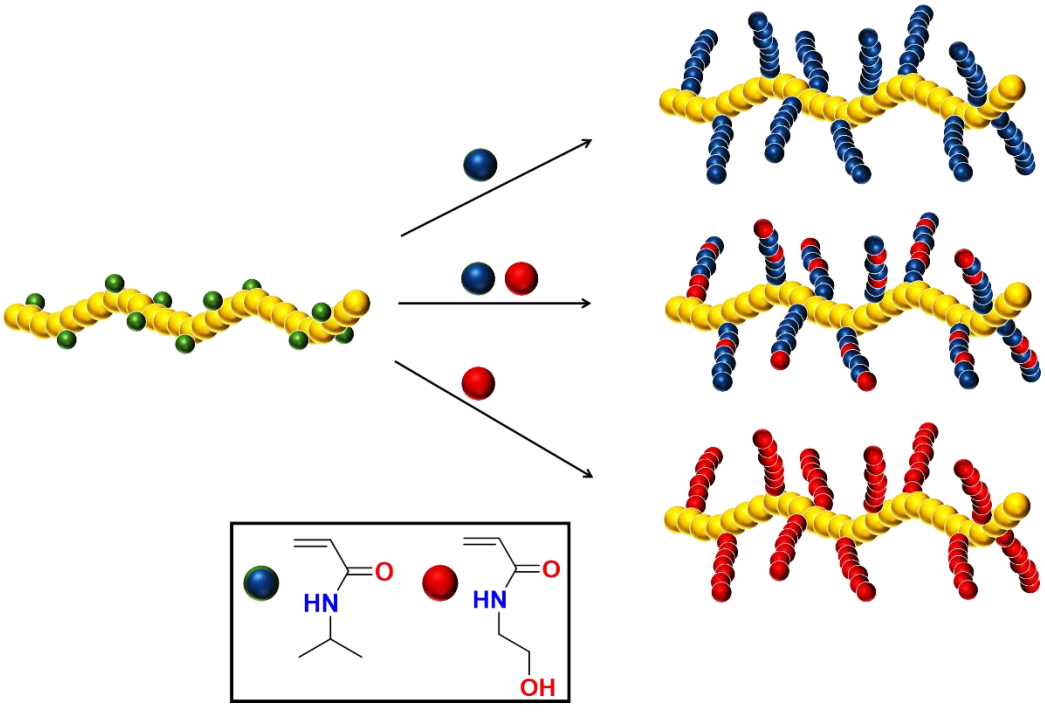

Scheme 4.2: Schematic presentation of the obtained polymers of NIPAM and HEAm.

After the disproportionation of CuBr, pre-disolved **MI1** and NIPAM were introduced *via* a degassed syringe. The polymerization of NIPAM was allowed to proceed for

3 hours to ensure full monomer conversion. A small aliquot from the mixture was subjected to SEC and ^{1}H NMR. The obtained spectra of PEtOx-*g*-PNIPAM (**P4**) are presented below.

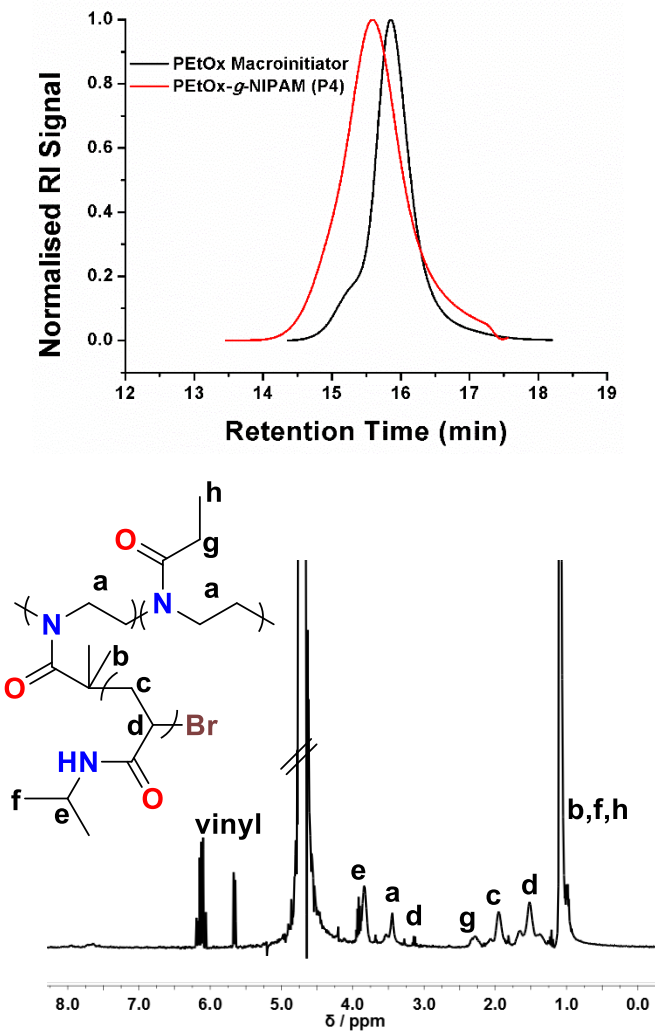

Figure 4.5: Overlaid SEC traces of PEtOx macroinitiator and PEtOx-*g*-PNIPAM (**P4**) (**top**) and ^{1}H NMR spectrum of the product $M_{n,SEC}$ = 15500 g·mol^{-1} and PDI = 1.33 (**bottom**).

The disappearance of the vinyl peaks, displaying 92% monomer conversion for **P4** with $M_{n,SEC}$ = 15500 g·mol^{-1} and PDI = 1.33. The sudden increase in dispersity can be explained with the reaction rate.[19] Initiators based on amides are typically known to initiate faster, which decreases control over the polymerization, leading to broader dispersities. One way to maintain control is to increase the CuBr:**MI1** ratio that will lead to an increase in the effective $CuBr_2$ concentration, which slows down the reaction.

In an attempt to assess monomer compatibility with functional monomers, HEAm was polymerized using the same conditions to obtain PEtOx-*g*-PHEAm (**Figure 4.6**). The SEC traces and the ^{1}H NMR spectrum used to calculate conversion is shown below. With the increase with molecular weight, a slight shoulder appears towards higher and lower retention times, which is respectively indicative of intramolecular coupling reactions and early termination taking place, although full conversion is reached. Nevertheless, the dispersity of the end product obtained, indicates good control over the polymerization ($M_{n,SEC}$ = 15300 gmol^{-1} and PDI = 1.33).

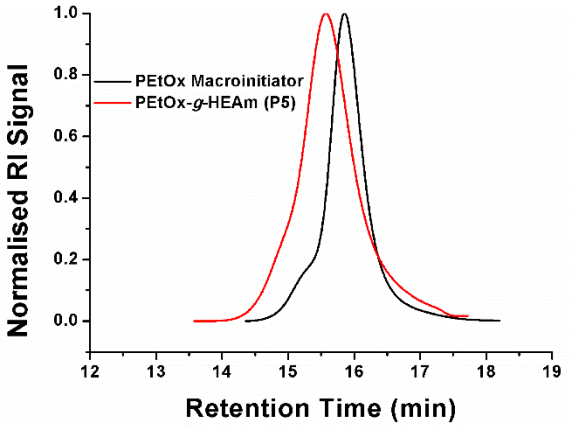

Figure 4.6: Overlaid SEC traces of PEtOx macroinitiator and PEtOx-*g*-PHEAm (**P5**) of the product $M_{n,SEC}$ = 15300 g·mol^{-1} and PDI = 1.33.

Finally, a random graft copolymer was polymerized consisting of equal amounts of NIPAM and HEAm. The obtained SEC trace and ^{1}H NMR spectrum for PEtOx-*g*-(PNIPAM-*r*-PHEAm) is given in the following

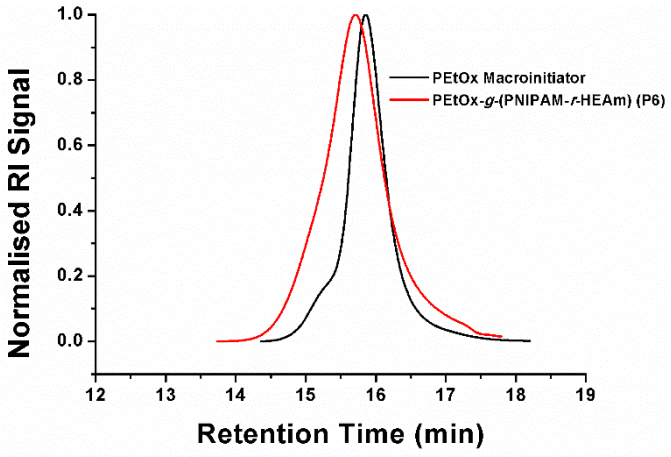

Figure 4.7: Overlaid SEC traces of PEtOx macroinitiator and PEtOx-*g*-PHEAm (**P5**) of the product $M_{n,SEC}$ = 14100 g·mol^{-1}, PDI = 1.34.

In all three cases, the polymerizations reached to full monomer conversion, inititated by a PEtOx based macroinitiator. Furthermore, although the control over the polymerization was moderately maintained, it can be further optimized by adjusting the [CuBr]:[Me_6TREN]:[**MI1**] ratios.

4.3. Conclusion

In conclusion a novel aqueous SET-LRP system was shown employing an oxazoline based macroinitiator to obtain graft polymers. The hydrolysis and subsequent synthesis of the initiator was demonstrated, while maintaining targeted hydrolysis and good control over the molecular weight distribution. The macroinitiator was then used to obtain polymers of NIPAM, HEAm and a random copolymer of NIPAM and HEAm, which was characterized with the help of SEC and ^{1}H NMR. It is believed that the newly established route over an oxazoline initiator will expand the use of the aqueous SET-LRP system to be employed more in the synthesis of graft copolymers.

4.4. Experimental

4.4.1. Materials

N-Isopropylacrylamide (NIPAM, 97%, Sigma Aldrich) was recrystallized from *n*-Hexane and stored at 4°C. 2-Hydroxyethyl acrylamide (HEAm, 97%, Sigma Aldrich) was passed over a short column of basic aluminium oxide to remove the inhibitor prior to use. Methyl p-toluenesulfonate, 2-Ethyl-2-oxazoline (EtOx), α-Bromoisobutyryl bromide (BIBB, 98%) and Triethylamine (TEA, ≥99%) were purchased from Sigma-Aldrich and used as received. All other chemicals and solvents were purchased from Sigma-Aldrich (UK) at the highest purity available and used as received unless stated otherwise. Used for the disproportionation and reaction solvent; water (H_2O, HiPerSolv Chromanorm for HPLC) was purchased from VWR International (UK). Tris(2-(dimethylamino)ethyl)amine (Me_6TREN) was synthesized according to literature procedures and stored at 4°C prior to use.[20,21] Copper(I) bromide (CuBr, 98%, Sigma-Aldrich) was purified by stirring in acetic acid overnight and washing with copious amounts of ethanol before drying under vacuum at 40°C overnight to constant weight.

4.4.2. Instruments and analysis

Proton nuclear magnetic resonance (^{1}H NMR) spectra were recorded on a Bruker AV-III 400 using D_2O at 303 K unless stated otherwise. Full monomer conversion was shown by the disappearance of the vinyl protons (H_2C=CH-CO–) (≈6.5-5.5 ppm). Otherwise, monomer conversion for NIPAM and HEAm was determined, comparing the integral of vinyl protons with isopropyl (–CH(CH_3)$_2$) (≈3.90-3.50 ppm) and (NH(–CH_2–) (≈3.3 ppm) respectively. All samples taken were immediately diluted with D_2O for analysis.

Size exclusion chromatography (SEC) measurements were conducted on an Agilent 1260 infinity system operating in DMF with 5mM NH_4BF_4 and equipped with refractive index and variable wavelength detector, 2 PLgel 5 μm mixed-C columns (300×7.5mm), a PLgel 5 mm guard column (50x7.5mm) and an autosampler. The instrument was calibrated with linear poly(methyl methacrylate) standards in range of 550-46890 g/mol. All samples were passed through neutral aluminium oxide to remove any catalyst residues and filtered with a 0.2 μm Nylon 6,6 filter before analysis.

Turbidity measurements were performed on a Cary 100 UV-Vis spectrophotometer (Agilent) at a wavelength of 500 nm. Solutions of polymers were prepared in water (HPLC grade) at a concentration of 1 mg·mL^{-1} and stirred until fully dissolved. The samples were thermostatted at 20°C for 15 minutes prior to measurement. The transmittance was measured between 20°C and 80°C at a rate of 1°C·min^{-1} in a heating and cooling cycle. The cloud points reported were determined as the 50% transmittance point during the heating cycle.

All reactions were carried out using standard Schlenk techniques under inert atmosphere of oxygen-free argon.

4.4.3. Synthesis

Synthesis of PEtOx

In a microwave vial was charged methyl tosylate, 2-Ethyl-2-Oxazoline (4M) and freshly distilled acetonitrile with a stirrer bar. The vial was sealed with a rubber septum and allowed to polymerize for 15 minutes at 140°C. After 15 minutes, the vial was

cooled to room temperature, before the polymer was precipitated into cold diethylether.

^{1}H NMR (300MHz, $CDCl_3$, δ): 3.80–3.21 (4H, -CH_2-CH_2-N-), 3.1–2.8 ($3H_{init}$,CH_3-NCOCH_2CH_3), 2.60–2.15 (2H; -NCOCH_2-), 1.23–0.95 (3H; -NCOCH_2CH_3).

Synthesis of PEtOx-*r*-PEI

In a microwave vial, desired amount of PEtOx ([Amide]=0.48M in total volume) was dissolved in water. 1M HCl was slowly added and the microwave vial was sealed. The polymer was allowed to hydrolyse under acidic conditions at 120°C for various times.

^{1}H NMR (300 MHz, CD_3OD, δ): PEtOx, + hydrolysis products: 3.80 – 3.30 (4H, -CH_2-CH_2-N-), 3.00 – 2.65 (4H, -NH-CH_2-CH_2-), 2.65 – 2.25 (2H; -NCOCH_2-), 2.25 - 2.00 (CH_3CH_2COOH), 1.25 – 0.85 (3H, -NCOCH_2CH_3, 3H, CH_3CH_2COOH).

Synthesis of the macroinitiator

PEtOx-*r*-PEI was dissolved in a roundbottom flask fitted with a stirrer bar containing DCM. Then, TEA was added and cooled the reaction to 0°C. Next, BIBB dissolved in DCM was added over a period of 1h. Upon completion of the addition, the reaction was allowed to warm up to room temperature and reacted for another 16 hours. The polymer was extracted twice with DCM, dried over $MgSO_4$, after which the solvent was removed, to obtain the initiator. $M_{n,SEC}$ = 10800 g·mol^{-1}, PDI = 1.19

^{1}H NMR (300MHz, $CDCl_3$, δ): 3.80–3.21 (4H, -CH_2-CH_2-N-), 3.1–2.8 ($3H_{init}$,CH_3-NCOCH_2CH_3), 2.60–2.15 (2H; -NCOCH_2-), 2.15–2.00 (6H, -$(CH_3)_2$ 1.23–0.95 (3H; -NCOCH_2CH_3).

SET-LRP reactions

In a typical reaction, CuBr (5 mg) was weighed into a Schlenk tube and fitted with a stirrer bar and deoxygenated with Argon for 20 minutes. The Schlenk tube was sealed with a rubber septum under a positive pressure of Argon and lowered into an ice bath. In the meanwhile, Me_6TREN (21 µL) was added to a vial with 2.5 mL of H_2O and sealed and degassed for 15 minutes (Vial 1) in an ice bath. Vial 1 was then transferred with a degassed syringe into the Schlenk tube and allowed to disproportionate for 30 minutes. In another vial (Vial 2), NIPAM (DP_n = 200), HEAm (DP_n = 200) and **MI1**

(63 mg, $M_{n,SEC}$ = 10800 g·mol^{-1}, PDI = 1.19) were dissolved in H_2O under stirring and deoxygenated with Argon for 20 minutes at 0° C. Vial 2 was then transferred with a degassed syringe into the Schlenk tube to start the polymerization. The transfer of Vial 2 defines t_0.

4.5. References

1. X. Li, S. L. Prukop, S. L. Biswal and R. Verduzco, *Macromolecules*, 2012, **45**, 7118-7127.
2. A. Chremos and P. E. Theodorakis, *ACS Macro Lett.*, 2014, **3**, 1096-1100.
3. Y. Xia, B. D. Olsen, J. A. Kornfield and R. H. Grubbs, *J. Am. Chem. Soc.*, 2009, **131**, 18525-18532.
4. J. A. Johnson, Y. Y. Lu, A. O. Burts, Y.-H. Lim, M. G. Finn, J. T. Koberstein, N. J. Turro, D. A. Tirrell and R. H. Grubbs, *J. Am. Chem. Soc.*, 2011, **133**, 559-566.
5. X. Banquy, J. Burdyńska, D. W. Lee, K. Matyjaszewski and J. Israelachvili, *J. Am. Chem. Soc.*, 2014, **136**, 6199-6202.
6. R. Verduzco, X. Li, S. L. Pesek and G. E. Stein, *Chem. Soc. Rev.*, 2015, **44**, 2405-2420.
7. A. Hucknall, S. Rangarajan and A. Chilkoti, *Adv. Mater.*, 2009, **21**, 2441-2446.
8. H. Y. Cho, P. Krys, K. Szcześniak, H. Schroeder, S. Park, S. Jurga, M. Buback and K. Matyjaszewski, *Macromolecules*, 2015, **48**, 6385-6395.
9. T. Zhou, H. Qi, L. Han, D. Barbash and C. Y. Li, *Nat. Commun.*, 2016, **7**, 11119.
10. Y. Cui, X. Jiang, C. Feng, G. Gu, J. Xu and X. Huang, *Polym. Chem.*, 2016, **7**, 3156-3164.
11. F. Sun, C. Feng, H. Liu and X. Huang, *Polym. Chem.*, 2016, **7**, 6973-6979.
12. M. Vorobii, O. Pop-Georgievski, A. de los Santos Pereira, N. Y. Kostina, R. Jezorek, Z. Sedlakova, V. Percec and C. Rodriguez-Emmenegger, *Polym. Chem.*, 2016, **7**, 6934-6945.
13. V. R. de la Rosa, E. Bauwens, B. D. Monnery, B. G. De Geest and R. Hoogenboom, *Polym. Chem.*, 2014, **5**, 4957-4964.
14. R. Hoogenboom and H. Schlaad, *Polym. Chem.*, 2017, **8**, 24-40.
15. B. Verbraeken, B. D. Monnery, K. Lava and R. Hoogenboom, *European Polymer Journal*, 2017, **88**, 451-469.
16. B. Verbraeken and R. Hoogenboom, *Angew. Chem. Int. Ed.*, 2017, **56**, 7034-7036.
17. R. Hoogenboom, F. Wiesbrock, H. Huang, M. A. M. Leenen, H. M. L. Thijs, S. F. G. M. van Nispen, M. van der Loop, C.-A. Fustin, A. M. Jonas, J.-F. Gohy and U. S. Schubert, *Macromolecules*, 2006, **39**, 4719-4725.
18. R. Aksakal, M. Resmini and C. R. Becer, *Polym. Chem.*, 2016, **7**, 171-175.
19. P. Wilson, A. Anastasaki, M. R. Owen, K. Kempe, D. M. Haddleton, S. K. Mann, A. P. R. Johnston, J. F. Quinn, M. R. Whittaker, P. J. Hogg and T. P. Davis, *J. Am. Chem. Soc.*, 2015, **137**, 4215-4222.
20. M. Ciampolini and N. Nardi, *Inorg. Chem.*, 1966, **5**, 41-44.

21. J. Queffelec, S. G. Gaynor and K. Matyjaszewski, *Macromolecules*, 2000, **33**, 8629-8639.

6. Conclusions and Future Outlook

The aim of this work was to push the polymerization system to its limits and investigate new synthetic possibilities to polymerize functional branched structures, in particular star-shaped and graft-shaped polymers.

The initial findings were based on the synthesis of a star-shaped polymer *via* aqueous SET-LRP, demonstrated for the first time. It was shown that various hydrophilic acrylamides can be polymerized to obtain a multiblock star-shaped polymer in just under 90 minutes. The ability to achieve a pentablock star polymer, displays the high chain end fidelity of the polymer prior to chain extension. The low dispersity of the polymers obtained proves that very well-defined polymers can be obtained using this novel approach.

In the second part of this thesis, the use of a 1 penny coin as a catalyst for organic SET-LRP systems was demonstrated. Various hydrophobic and hydrophilic monomers were employed to obtain linear and star shaped polymers, reaching full monomer conversion whilst maintaining excellent control over molecular weight distribution and no induction period. The results clearly demonstrate that copper wire, which is typically used in this type of polymerizations, can easily be replaced by a copper coin. Furthermore, as no visible damage on the coin surface was observed, it is possible to recirculate the penny, effectively giving a "free catalyst".

Next, the first synthesis of graft polymers in aqueous SET-LRP *via* the grafting from approach was reported, in Chapter 3. For this, a homopolymer of Poly(2-Ethyl-2-Oxazoline) with 100 repeating units was synthesized on a microwave reactor. The purified polymer was hydrolysed to Poly(ethylene imine) under acidic conditions to yield PEtOx-*r*-PEI. The PEI segments of the copolymer were functionalised into an ATRP initiator, which was subsequently employed in the synthesis of graft polymer *via* aqueous SET-LRP.

Finally, glycomonomers with one, two or three carbohydrates were synthesized that were successfully polymerized *via* aqueous SET-LRP, showing that even high molecular weight glycomonomers can be polymerized. Furthermore, the new type of

monomers can be employed to investigate the effects of carbohydrate density on lectin affinity, which would allow us to better understand their role in recognition.

The current state of aqueous SET-LRP is well established to allow the synthesis of complex compositions. This report adds to the synthesis of new topologies that can be realized within very simple reaction conditions and rapid polymerization times. Implementing these findings on the synthesis of novel materials and glycopolymers will be the next interesting area to be investigated.